ZooKeys 328: 1–3 (2013)
doi: 10.3897/zookeys.328.6171
www.zookeys.org

EDITORIAL

A peer-reviewed open-access journal
ZooKeys
Launched to accelerate biodiversity research

Revolving images and multi-image keys open new horizons in descriptive taxonomy: ZooKeys working examples

Pavel Stoev[1], Lyubomir Penev[2], Nesrine Akkari[3], David Koon-Bong Cheung[3], Henrik Enghoff[3], Adam Brunke[3], Carina Mara de Souza[4], Thomas Pape[3], Daniel Mietchen[5], Terry Erwin[6]

1 *National Museum of Natural History, Bulgarian Academy of Sciences and Pensoft Publishers, 12, Prof. Georgi Zlatarski St., 1700 Sofia, Bulgaria* **2** *Institute of Biodiversity and Ecosystem Research, Bulgarian Academy of Sciences and Pensoft Publishers, 12, Prof. Georgi Zlatarski St., 1700 Sofia, Bulgaria* **3** *Natural History Museum of Denmark (Zoological Museum), University of Copenhagen, Universitetsparken 15, Copenhagen, Denmark, 2100* **4** *Department of Animal Biology, Institute of Biology, State University of Campinas (UNICAMP), Barão Geraldo, Campinas, São Paulo, Brazil, P.O.B. 6109, 13083-970* **5** *Museum für Naturkunde – Leibniz-Institut für Evolutions- und Biodiversitätsforschung, Invalidenstraße 43, 10115 Berlin, Germany and Pensoft Publishers, 12, Prof. Georgi Zlatarski St., 1700 Sofia, Bulgaria* **6** *Department of Entomology, MRC 187, National Museum of Natural History, Smithsonian Institution, P. O. Box 37012, Washington, DC 20013-7012 USA*

Corresponding author: *Pavel Stoev* (pavel.e.stoev@gmail.com)

Received 28 August 2013 | Accepted 30 August 2013 | Published 3 September 2013

Citation: Stoev P, Penev L, Akkari N, Cheung DK-B, Enghoff H, Brunke A, de Souza CM, Pape T, Mietchen D, Erwin T (2013) Revolving images and multi-image keys open new horizons in descriptive taxonomy: ZooKeys working examples. ZooKeys 328: 1–3. doi: 10.3897/zookeys.328.6171

Illustrations are indispensable in the recognition of species, irrespective of whether they are used for taxonomic, biological or conservational purposes. With the development of Web 2.0 and Open Access publishing, the demand for image quality and methods for visualizing taxonomic traits has significantly increased. Since its launch in 2008, ZooKeys has been supporting the development of new methods in taxonomy and advocating new tools for the visualization of taxonomic content. Publishing interactive keys as part of taxonomic revisions has become a routine practice for the journal (see e.g., Sharkey et al. 2009a,b, van Noort and Johnson 2009, Stoev et al. 2010, Cerretti et al. 2012). With the development of the journal's web platform, ZooKeys has also started to support the publication of various types of multimedia and audio records, either as supplementary materials or as files embedded in the paper itself (see e.g. Hertz et al. 2012, Faulwetter et al. 2013, Akkari et al. 2013).

A novel approach for the visualization of taxonomic traits exemplified by a modern revision of millipedes of the genus *Ommatoiulus* is published in this issue of ZooKeys (Akkari et al. 2013), along with a detailed technical description and applied workflow (Cheung et al. 2013). It presents an innovative case study aiming to overcome the challenges faced by taxonomists in describing the complex structures essential for species description and identification. The authors use multiple techniques, including an interactive key and a new rotatable scanning electron microscope (rSEM) model to meet these challenges. They present a key design which prioritizes the visual delivery of taxonomic information via interactive media, including line drawings, photographs and scanning electron micrographs of the male genitalia (gonopods). The development of rSEM is widely accessible, requiring no more than access to a scanning electron microscope and some form of software for image integration (Flash, Java Script based programs, etc.). This technique is used for the first time to enhance taxonomic descriptions and allows the structure in question to be seen from multiple angles of view.

The yet slow rate of utilization and acceleration of multimedia in taxonomic research is very likely due to the perception that sophisticated imaging requires special software, e-infrastructure, and significant funding. The method applied here proves that wrong as it enables the visualization of important taxonomic characters in great detail from various angles and can be achieved comparatively effortlessly with conventional technology and software. In addition to providing new insights on the application of SEM and bringing a touch of modernism to taxonomic studies in general, the use of detailed rotating illustrations for small and complex anatomical structures, such as millipede genitalia, revealed diagnostic characters that would have remained unnoticed with conventional methods. The use of these rSEM as a replacement for static illustrations in taxonomic revisions puts us one step closer to the development of a software capable of automatically extracting morphological character data from images of organisms and providing users with the species name (La Salle et al. 2009). Though conceived only to better visualize surface structures, the rSEM model is in a way proving that creating three-dimensional imaging libraries and virtual specimen collections is possible, with a rapid access to "cybertypes," a term recently introduced by Faulwetter et al. (2013).

Acknowledgments

Pensoft has received financial support by the ViBRANT (Virtual Biodiversity Research and Access Network for Taxonomy, www.vbrant.eu) FP7 project.

References

Akkari N, Cheung DK-B, Enghoff H, Stoev P (2013) Revolving SEM images visualising 3D taxonomic characters: application to six species of the millipede genus Ommatoiulus Latzel, 1884, with description of seven new species and an interactive key to the Tunisian members of the genus (Diplopoda, Julida, Julidae). ZooKeys 328: 5–45. doi: 10.3897/zookeys.328.5763

Cerretti P, Tschorsnig H-P, Lopresti M, Di Giovanni F (2012) MOSCHweb – a matrix-based interactive key to the genera of the Palaearctic Tachinidae (Insecta, Diptera). ZooKeys 205: 5–18. doi: 10.3897/zookeys.205.3409

Cheung DK-B, Brunke AJ, Akkari N, Souza CM, Pape T (2013) Rotational Scanning Electron Micrographs (rSEM): A novel and accessible tool to visualize and communicate complex morphology. ZooKeys 328: 47–57. doi: 10.3897/zookeys.328.5768

Faulwetter S, Vasileiadou A, Kouratoras M, Dailianis T, Arvanitidis C (2013) Micro-computed tomography: Introducing new dimensions to taxonomy. ZooKeys 263: 1–45. doi: 10.3897/zookeys.263.4261

Hertz A, Hauenschild F, Lotzkat S, Köhler G (2012) A new golden frog species of the genus *Diasporus* (Amphibia, Eleutherodactylidae) from the Cordillera Central, western Panama. ZooKeys 196: 23–46. doi: 10.3897/zookeys.196.2774

La Salle J, Wheeler Q, Jackway P, Winterton S, Hobern D, Lovell D (2009) Accelerating taxonomic discovery through automated character extraction. Zootaxa 2217: 43–55.

Sharkey M, van Noort S, Whitfield J (2009a) Revision of Khoikhoiinae (Hymenoptera, Braconidae). In: Johnson N (Ed) Advances in the systematics of Hymenoptera. Festschrift in honour of Lubomír Masner. ZooKeys 20: 299–348. doi: 10.3897/zookeys.20.108

Sharkey M, Yu D, van Noort S, Seltmann K, Penev L (2009b) Revision of the Oriental genera of Agathidinae (Hymenoptera, Braconidae) with an emphasis on Thailand and interactive keys to genera published in three different formats. ZooKeys 21: 19–54. doi: 10.3897/zookeys.21.271

Stoev P, Akkari N, Zapparoli M, Porco D, Enghoff H, Edgecombe GD, Georgiev T, Penev L (2010) The centipede genus *Eupolybothrus* Verhoeff, 1907 (Chilopoda: Lithobiomorpha: Lithobiidae) in North Africa, a cybertaxonomic revision, with a key to all species in the genus and the first use of DNA barcoding for the group. ZooKeys 50: 29-77. doi: 10.3897/zookeys.50.504

van Noort S, Johnson NF (2009) New species of the plesiomorphic genus *Nixonia* Masner (Hymenoptera, Platygastroidea, Platygastridae, Scelioninae) from South Africa. In: Johnson N (Ed) Advances in the systematics of Hymenoptera. Festschrift in honour of Lubomír Masner. ZooKeys 20: 31–51. doi: 10.3897/zookeys.20.112

ZooKeys 328: 5–45 (2013)
doi: 10.3897/zookeys.328.5763
www.zookeys.org

RESEARCH ARTICLE

A peer-reviewed open-access journal
ZooKeys
Launched to accelerate biodiversity research

Revolving SEM images visualising 3D taxonomic characters: application to six species of the millipede genus *Ommatoiulus* Latzel, 1884, with description of seven new species and an interactive key to the Tunisian members of the genus (Diplopoda, Julida, Julidae)

Nesrine Akkari[1,†], David Koon-Bong Cheung[1,‡], Henrik Enghoff[1,§], Pavel Stoev[2,3,|]

1 *Natural History Museum of Denmark, University of Copenhagen, Universitetsparken 15, DK-2100 København Ø, Denmark* **2** *National Museum of Natural History, Bulgarian Academy of Sciences* **3** *Pensoft Publishers, 12, Prof. Georgi Zlatarski St., 1700 Sofia, Bulgaria*

† *http://zoobank.org/8DF67798-8E47-4286-8A79-C3A66B46A10F*
‡ *http://zoobank.org/B47D6016-19EC-48F3-BF55-F758478E1B8C*
§ *http://zoobank.org/9B9D901F-D6C8-4BCA-B11B-CF6EE85B16DC*
| *http://zoobank.org/333ECF33-329C-4BC2-BD6A-8D98F6E340D4*

Corresponding author: *Nesrine Akkari* (nakkari@snm.ku.dk; nes.akkari@gmail.com)

Academic editor: *Robert Mesibov* | Received 10 June 2013 | Accepted 31 July 2013 | Published 3 September 2013

http://zoobank.org/EAEE5ABC-5C3E-42EB-B614-7653C8B9B2DD

Citation: Akkari N, Cheung DK-B, Enghoff H, Stoev P (2013) Revolving SEM images visualising 3D taxonomic characters: application to six species of the millipede genus *Ommatoiulus* Latzel, 1884, with description of seven new species and an interactive key to the Tunisian members of the genus (Diplopoda, Julida, Julidae). ZooKeys 328: 5–45. doi: 10.3897/zookeys.328.5763

Abstract

A novel illustration technique based on scanning electron microscopy is used for the first time to enhance taxonomic descriptions. The male genitalia (gonopods) of six species of millipedes are used for construction of interactive imaging models. Each model is a compilation of a number of SEM images taken consecutively while rotating the SEM stage 360°, which allows the structure in question to be seen from all angles of view in one plane. Seven new species of the genus *Ommatoiulus* collected in Tunisia are described: *O. chambiensis*, *O. crassinigripes*, *O. kefi*, *O. khroumiriensis, O. xerophilus*, *O. xenos,* and *O. zaghouani* **spp. n.** Size differences between syntopic adult males of *O. chambiensis* and *O. xerophilus* **spp. n.** from Châambi Mountain are illustrated using scatter diagrams. A similar diagram is used to illustrate size differences in *O. crassinigripes*, *O. khroumiriensis* **spp. n.** and *O. punicus* (Brölemann, 1894). In addition to morphological differences, the latter three species display allopatric distribution and different habitat

preferences. A dichotomous interactive key with a high visual impact and an intuitive user interface is presented to serve identification of the 12 *Ommatoiulus* species so far known from Tunisia. Updates on the North African *Ommatoiulus* fauna in general are presented.

Keywords
Taxonomy, millipedes, Diplopoda, *Ommatoiulus*, new species, North Africa, interactive SEM images, interactive key

Introduction

Description of new species is just one among many tasks of taxonomists (Enghoff and Seberg 2006), but this task is becoming increasingly urgent due to the continuing global decline of biodiversity. However, descriptive taxonomy has a big problem with keeping up to speed. Thus, it has recently been estimated that it takes on average 21 years for a species from being discovered and collected to be formally named and described (Fontaine et al. 2012). The 'shelf life' was, for example, ca. 150 years for *Ommatoiulus schubarti* Akkari & Enghoff, 2012, a species collected for the first and hitherto only time in 1863 (Akkari and Enghoff 2012).

Enhancing and modernizing taxonomy constitutes one of the main challenges of this century, and several pilot projects and initiatives have been taken in this respect (see La Salle et al. 2009, Deans et al. 2012, Erwin et al. 2012). Nevertheless, there is still scope for improvement of efficiency. Costello et al. (2013) listed 14 "Actions to increase the species description rates and taxonomic efficiency", including "Use of digital imaging and molecular technologies to accelerate the description of species" and "Increased availability and access to museum and herbarium specimens, particularly type specimens through exchanges, loans, and on-line imaging …..".

It is natural that the word "imaging" appears in two of Costello et al.'s 14 action points, because nowhere is the saying "a picture is worth a thousand words" more true than in taxonomic descriptions. Early taxonomic works often included excellent drawings. In the course of time, drawings have been supplemented with photographs, microphotographs, SEM micrographs, multi-focus images, and (most recently) images produced by confocal laser scanning microscopy (cLSM), optical projection tomography (OPT), magnetic resonance imaging (MRI) and micro-Computed Tomography scan (e.g., Heim and Nickel 2010, Błażejowski et al. 2011, Görög et al. 2012, Faulwetter et al. 2013). The latter authors in particular have made a significant contribution in this field, suggesting that virtual specimens prepared by means of micro-CT scan may replace type specimens for some purposes.

To demonstrate a new technique for visualization of taxonomic characters described in detail in Cheung et al. (2013) we use six species of the millipede genus *Ommatoiulus* Latzel, 1884 from Tunisia. We describe 7 new *Ommatoiulus* species and offer an interactive and highly visual key to all 12 *Ommatoiulus* species from Tunisia for users with a suitable browser plug-in or Flash viewer.

This work is part of an ongoing project of revising the tribe Schizophyllini (Akkari and Enghoff 2011, 2012, Akkari 2013).

Taxonomic characters in millipedes and associated problems

The male copulatory organs, or gonopods, are of prime importance for characterising millipede species and higher taxa. There are exceptions, where different species have identical or almost identical gonopods, e.g., several genera of Juliformia, such as *Nepalmatoiulus* Mauriès, 1983 (Enghoff 1987), *Dolichoiulus* Verhoeff, 1900 (Enghoff 1992), *Pachyiulus* Berlese, 1883 (Frederiksen et al. 2012), *Anadenobolus* Silvestri, 1897 (Bond and Sierwald 2002) and *Thyropygus* Pocock, 1894 (Pimvichai et al. 2011a, b), and of Nematophora, e.g., *Sinocallipus* Zhang, 1993 (Stoev and Enghoff 2011). By and large, however, the gonopods carry enough information to recognize species, and for more than 150 years authors have focused on describing and illustrating these structures in the most reliable way (Highton 2009).

As useful as gonopod illustrations are for taxonomic descriptions, they can sometimes be grossly misleading and result in misidentification and production of synonymic names, the Achilles' heel of descriptive taxonomy. There are several examples of this in the literature about millipedes, but most striking is perhaps the case presented by Hauser (2000) who demonstrated that amongst 11 subspecies and 100 varieties described for *Craspedosoma alemannicum* Verhoeff, 1910 (see Schubart 1963a), based on differences in the length of podosternite (posterior gonopods) processes, only 9% are valid while the rest can be discarded. The reason for this is that the 'heterodactyly' on which Verhoeff (1915, 1916, 1917, 1939) based his infraspecific *Craspedosoma* taxonomy and which was subsequently adopted by most authors studying the taxonomy and ecology of the genus, was simply due to observation error. When the podosternite of *Craspedosoma* is viewed from varying angles, the relative lengths of its processes change (see Hauser 2000, figs 1, 2, 3).

Useful taxonomic characters in *Ommatoiulus* are almost exclusively derived from the gonopods. Differences between species are often subtle, and the pronouncedly "3D" nature of the gonopods makes recognition of the differences difficult. In many older papers dealing with *Ommatoiulus* taxonomy, authors have dissected the different parts of the gonopods and have illustrated them separately which has led not only to "angle-of-view" problems, but also to difficulties of relating the various gonopod components spatially to each other. By applying the novel imaging technique we have overcome these problems.

The study group: *Ommatoiulus* millipedes from Tunisia

Ommatoiulus is the dominant genus of julid millipedes in North Africa and the Iberian Peninsula. A total of 70 species have been described so far, and many more remain to be recognised and named. For example, Akkari and Enghoff (2012) recorded 19 *Ommatoiulus* species in the southernmost Spanish region, Andalusia, 10 of which they described as new. These authors further provided a historical overview tracing the general inconclusive taxonomic situation and gave an updated definition of the genus based on

morphological characters and a key to the 19 Andalusian species which they estimated to constitute at most 1/6 of the total species richness for the genus. In spite of the wide distribution of a few species, e.g. *O. sabulosus* (Linnaeus, 1758) reaching 64°N in Fennoscandia, and *O. moreleti* (Lucas, 1860) with a near-cosmopolitan, synanthropic distribution, most *Ommatoiulus* species are confined to the Mediterranean region of North Africa and Iberia, and tend even to display small-scale endemism. For instance, of the 19 species recorded from Andalusia, only five were found in other areas (Akkari and Enghoff 2012).

North African species of the genus were examined in considerable detail by several authors, especially Brolemann (1921, 1924, 1925a, b) and Schubart (1952, 1960, 1963b). Recent studies have mostly targeted the Tunisian fauna, describing new species (Akkari and Voigtländer 2007, Akkari and Enghoff 2011) and in some cases detailing some aspects of developmental modalities (Akkari and Enghoff 2011). Akkari et al. (2009) presented detailed species accounts and new records from Tunisia in addition to a complete bibliographical review of the order Julida in North Africa, listing 24 *Ommatoiulus* species for the region.

Despite these contributions, the North African *Ommatoiulus* fauna is far from being thoroughly assessed, nor is its taxonomy close to being fully revised. Without doubt, numerous new species still await discovery, and several taxonomic questions still remain unsolved, such as the correct placement of the highly deviating species *O. lapidarius* (Lucas, 1846), type species of the subgenus *Apareiulus* Brölemann, 1897 (e.g., Attems 1952, Schubart 1963b). The same applies to the *O. punicus* species group established to facilitate understanding species affinities (Akkari and Voigtländer 2007) but which, in the light of recent revisionary work on the genus (Akkari and Enghoff 2012), might not reflect true relationships. To solve these questions an exhaustive revision of the genus in this area is needed.

Material and methods

Most specimens were hand collected during spring 2008 by N.A. and P.S. Supplementary material was obtained from museum collections. All studied specimens are preserved in 70% alcohol. Measurements were made using a Leica Wild M10 microscope equipped with an ocular micrometre. Photographs were taken using Visionary Digital's BK Plus Lab with a Canon EOS 7D. For scanning electron microscopy, parts of the specimens were cleaned with ultrasound, transferred to 96% ethanol then to acetone, air-dried, mounted on adhesive electrical tape attached to aluminium stubs, coated with platinum/palladium and studied in a JEOL JSM-6335F scanning electron microscope. Photographs were processed with a Leica Application Suite program and final stacking made with Zerene Stacker 1.04. The rotatable images were constructed from 18 SEM images taken at 20 degrees intervals starting from the mesal view and continuing until all 360 degrees were captured by rotating the SEM stage. The images were processed using Adobe Lightroom 4.3 by adjusting the black, highlight and white levels to achieve a uni-

form background and contrast. Each image was then cropped to ensure a smooth transition between each frame during rotation. The images were imported into Adobe Flash CS5, where each image was made into a single frame and the series combined to form a rotating animation. The animation controls (moving from one frame to the next) were mapped to the mouse cursor using Actionscript 3.0. The html version available online was compiled using Magic 360. The interactive key was developed in Adobe Flash CS5.5 using Actionscript 2.0 to handle screen transitions and image swapping. Plates were assembled using Adobe Indesign CS 5.5. Respective image libraries of the interactive rSEM have been deposited in MorphBank. More details on the method of creation of the interactive models can be found in Cheung et al. (2013). The number of body rings is given as recommended by Enghoff et al. (1993): Number of podous rings (PR) + number of apodous rings (AR) + telson (T). The developmental stadium of a number of individuals was taken as being represented by the number of vertical rows of ocelli (RO). The real stadium number in julid millipedes has been shown to equal the number of RO+1 (Enghoff et al. 1993), e.g., a specimen with 9RO belongs to developmental stadium 10.

Abbreviations

AR	apodous rings
H	vertical midbody diameter (height)
L	body length
MNHN	Muséum National d'histoire Naturelle, Paris
MSNB	Museo Civico di Storia Naturale 'Enrico Caffi', Bergamo, Italy
NMNHS	National Museum of Natural History, Sofia
PR	podous rings
RO	vertical rows of ocelli
T	telson
ZMUC	Natural History Museum of Denmark (Zoological Museum), University of Copenhagen

Results

Order Julida Brandt, 1833
Family Julidae Leach, 1814
Tribe Schizophyllini Verhoeff, 1909

Genus *Ommatoiulus* Latzel, 1884
http://species-id.net/wiki/Ommatoiulus

Remarks. A general characterisation of *Ommatoiulus* was given by Akkari and Enghoff (2012). Delimitation of *Ommatoiulus* vis-à-vis related nominal genera such as *Tachy-*

podoiulus Verhoeff, 1893 and *Rossiulus* Attems, 1926 is not very clear at present and will probably remain so until the ongoing comprehensive revision of Schizophyllini has been completed (see Akkari and Enghoff 2012).

Of the ca. 70 species of *Ommatoiulus* currently recognized, the following occur in Tunisia:

Ommatoiulus chambiensis Akkari & Enghoff, sp. n.
Ommatoiulus crassinigripes Akkari & Enghoff, sp. n.
Ommatoiulus fuscounilineatus (Lucas, 1846)
Ommatoiulus kefi Akkari & Enghoff, sp. n.
Ommatoiulus khroumiriensis Akkari & Enghoff, sp. n.
Ommatoiulus malleatus Akkari & Voigtländer, 2007
Ommatoiulus punicus (Brölemann, 1894)
Ommatoiulus sempervirilis Akkari & Enghoff, 2011
Ommatoiulus seurati (Brolemann, 1925)
Ommatoiulus xenos Akkari & Enghoff, sp. n.
Ommatoiulus xerophilus Akkari & Enghoff, sp. n.
Ommatoiulus zaghouani Akkari & Enghoff, sp. n.

Ommatoiulus chambiensis Akkari & Enghoff, sp. n.

http://zoobank.org/C6950942-CCF3-43CA-96FF-75F9166168ED
http://species-id.net/wiki/Ommatoiulus_chambiensis
Figs 1–6

Material. Holotype: ♂, W Tunisia, Kasserine Governorate, Châambi National Park, surroundings of the park´s guest house, 35°10.139'N, 8°40.486'E, alt. 950–1000m, scarce trees, *Pinus halepensis*, under stones, 7.3.2008, P. Stoev & N. Akkari leg. (ZMUC). **Paratypes**: 17 ♂♂, 31 ♀♀, 1 immature, same data as holotype (ZMUC); 2 ♂♂, 2 ♀♀, same data as holotype (NMNHS); 1 ♂, 2 ♀♀, W Tunisia, Kasserine Governorate, Châambi National Park, 35°11. 901'N, 8°39.505'E, alt. 1291m, *Quercus ilex*, *Pinus halepensis*, slope, under stones and in leaf litter, 9.3.2008, P. Stoev & N. Akkari leg. (ZMUC).

Diagnosis. Most similar to *O. xerophilus* sp. n., but easily distinguished by the shape of promerite and the presence of a distal notch and a small pointed process on solenomerite.

Etymology. Named after the type locality. Châambi Mountain is the highest mountain range in Tunisia, reaching 1550 m at peak Châambi.

Description. Males: L: 17–23 mm, H: 1.6–2 mm, 46–49 PR+1-2 AR+T; females: L: 18.5–32.2 mm, H: 2.4–3.6 mm, 44–50 PR+1-2 AR+T. General colour brownish with a black sputter, dorsally darker, with a black mid-dorsal line. Head

dark brown to black with yellow spots in the occipital area, uniformly black frontally, with yellow spots at antennal level and labrum, the latter yellow and brighter; antennae dark brown. Prozonites covered with yellowish-brown spots on a blackish background, also laterally, interrupted by big black spots at ozopore level, dorsally black with a narrow transverse row of yellow spots anteriorly; metazonites glossy pale to whitish; legs light brown to yellowish. Telson: anal valves black, with a yellow sputter, preanal ring black, somewhat paler on the caudal projection; subanal scale light brown. Prozonites with fine oblique striae; metazonites with regular striation, laterally narrower; suture complete, strongly curving at ozopore level; ozopores small, rounded, situated on metazonites, at about their diameter from the suture. Anal valves with numerous submarginal and marginal setae, ca. 2 setae on the surface; subanal scale rounded and setose; preanal ring protruding in a caudal projection with ca. 3+3 setae on the tip and a small hyaline process.

Male sexual characters. Mandibular stipites expanded in well-rounded posterior-ventral lobes, first pair of legs hook-shaped, remaining legs with postfemoral and tibial pads.

Gonopods. Promerite (**P**) bent anteriad (Figs 1, 2), proximally subrectangular, gradually narrowing in its distal third (Figs 1, 2); lateral margin with a moderately deep rounded incision (**i**). In a posterior view showing a distal process expanded in a subtriangular shape, bearing an apical blunt process (**ap**) and a lateral broad process pointing basad (**lp**); mesal ridge (**M**) apically broadened and delimiting a serrated lateral lamellar process; distal process laterally bearing a strong serrated ridge (**se**) marking a thickness on the posterior surface; telopodite (**T**) remnant ovoid located in the middle of the proximal part.

Posterior gonopod (Figs 3–6): Mesomerite (**Ms)** longer than the other processes of the gonopods, distally curved mesad and narrowing into an apical process folded and tapering toward the apex. Solenomerite (**S**) broad, slightly narrowing at mid-length, proximally with several strong spikes (**sp**) on the posterior margin; anterior margin with a big, serrated process (**pr**) pointing distad, separated from the apical part by a rounded notch (**n**); apical part with an anterior marginally furrowed lamella (Figs 1, 4–6), and a setose wrinkled protruding lamella (**wl**) covering a protruding slender process (**ds**) (Figs 1, 3–6) housing the distal part and the opening of the seminal groove (**g**), the latter running from the fovea (**F**) at the base of the solenomerite up to process **ds**. Paracoxite (**Px**) broad and curved, emerging from a well-rounded coxite (**Co**), distal third broad then gradually narrowing in a rounded apex pointing mesad (Figs 3–6).

Distribution. Known only from the type locality, Châambi Mountain, Arid Bioclimatic zone, central Tunisia.

Habitat. Mixed forest with *Quercus ilex* and *Pinus halepensis*, under stones and in leaf litter.

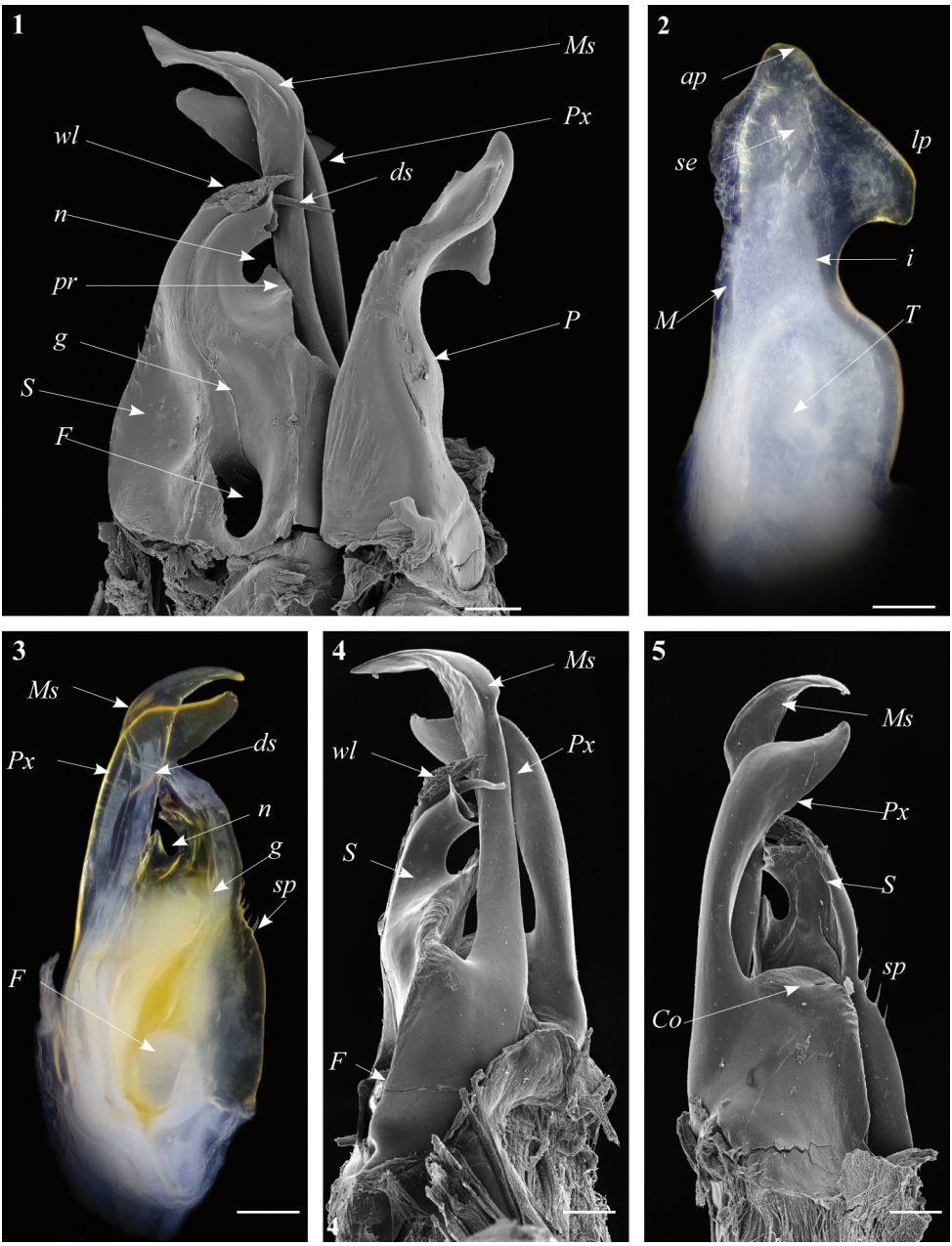

Figures 1–5. *Ommatoiulus chambiensis* sp. n. paratype, gonopod structures. **1** Right gonopod, mesal view **2** Left promerite, posterior view **3** Left posterior gonopod, mesal view **4** Right posterior gonopod, anterior view **5** Right posterior gonopod, posterior view. Abbreviations: **ap** apical process, **ds** distal process of the solenomerite, **F** fovea, **g** seminal groove, **i** incision on lateral margin of the promerite, **lp** lateral apical process of promerite, **M** mesal ridge, **Ms** mesomerite, **P** promerite, **pr** triangular process of the solenomerite, **Px** paracoxite, **S** solenomerite, **se** serrations, **sp** spikes, **T** remnant of telopodite, **wl** wrinkled lamella. Scale bar: 0.1 mm.

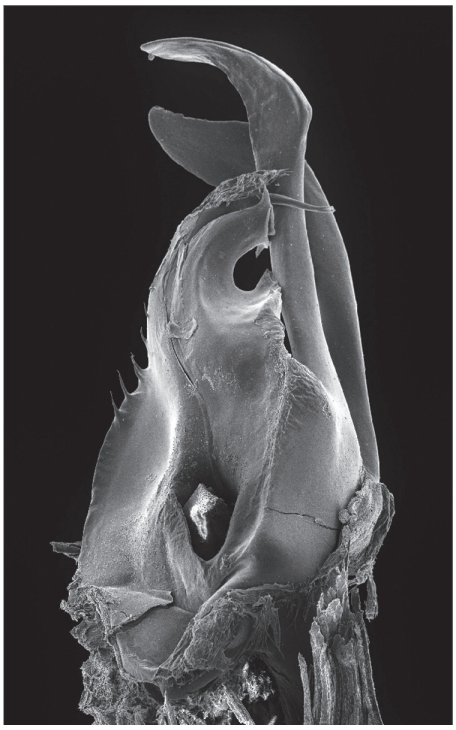

Figure 6. *Ommatoiulus chambiensis* sp. n. paratype, right posterior gonopod. Interactive rotating SEM image. [Morphbank # 831160–831177, 831188]

***Ommatoiulus crassinigripes* Akkari & Enghoff, sp. n.**
http://zoobank.org/82B068D7-2ABD-4771-9899-2F2E2C51B9CA
http://species-id.net/wiki/Ommatoiulus_crassinigripes
Figs 7–13

Schizophyllum punicum: Attems 1903: 144, figs 77–81.
Ommatoiulus punicus: Akkari et al. 2009, in part.

Material. Holotype: ♂, W Tunisia, Kasserine Governorate, Châambi National Park, Châambi peak and its surroundings, 35°12.285'N, 8°40.653'E, alt. 1500–1540m, *Quercus ilex*, *Pinus halepensis*, under stones and leaf litter, 9.3.2008, P. Stoev & N. Akkari leg. (ZMUC). **Paratypes**: 4 ♂♂, 2 ♀♀, same data as holotype (ZMUC); 1 ♂, 1 ♀, same data as holotype (NMNHS); 1 ♂, 3 ♀♀, 3 juveniles, CW Tunisia, El Kef, 21.4.1983, Bianchi & Moretti leg. (MSNB); 3 ♂♂, 11 ♀♀, 1 intercalary male, 30 juveniles, CW Tunisia, Makthar, 9.3.1986, Bianchi & Moretti leg. (MSNB); 6 ♀♀, 2 subadults, CW Tunisia, 12 km S Thala, 10.3.1986, Bianchi & Moretti leg. (MSNB); 2 ♂♂, 12 ♀♀, 4 juveniles, C Tunisia, Kairouan Governorate, El Manara, on the road Kairouan-Sidi Bouzid, open and dry area, 35°14'N, 09°45'E, alt. 673m, 17.3.2005, N. Akkari leg. (ZMUC).

Diagnosis. Gonopods resembling those of *O. punicus* and *O. khroumiriensis* sp. n., but differing by the shape of promerite, a much broader and strongly serrated paracoxite, a broader mesomerite bearing subapical serrations on the mesal margin, and the apical processes on solenomerite.

Etymology. An adjunction of Latin words referring to the body size and leg colour, *crassus* meaning fat and *nigripes*, black leg.

Description. Males: L: 24.8–30 mm, H: 2.7–3.6 mm, 45–53 PR+1–2 AR+T. Females: 30–34 mm, H: 3.4–3.9 mm, 45–47 PR+1–2 AR+T. General colour grey, with alternating pale grey and golden brown, darker laterally, with a thin black mid-dorsal line. Head grey, with black sputter frontally, labral zone reddish-brown, brighter at the margin, antennae dark brown. Prozonites pale grey, with big black spots at the level of ozopores and below, a dense black sputter; metazonites whitish anteriorly and golden brown posteriorly, legs black. Telson: anal valves dark grey, bordered with black, preanal ring golden brown, darker on the tip of the caudal projection; subanal scale yellowish. Prozonites with scattered oblique striae; metazonites with regular striation becoming dense laterally; ozopores small and rounded, appearing as brown rounded spots located on metazonites, situated at about their diameter from the suture; the latter complete, only slightly curving at the level of ozopores. Anal valves mostly glabrous at the surface but bearing several submarginal and shorter marginal setae; subanal scale triangular, blunt and setose; preanal ring protruding in a caudal projection, with ca. 2+2 setae and a small hyaline process on the tip.

Male sexual characters. Mandibular stipites expanded in well-rounded posterior-ventral lobes, first pair of legs hook-shaped, remaining legs with postfemoral and tibial pads.

Gonopods. Promerite (Fig. 7) broad, proximally almost rectilinear, bent 90 degrees at notch level; strongly narrowing in its distal third with a deep incision (**i**) on the lateral margin, latter almost rectilinear; mesal ridge (**M**) broad distally, protruding in a blunt process (**mp**) (Fig. 7); posterior surface irregular on the mesal side, bearing a number of strong setae aligned in front of the notch; distal process (**ap**) laterally broadened and rounded, showing a small mesal serrated process (**ap1**); remnant of telopodite (**T**) as a small bump located proximally.

Posterior gonopod (Figs 8–13). Mesomerite (**Ms**) long, sinuous, distal part asymmetrically enlarged mesolaterally, and showing in lateral view strong serrations at different levels on both margins (Figs 8, 9, 13), gradually narrowed apically in a hook-shaped process (**ho**) curved and tapering toward the apex (Figs 11, 12, 13). Solenomerite (**S**) broadest at the base, narrowing at mid-length and bearing a number of strong setae near the posterior margin (Figs 10, 12, 13); in mesal view showing at mid-length a triangular process (**pr**) pointing distad (Figs 10, 13), latter separated from the apical part by a deep rounded notch (**n**); apically bearing a long curved process (**ds**) pointing mesad, housing the distal part and the opening of the seminal groove (**g**) and emerging between a posterior and an anterior folded hyaline processes (**hp1**, **hp2**) (Figs 11–13). Seminal groove running from the fovea (**F**) at the base of the solenomerite up to process **ds** (Figs 10, 13). Paracoxite (**Px**) lamellar, broad and folded, emerging from a rounded coxite (**Co**), distally broadened, apical margin almost

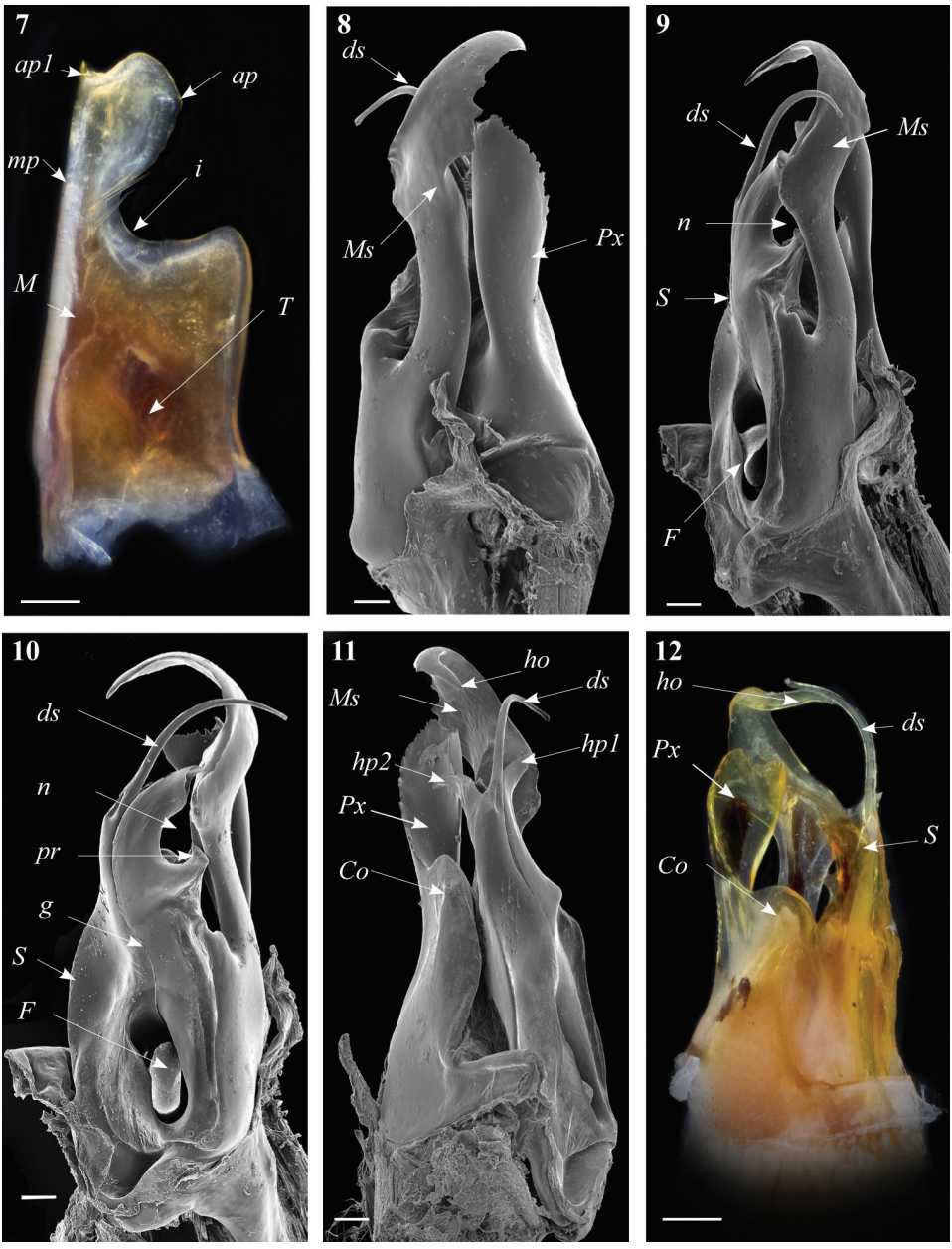

Figures 7–12. *Ommatoiulus crassinigripes* sp. n. paratype, gonopod structures. **7** Left promerite, posterior view **8** Right posterior gonopod, lateral view **9** Right posterior gonopod, anterior view **10** Right posterior gonopod, mesal view **11** Right posterior gonopod, posterior view **12** Right posterior gonopod latero-posterior view. Abbreviations: **ap** distal process of the promerite, **ap1** apical mesal process, **Co** coxite, **ds** distal process of the solenomerite, **F** fovea, **g** seminal groove, **ho** hook-shaped process, **hp1, hp1** distal processes of the solenomerite, **i** lateral margin incision of the promerite, **M** mesal ridge, **Ms** mesomerite, **mp** distal blunt process of the mesal ridge, **n** notch of the solenomerite, **pr** triangular process of the solenomerite, **Px** paracoxite, **S** solenomerite, **T** remnant of telepodite. Scale bar: 0.1 mm

Figure 13. *Ommatoiulus crassinigripes* sp. n. paratype, right posterior gonopod. Interactive rotating SEM image. [Morphbank # 831189–831207]

horizontal, and together with the posterior margin showing many strong, short serrations (Figs 8, 11–13).

Distribution. Semi-arid and Arid bioclimatic zones in west central Tunisia, recorded from the governorates Kasserine, El Kef, Thala and Kairouan.

Habitat. Dry and open habitats, to 1500 m in Châambi Mountain.

***Ommatoiulus kefi* Akkari & Enghoff, sp. n.**
http://zoobank.org/93E41C97-AA12-45D5-BD86-F2B0ACF02465
http://species-id.net/wiki/Ommatoiulus_kefi
Figs 14–19

Material. Holotype: ♂, W Tunisia, El Kef Governorate, 13 km S El Kef, 22.iv.1981, Bianchi & Moretti leg. (MSNB).

Diagnosis. Differing from all congeners by having a tri-lobate distal part of promerite and a bifurcated apical part of mesomerite, the latter divided in two short oppositely directed processes.

Etymology. Named after El Kef city, the type locality of the species.

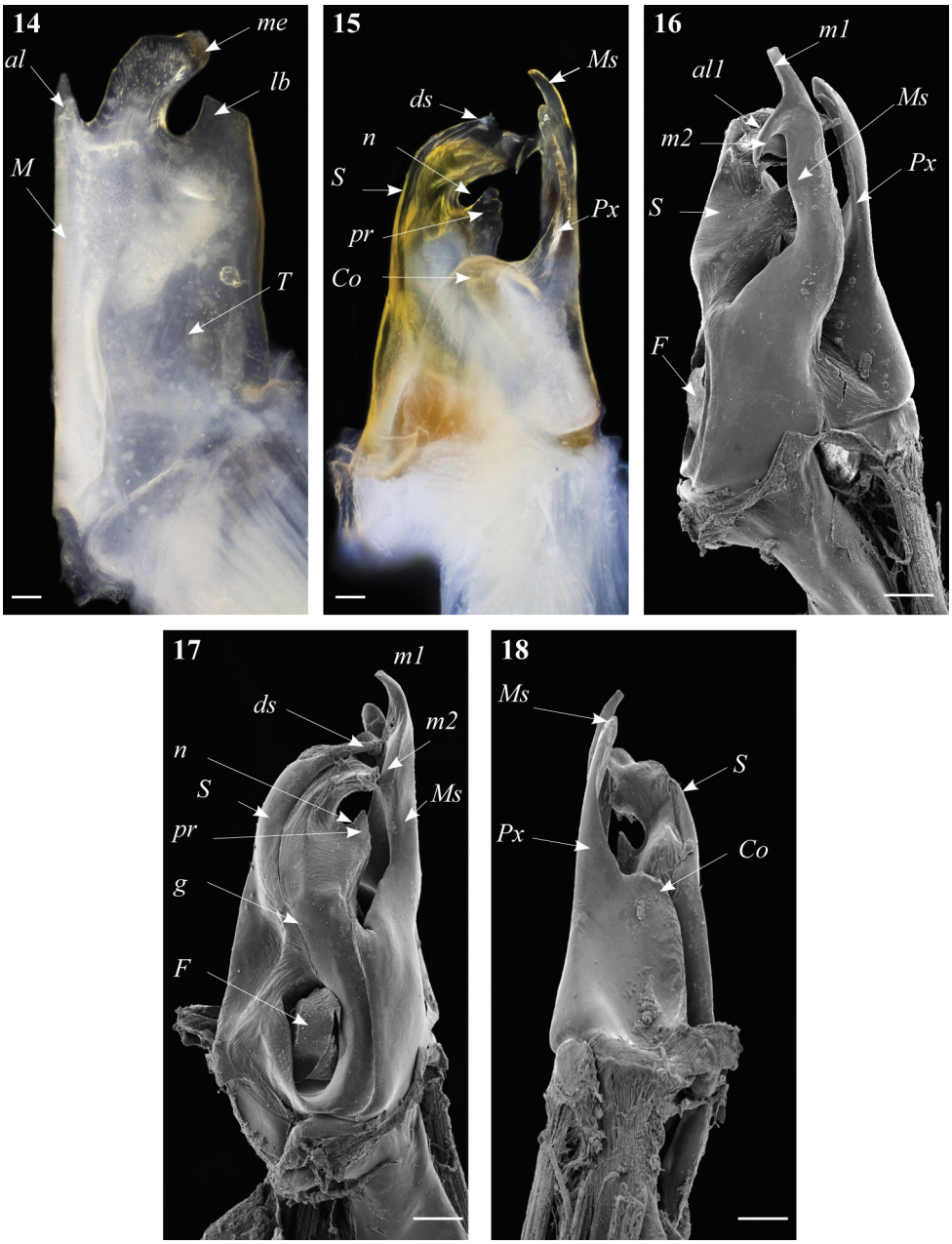

Figures 14–18. *Ommatoiulus kefi* sp. n. holotype, gonopod structures. **14** Left promerite, posterior view **15** Left posterior gonopod, posterior view **16** Right posterior gonopod, anterior view **17** Right posterior gonopod, mesal view **18** Right posterior gonopod, mesal view. Abbreviations: **al** apical lobe of the promerite, **al1** apical folded lamella of the solenomerite, **Co** coxite, **ds** distal process of the solenomerite, **F** fovea, **g** seminal groove, **lb** lateral lobe, **m1, m2** apical processes of the mesomerite, **M** mesal ridge, **me** median lobe, **Ms** mesomerite, **n** notch of the solenomerite, **pr** triangular process of the solenomerite, **Px** paracoxite, **S** solenomerite, **T** telopodite. Scale bar: 0.1 mm

Figure 19. *Ommatoiulus kefi* sp. n. holotype, right posterior gonopod. Interactive SEM image. [Morphbank # 831208-831227]

Description. Male: L: 26 mm, H: 2.7 mm, 53 PR+1 AR+T. General colour alternating whitish and blackish with a thin black mid-dorsal line. Head brown, lighter on the frontal part, with yellowish spots at antennal level, labral zone yellowish, becoming brighter at the margin, antennae brownish. Prozonites pale grey, dorsally scarcely sputtered with black; metazonites anteriorly dark, with a blackish background and a line of light brown spots below ozopores; legs whitish. Telson: anal valves and preanal ring blackish, paler towards caudal projection, subanal scale yellowish. Prozonites with scattered oblique striae; metazonites with regular striation becoming dense laterally; suture complete and rectilinear; ozopores small, rounded and located in metazonites, well apart from the suture. Anal valves with numerous submarginal and marginal setae and ca. 1-2 setae on the surface; subanal scale triangular, blunt and setose; preanal ring protruding in a caudal projection, with ca. 3+3 setae and a small hyaline process on the tip.

Male sexual characters. Mandibular stipites expanded in rounded posterior-ventral lobes, first pair of legs hook-shaped, remaining legs with postfemoral and tibial pads.

Gonopods. Promerite (Fig. 14) in posterior view subrectangular, mesal ridge (**M**) fairly broad, distally narrowing and protruding into a pointed apical lobe (**al**); apical margin protruding in a curved median lobe (**me**) pointing laterad and a shorter broad lateral lobe (**lb**); the three apical lobes separated by two rounded incisions; lateral margin almost rectilinear. Remnant of telopodite (**T**) ovoid, located at mid-length of promerite.

Posterior gonopod (Figs 15–19): Mesomerite (**Ms**) broadest at the base, distally protruding in a uniformly broad process, apically splitting into two short and curved

processes, pointing in opposite directions (**m1**, **m2**) (Fig 16, 17, 19); solenomerite (**S**) broad at the base, slightly narrowing at mid-length and showing a triangular process (**pr**) separated from the rest of the processes by a rounded (**n**) (Figs 17, 19), apical part of the solenomerite complex with a broad lamella (**al1**) extended latero-mesad, downturned and marginally furrowed (Fig. 16). Seminal groove (**g**) running from the fovea (**F**) at the base of solenomerite up to a slender and short conical process (**ds**) emerging on top of the median part of the apical lamella and pointing anteriad (Figs 15, 17). Paracoxite (**Px**) stout, with smooth margins, emerging from a broad rounded coxite (**Co**) (Figs 18, 19).

Distribution. Semi-arid bioclimatic zone in western Tunisia; hitherto known only from the type locality near El Kef city.

Comments. We have examined three females (MSNB) collected from the same locality but could not assign them with certainty to *O. kefi* as they show a different colour pattern.

***Ommatoiulus khroumiriensis* Akkari & Enghoff, sp. n.**
http://zoobank.org/05BAED95-725C-4395-92C3-6BF22A01CE18
http://species-id.net/wiki/Ommatoiulus_khroumiriensis
Figs 20–26

Archiulus punicus: Attems (1926): 191, figs 240, 241.
Ommatoiulus punicus: Akkari et al. 2009, in part.
Ommatoiulus cf. *punicus*: Enghoff et al. 2011: 610.

Material. Holotype: ♂, NW Tunisia, Jendouba Governorate, Aïn Draham, Col des Ruines, 1.11.2009, N. Akkari leg. (ZMUC). **Paratypes**: 2 ♂♂, 5 ♀♀, NW Tunisia, Jendouba Governorate, Aïn Draham, Col des Ruines, 1.11.2009, N. Akkari leg. (ZMUC); 2 ♂♂, 6 ♀♀, NW Tunisia, Jendouba Governorate, 7 km south Aïn Draham, les chênes, 22.3.1986, ZMUC expedition; 1 ♂, 1 ♀, 4 immatures, 5-18.3.1988, NW Tunisia, Jendouba Governorate, Aïn Draham area, ZMUC expedition; 1 ♂, 1 ♀, 1 intercalary male, NW Tunisia, Jendouba Governorate, Aïn Draham, 19.11.2003, forest with *Quercus suber* and *Quercus faginea*, under stones, N. Akkari leg. (NMNHS); 2 ♂♂, 5 ♀♀, 2 juveniles, NW Tunisia, Jendouba Governorate, Hammam Bourguiba, 36°45'N, 08°35'E, alt. 158m, mixed forest with *Pinus pinaster* and *Quercus suber*, under stones, 31.10.2009, N. Akkari leg. (ZMUC); 3 ♂♂, NW Tunisia, Jendouba Governorate, Aïn Draham, 36°47'N, 8°41'E, alt. 511m, 3.10.2005, N. Akkari leg. (ZMUC); 1 ♂, 2 ♀♀, NW Tunisia, Jendouba Governorate, Aïn Draham, 36°47'N, 8°41'E, 760m, *Quercus suber-Erica* forest, 11.3.2009, N. Akkari & H. Enghoff leg. (ZMUC); 3 ♂♂ Jendouba Governorate, route Aïn Draham- Fernana, 36°43'N, 8°40'E, *Quercus suber-Erica* forest, 9.3.2009, N. Akkari & H. Enghoff leg. (ZMUC); 1 ♂, 2 ♀♀, Jendouba Governorate, route Aïn Draham- Béni M'tir, 36°43'N, 8°42'E, *Quercus suber-Erica* forest, 10.3.2009, N. Akkari & H. Enghoff leg. (ZMUC).

Diagnosis. Similar to *O. punicus* and *O. crassinigripes* sp. n. but readily distinguished by the shape of promerite having a deeper notch extended basad, much slen-

derer processes of posterior gonopods, and a more sinuous mesomerite devoid of conspicuous serrations.

Etymology. The species name refers to the natural region of Khroumirie, NW Tunisia, to which the species seems confined.

Description. Males: L: 26–27 mm, H: 2–2.8 mm, 43–48 PR+1–2 AR+T, females: L: 30–37 mm, H: 4–4.3, 44–48 PR+1 AR+T. General colour dark grey, alternating with brown-yellow laterally, and with a thin black mid-dorsal line. Head dark reddish-brown; occipital area blackish, with brown-reddish- spots; frontal part uniformly black, labral zone brown-reddish- to yellowish at margin, antennae brownish. Prozonites uniformly grey, with a pale narrow stripe anteriorly; metazonites darker, brown-greyish, densely sputtered with black, colour gradually vanishing on the sides, below ozopore level yellow-brownish; legs light brown. Telson: anal valves black, preanal ring blackish, caudal projection brown-reddish, subanal scale light brown to yellowish.

Prozonites with scattered oblique striae; metazonites densely striated; suture complete, curving at ozopore level; ozopores small, rounded and located on metazonites, situated at about their diameter from the suture. Anal valves with 4-5 setae on the surface, a submarginal row of 12-13 setae and numerous short marginal ones; subanal scale triangular and setose; preanal ring protruding in a caudal projection with ca. 3+3 setae and a small hyaline process on the tip.

Male sexual characters. Mandibular stipites expanded in rounded posterior-ventral lobes, first pair of legs hook-shaped, remaining legs with postfemoral and tibial pads.

Gonopods. Promerite (Fig. 20) strongly narrowed distally with a deep lateral incision (**i**) extending meso-basad, distal process (**ap**) broad, subtriangular, with two pointed edges, the tip of apical process with a small pointed lobe (**ap2**); mesal ridge (**M**) distally protruding in a blunt small cylindrical process (**mp**), posterior surface of promerite with a row of strong setae emerging at the level of the notch, in close proximity to the mesal ridge.

Posterior gonopod (Figs 21–26). Mesomerite (**Ms**) large, longer than the other processes, uniformly broad, sinuous; distal third constricted to less than half breadth and apically protruding into a slender curved process, latter tapering and pointing mesad (Figs 21, 23, 24, 26). Solenomerite (**S**) broadest at the base, narrowing at mid-length, and bearing a number of strong setae near the posterior margin, distally with a broad, blunt triangular process (**pr**) separated from the apical part by a rounded notch (**n**), and with a long curved process (**ds**) protruding between two apical hyaline processes (**hp3, hp4**) and housing the apical part of seminal groove (**g**), the latter (**g**) running from the fovea (**F**) located at the base of the solenomerite (**S**) up to process **ds**. Paracoxite (**Px**) emerging from a depressed coxite (**Co**); **Px** curved, half as broad as in *O. crassinigripes*, gradually narrowing distad; lateral and apical margins, with a saw-like strongly jagged margin (Figs 22–26).

Distribution. Humid bioclimatic zone in northwestern Tunisia; known from Aïn Draham, Fernana and Hammam Bourguiba in Khroumirie, Jendouba Governorate.

Habitat. Mixed forests dominated by *Quercus faginea* and *Q. suber*, or *Pinus pinaster* and *Quercus suber*.

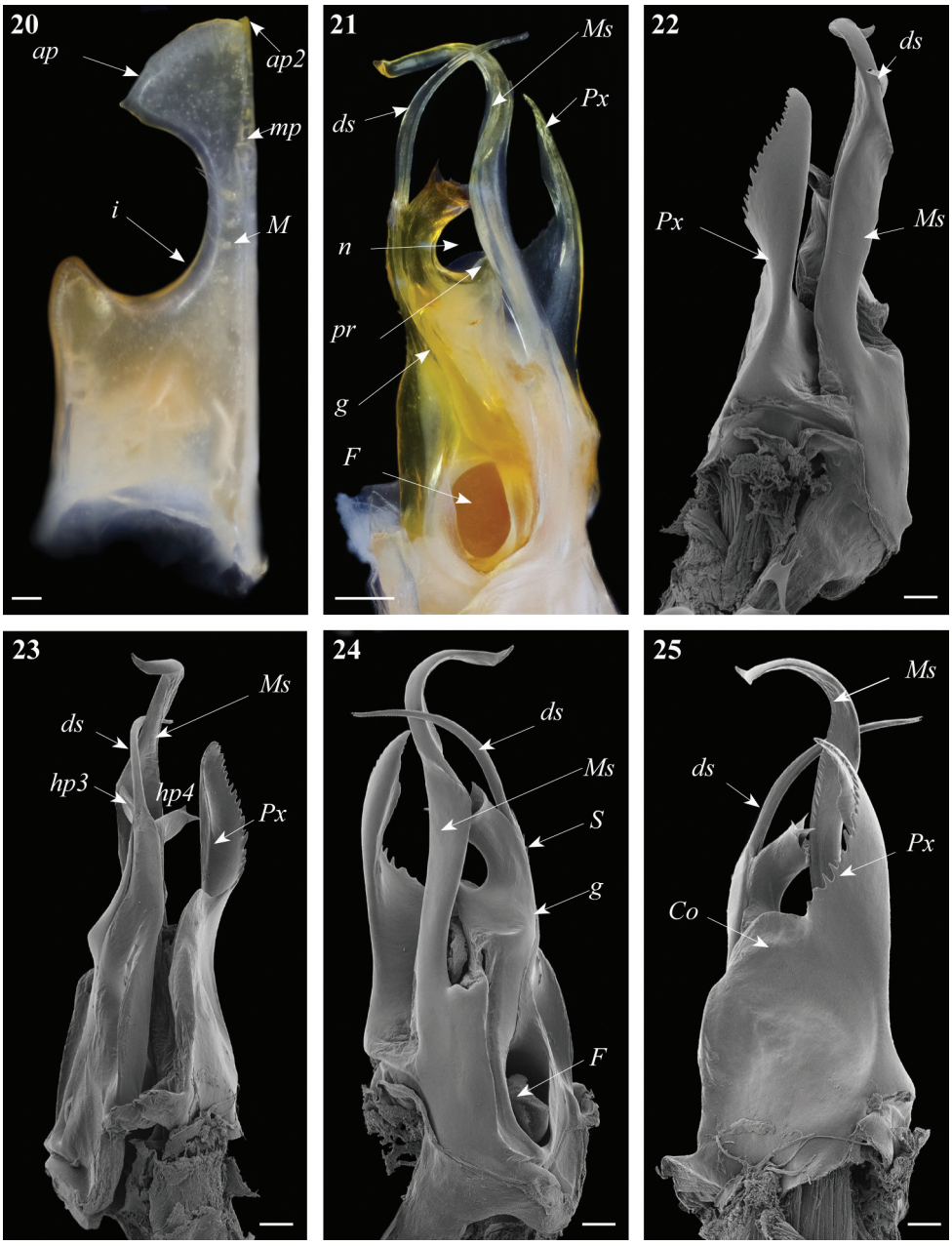

Figures 20–25. *Ommatoiulus khroumiriensis* sp. n. paratypes, gonopod structures. **20** Right promerite, posterior view **21** Right posterior gonopod, mesal view **22** Right posterior gonopod, lateral view **23** Right posterior gonopod, meso-posterior view **24** Right posterior gonopod, anterior-mesal view **25** Right posterior gonopod, anterior view. Abbreviations: **ap** distal process of the promerite, **ap2** lobed process, **Co** coxite, **ds** distal process of the solenomerite, **F** fovea, **g** seminal groove, **hp3, hp4** distal processes of the solenomerite, **i** lateral incision of the promerite, **mp** blunt mesal process, **M** mesal ridge, **Ms** mesomerite, **n** notch of the solenomerite, **pr** triangular subapical process of the solenomerite, **Px** paracoxite, **S** solenomerite. Scale bar: 0.1 mm.

Figure 26. *Ommatoiulus khroumiriensis* sp. n. paratype, left posterior gonopod. Interactive SEM image. [Morphbank # 831016–831034]

***Ommatoiulus xenos* Akkari & Enghoff, sp. n.**
http://zoobank.org/09D98AF5-9AD3-41E0-8B54-624E31B72480
http://species-id.net/wiki/Ommatoiulus_xenos
Figs 27–30

Material. Holotype: ♂, Tunisia ("Tunis"), 1861, J.P. Coindé leg. (MNHN). **Paratypes**: 5 ♀♀, Tunisia ("Tunis"), 1861, J.P. Coindé leg. (MNHN).

Diagnosis. Resembling *O. chambiensis* and *O. xerophilus* spp. n. in size and general shape of gonopods, but distinguished by the shape of promerite, a much more slender mesomerite and shorter and stouter paracoxite.

Etymology. The species name is a Greek noun meaning 'stranger', emphasising the fact that this species, found surprisingly in the collection of the MNHN shortly before completion of the manuscript, had remained unknown and out of the sight of a number of myriapodologists for more than 150 years.

Description. Male: L: 20.5 mm, H: 1.85 mm, 47 PR+2 AR+T; females: L: 18.5–21 mm, H: 2.26–2.46 mm, 42–48 PR+2–3 AR+T. General colour faded, generally grey-greenish (very likely an artefact from the decomposition of the inserted label), somewhat lighter laterally. Head pale in the occipital and labral areas; antennae and legs darker. Prozonites with darker triangular spots laterally, latter situated along the ozopores line and forming two longitudinal dark bands, dorsally separated by a pale one; dorsum crossed

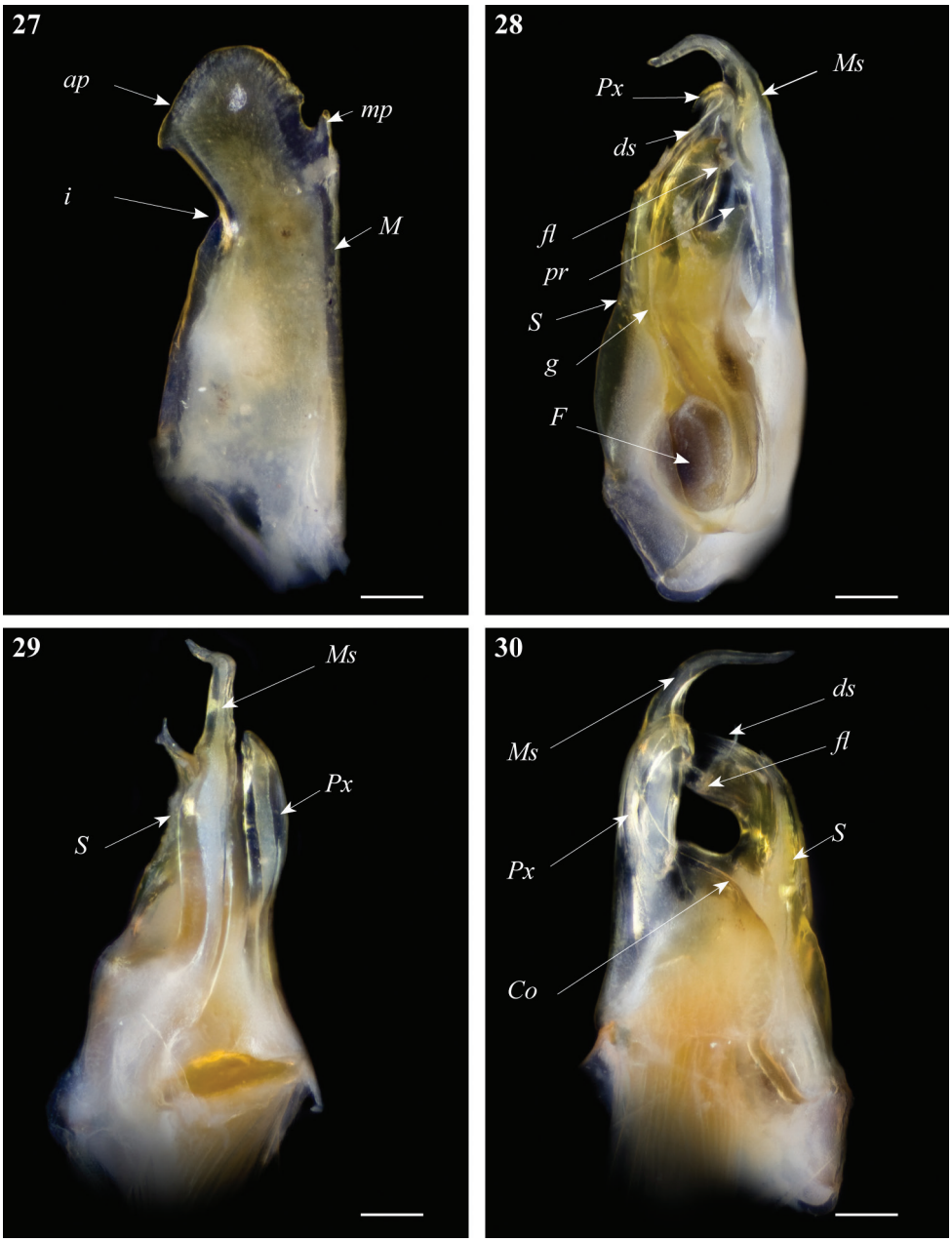

Figures 27–30. *Ommatoiulus xenos* sp. n. holotype, gonopod structures. **27** Right promerite, posterior view **28** Right posterior gonopod, mesal view **29** Right posterior gonopod, antero-lateral view **30** Right posterior gonopod, posterior view. Abbreviations: **Co** coxite, **ds** distal process of the solenomerite, **F** fovea, **fl** folded lamella, **g** seminal groove, **i** lateral incision of the promerite, **M** mesal ridge, **mp** distal process, **Ms** mesomerite, **pr** blunt process of the solenomerite, **Px** paracoxite, **S** solenomerite. Scale bar: 0.1 mm.

by dark triangular spots and showing a thin black mid-dorsal line; metazonites mostly pale and glossy. Telson: anal valves and preanal ring dark, subanal scale pale.

Prozonites with fine striae; metazonites with regular striae, denser on the sides, suture complete, curving at the level of ozopores; ozopores small, rounded, situated on metazonites situated at about their diameter from the suture. Anal valves setose; preanal ring with 3-4 setae on each lateral side, protruding in a short caudal projection with 1-4/5 setae and a small hyaline process on the tip. Subanal scale blunt to rounded and setose.

Male sexual characters. Mandibular stipites expanded in rounded posterior-ventral lobes, first pair of legs hook-shaped, remaining legs with postfemoral and tibial pads.

Gonopods. Promerite (Fig. 27) gradually narrowed distally, lateral margin with a shallow incision (**i**); apical process of promerite with a rounded margin pointing laterad; mesal ridge (**M**) narrow, distally protruding in a pointed apex (**mp**) separated from the apical process by a small apical incision; remnant of telopodite not very conspicuous.

Posterior gonopod (Figs 28–30): Mesomerite (**Ms**) uniformly broad proximally, strongly narrowed in its distal third and bent posteriad (Figs 28, 29); solenomerite (**S**) broad, with scattered setae on posterior margin, narrowing at mid-length, and bearing a large blunt process (**pr**); solenomerite apically with a broad folded lamella (**Fl**) and a small wrinkled lamella laying on the top of a slender and slightly protruding process (**ds)** housing the distal part of the seminal groove (**g**); seminal groove running from the fovea (**F**) and opening at the apex of process **ds** (Fig. 28). Paracoxite (**Px**) stout, distally curved mesad and narrowed into a slender apex pointing basad emerging from a broad and rounded coxite (**Co**) (Fig. 30).

Distribution. Exact locality unknown. The label mentions 'Tunis' which presumably refers to Tunisia in general.

Habitat. Unknown.

Remarks. The collector of this species, J.P. Coindé, who was a 'zoologist-traveler', made a collecting trip to Tunisia in 1861 during which he visited several localities throughout the country. Although we are certain that *O. xenos* sp. n., found by chance in an obscure jar among several unidentified myriapods from North Africa, labelled 'Brolemann unidentified', was collected in Tunisia, we couldn't determine with certainty the locality where this species was collected 152 years ago.

Ommatoiulus xerophilus Akkari & Enghoff, sp. n.

http://zoobank.org/6C3A27BC-A781-4EF3-B2BD-2275C59126FF
http://species-id.net/wiki/Ommatoiulus_xerophilus
Figs 31–35

Material. Holotype: ♂, W Tunisia, Kasserine Governorate, Châambi National Park, surroundings of the park´s guest house, 35°10.139'N, 8°40.486'E, alt. 950–1000m, scarce trees, *Pinus halepensis*, *Thuja*, under stones, logs and in leaf litter, 8.3.2008, P. Stoev & N. Akkari leg. (ZMUC). **Paratypes**: 1 ♂, 2 ♀♀, W Tunisia, Kasserine Governorate, Châambi National Park, surroundings of the park's guest house, 35°10.139'N, 8°40.486'E, alt. 950m, scarce trees, *Pinus halepensis*, under stones, 7.3. 2008, N. Akkari & P. Stoev leg. (ZMUC); 2 ♂♂, 12 ♀♀, 8 subadult ♀♀, 8 juveniles, W Tunisia, El Kasserine Governorate, Châambi

National Park, surroundings of the park's guest house, 35°10. 139'N, 8°40.486'E, alt. 950–100m, scarce trees, *Pinus halepensis*, *Thuja*, under stones, logs and in leaf litter, 8.3.2008, P. Stoev & N. Akkari leg. (ZMUC); 1 ♂, 2 ♀♀, same data (NMNHS).

Diagnosis. Resembling *O. chambiensis* in the structure of mesomerite, paracoxite, but well distinguished from the latter by the characteristic globular apex of promerite and the shape of solenomerite devoid of a rounded notch.

Etymology. The species name is a Greek adjective referring to the affinity of the species for dry habitats.

Description. Males: L: 15.7–15.9 mm, H: 1.54–1.65 mm, 44–46 PR+1–2 AR+T; females: L: 10.2–23.1 mm, H: 1.44–2.56 mm, 39–46 PR+1–4 AR+T. General colour black to brownish, light brown on the sides; dorsum pale yellow, crossed by thick black mid-dorsal spots. Head dark to blackish with yellow spots in the occipital area, frontal part uniformly black showing yellow spots at antennal level, labral zone yellowish, brighter at margin; antennae brownish. Prozonites blackish with light brown-yellowish spots becoming dominant laterally, just below the ozopore line; dorsally pale, with big, irregularly shaped black spots; metazonites predominantly grey-whitish and glossy, legs yellowish. Telson: anal valves dark brown-blackish, with dense yellow sputter, preanal ring blackish sputtered with yellow, dorsal side and caudal projection mostly pale, subanal scale yellowish.

Prozonites with fine striae; metazonites with regular striae, becoming denser laterally, suture complete, curving at the level of ozopores; latter small, rounded, situated on metazonites situated at about their diameter from the suture. Anal valves setose, with 6-7 setae on the surface and numerous submarginal and marginal setae; subanal scale rounded and setose; preanal ring with 1+1 setae on the sides, protruding in a caudal projection with 3+3 setae and a small hyaline process on the tip.

Male sexual characters. Mandibular stipites expanded in rounded posterior-ventral lobes, first pair of legs hook-shaped, remaining legs with postfemoral and tibial pads.

Gonopods. Promerite (**P**) (Figs 31, 32) bent anteriad, not very broad, with parallel margins, mesal ridge (**M**) broad, distally narrowing and truncate, bearing several serrations (**se**) and separated from the apical lobe (**ap**); by an incision; lateral margin mostly rectilinear, only slightly narrowing subapically at the level of the mesal incision; apical lobe globular, with rounded margin, curved laterad; posterior surface with a number of strong setae aligned distally; telopodite remnant inconspicuous.

Posterior gonopod (Figs 31, 33–35): Mesomerite (**Ms**) similar to *O. chambiensis* but broader, strongly truncated and distally bent mesad (Figs 33–35); solenomerite (**S**) broad, with scattered setae on posterior margin, strongly narrowing at mid-length, apical part with a wrinkled blunt lamella (**wl**) covering a slender and protruding process (**ds)** housing the distal part of the seminal groove (**g**) (Figs 31, 33, 35); the latter running from the fovea (**F**) (Figs 31, 33–35) up to process **ds**. Paracoxite (**Px**) broad, curved mesad, emerging from a depressed coxite (**Co**), distal third slightly enlarged, apically narrowing into a pointed apex, directed mesad (Figs 33–35).

Distribution. Arid bioclimatic zone, central Tunisia; hitherto known only from the type locality, Châambi Mountain.

Habitat. Open areas with scattered *Pinus halepensis* trees.

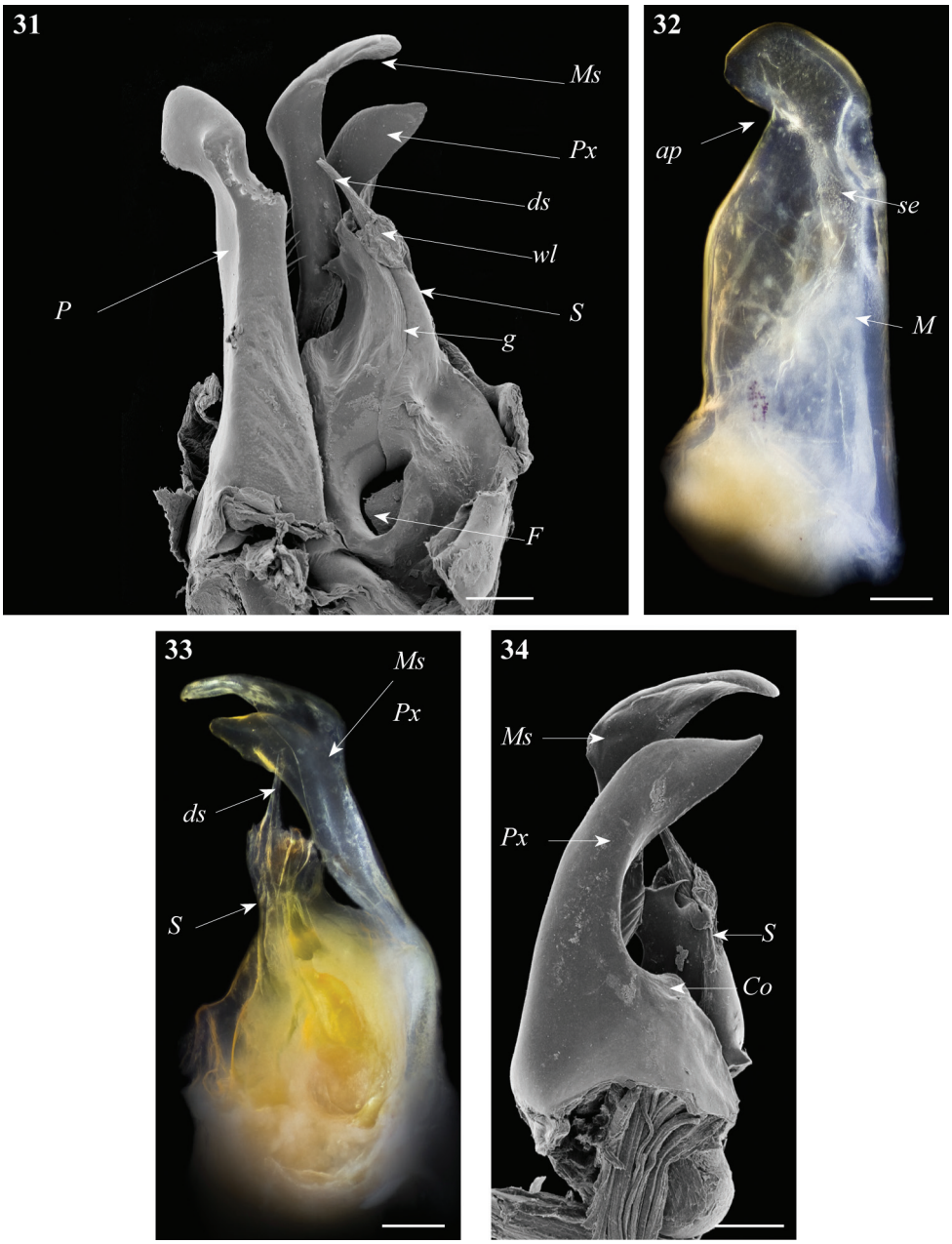

Figures 31–34. *Ommatoiulus xerophilus* sp. n. paratype, gonopod structures. **31** Left gonopod, mesal view **32** Right promerite, posterior view **33** Right posterior gonopod, mesal view **34** Right posterior gonopod, latero-posterior view. Abbreviations: **ap** distal process of the promerite, **Co** coxite, **ds** distal process of the solenomerite, **F** fovea, **g** seminal groove, **M** mesal ridge, **Ms** mesomerite, **P** promerite, **Px** paracoxite, **S** solenomerite, **se** serrations, **wl** wrinkled lamella. Scale bar: 0.1 mm.

Figure 35. *Ommatoiulus xerophilus* sp. n. paratype, right posterior gonopod. Interactive SEM image. [Morphbank # 831246–831263]

***Ommatoiulus zaghouani* Akkari & Enghoff, sp. n.**
http://zoobank.org/F23E46BA-1E8C-4B6D-BF46-73D9A37E8E42
http://species-id.net/wiki/Ommatoiulus_zaghouani
Figs 36–39

Material. Holotype: ♂, NE Tunisia, Zaghouan Governorate, Jebel Zaghouan, 36°23'N, 10°06E, alt. 365m, *Pinus* forest, 13.3.2009, N. Akkari & H. Enghoff leg. (ZMUC).

Diagnosis. Gonopods resembling those of *O. seurati* but distinguished by a broader distal part of the promerite, a subapical lateral projection on the mesomerite and a much shorter solenomerite.

Etymology. Named after Jebel Zaghouan, the type locality.

Description. Male: L: 28.5 mm, H: 2.56 mm, 49 PR+1 AR+T. General colour alternate dark and light golden brown; dorsum with a thin black axial line. Head dark to blackish, with brownish spots on the frontal part and on the mandibular stipites, labral zone and mouth parts pale, marginally bright yellow; antennae brownish. Prozonites dark to blackish, covered with yellowish spots; metazonites pale brown to whitish laterally and golden brown dorsally, legs yellowish. Telson: anal valves black, preanal ring blackish, caudal projection yellowish, subanal scale yellowish.

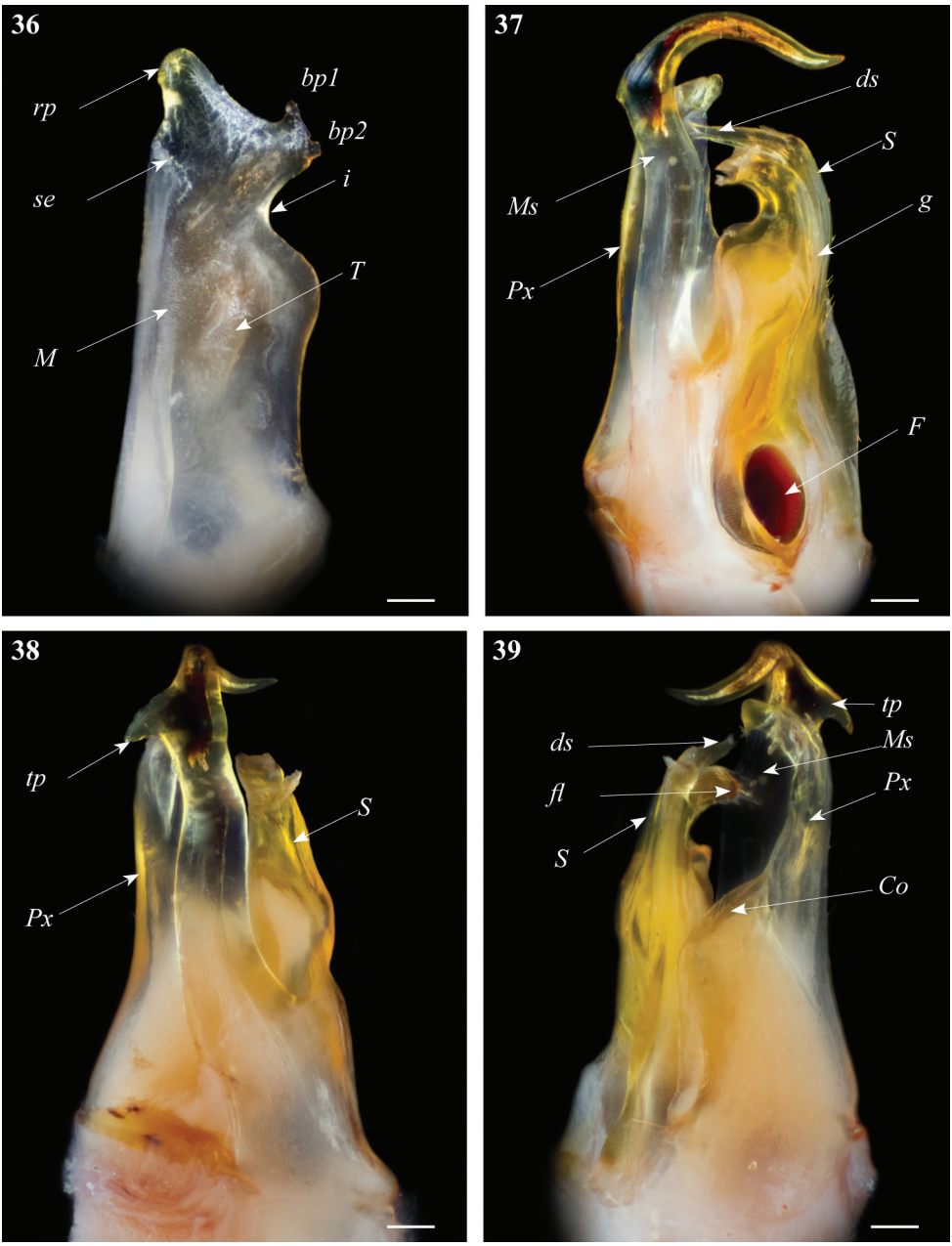

Figures 36–39. *Ommatoiulus zaghouani* sp. n. holotype, gonopod structures. **36** Left promerite, posterior view **37** Left posterior gonopod, mesal view **38** Left posterior gonopods, anterior view **39** Left posterior gonopods, postero-lateral view. Abbreviations: **bp1, bp2**: small bumps on the apical lateral process, **Co** coxite, **ds** distal process of the solenomerite, **F** fovea, **fl** folded lamella, **g** seminal groove, **M** mesal ridge, **Ms** mesomerite, **i** lateral incision on the promerite, **Px** paracoxite, **rp** apical mesal process of the promerite, **S** solenomerite, **se** serrated process, **tp**: triangular distal process. Scale bar: 0.1 mm.

Prozonites with fine irregular striae; metazonites with regular striae, becoming dense laterally, suture complete, curving at the level of ozopores; ozopores small, rounded, situated in metazonites, situated at about their diameter from the suture. Anal valves setose, with 4-6 setae on the surface, ca 14 submarginal and numerous marginal setae; subanal scale rounded and setose; preanal ring with 2+2 setae on the sides, protruding in a caudal projection with (6-7)+(6-7) setae on the tip and bearing a small hyaline process.

Male sexual characters. Mandibular stipites expanded in rounded posterior-ventral lobes, first pair of legs hook-shaped, remaining legs with postfemoral and tibial pads.

Gonopods. Promerite (Fig. 36) proximally subrectangular, strongly narrowed distally by a deep incision (**i**) on the lateral margin; mesal ridge (**M**) broad, distally protruding in a serrated edge (**se**); apical part with a mesal triangular blunt process (**rp**) protruding mesodistad, and a lateral protruding process with two small apical bumps (**bp1**, **bp2**); posterior surface of promerite showing few scattered setae near the mesal margin; remnant of telopodite (**T**) large and ovoid, located at mid-length of the process.

Posterior gonopod (Figs 37–39): Mesomerite (**Ms**) large, and uniformly broad (Figs 37, 38) with a distal triangular pointed extension on the lateral margin (**tp**), distal third strongly curved mesoposteriad and narrowed in a long and slender apical process (Figs 37, 38,39); solenomerite (**S**) broad, with scattered setae on posterior margin; anteriorly simply rounded devoid of processes; apically with a hyaline folded lamella (**fl**) and a slightly protruding process (**ds)** housing the distal part of the seminal groove (**g**); the latter running from the fovea (**F**) (Fig. 37) up to process **ds**. Paracoxite (**Px**) stout and curved apically slightly narrowing into a rounded apex directed mesad, coxite broad (**Co**) (Fig. 39).

Distribution. Semi-arid bioclimatic zone in northeastern Tunisia; known only from Zaghouan Mountain.

Habitat. Forest dominated by *Pinus halepensis*.

Updates to the list of *Ommatoiulus* species in North Africa

Akkari et al. (2009) summarized all records of julidan millipedes, including *Ommatoiulus* species, from Tunisia and provided a complete list of the North African members of the order. A number of additions and corrections to the lists are presented here:

- We refute the presence of *O. diplurus appendiculatus* (Brolemann, 1925) in Algeria. This taxon is based on females and juveniles only, and Akkari and Enghoff (2012) already regarded the presence of *O. diplurus* (Attems, 1903) in North Africa uncertain.
- The record of *O. aumalensis* (Brolemann, 1925) from Tunisia by Akkari et al. (2009) was due to a misidentification and actually refers to *O. fuscounilineatus* (Lucas, 1846).
- *Ommatoiulus sempervirilis* Akkari & Enghoff, 2011 was described from the Tunisian islands Galita and Zembretta (Akkari and Enghoff 2011).

- *Ommatoiulua chambiensis*, *O. crassinigripes*, *O. kefi*, *O. khroumiriensis*, *O. xerophilus*, *O. xenos* and *O. zaghouani* spp. n., are described from northern and central Tunisia in the present paper bringing the overall number of *Ommatoiulus* species in Tunisia to 12, and to 28 in North Africa.
- We refute the presence of *O. lapidarius* (Lucas, 1846) in Libya. This record was based on the synonymy of *Julus rimosus* Karsch, 1881 (see Manfredi 1939, Schubart 1952) with *O. lapidarius*, but re-examination of the holotype of *J. rimosus* (Museum für Naturkunde, Berlin) has shown that this is a valid species (Akkari 2013).

Discussion

Three of the new Tunisian *Ommatoiulus* species were found in Châambi Mountain, which is the highest mountain range in Tunisia. The mountain is located only a few kilometres from the Algerian border and in spite of its arid character is known to harbour a number of endemic species (cf. Kovařík 2006, Hartenberger 1986), which is here confirmed by the finding of *O. chambiensis*, *O. xerophilus* and *O. crassinigripes* spp. n. in semi-arid open habitats of the mountain. With regard to morphology, *O. chambiensis* and *O. xerophilus* show great resemblance in the gonopod structure as they both have apical serrations connecting the mesal ridge of the promerite with the apical processes of the promerite, which is reminiscent of similar structures found in the *O. fuscounilineatus* species group (see Akkari and Enghoff 2012, figs 94–96). The posterior gonopods of both species are outstanding in having a large, distally curved mesomerite and paracoxite, and a relatively short and simply structured solenomerite. However, clear differences between them were observed in the apex of the promerite: globular and with a blunt margin in *O. xerophilus*, and subtriangular in *O. chambiensis*; the paracoxite is apically more rounded in *O. chambiensis*, while the solenomerite has a notch and a distal pointed process in the latter species. With regard to somatic traits, *O. chambiensis* and *O. xerophilus* display differences in colour patterns and body size. *O. xerophilus* has clear pale dorsal longitudinal stripes which are lacking in *O. chambiensis*. Analysis of the variation of the maximum vertical diameter in relation to the number of podous rings for the different developmental stadia demonstrated that *O. chambiensis* is generally larger (more podous rings, higher body diameter) than *O. xerophilus* (Fig. 40). Of special importance is the fact that the size difference is apparent within each developmental stadium. Thus, *O. chambiensis* males with 8RO have more podous rings and larger diameter than *O. xerophilus* males with 8RO. The same is true for specimens with 9RO although the studied material is much smaller.

O. crassinigripes is the only schizophylline millipede collected at more than 1500 m elevation in Tunisia. However, it occurs also at lower elevation in central Tunisia (El Kef, Thala, Makthar, Kairouan) and is very unlikely to be an alticolous species like *Ommatoiulus gravieri* (Brolemann, 1924), which is known from 3000–3200 m altitude in Jebel Tachdirt of the High Atlas in Morrocco (Brolemann 1924, Akkari et

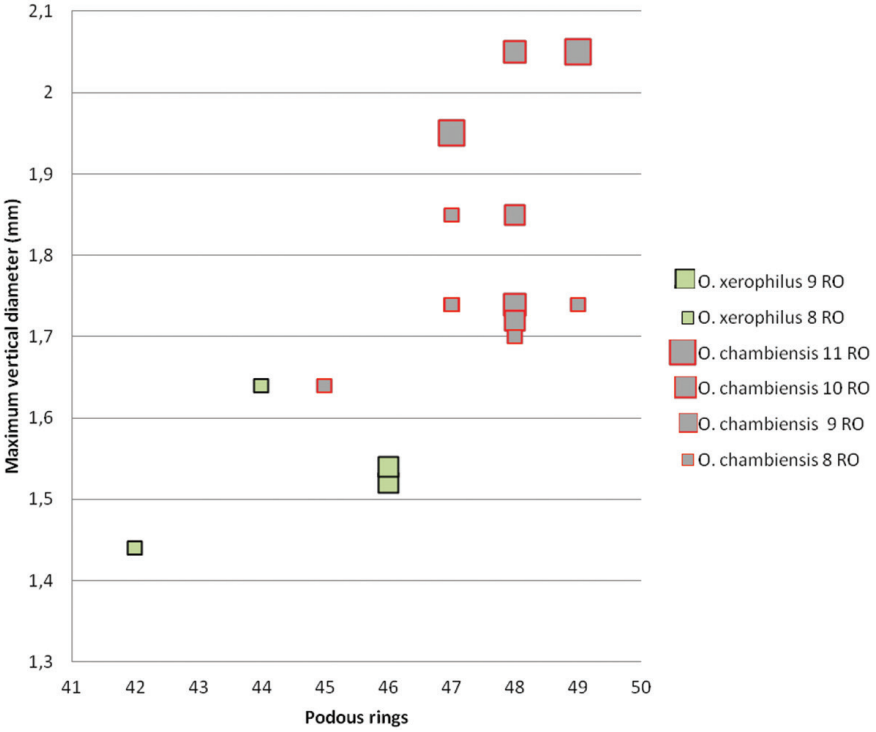

Figure 40. *O. chambiensis* and *O. xerophilus* spp. n. Scatter diagram illustrating size of adult males expressed as maximum vertical body diameter (mm) vs number of podous rings in different developmental stadia (8–11RO).

al. 2009). *O. crassinigripes* is one of the largest *Ommatoiulus* species in Tunisia and, together with *O. khroumiriensis*, is the closest to *O. punicus* with regard to gonopod shape (Fig. 41). The three species, which were all treated under *O. punicus* by Akkari et al. (2009), have quite similar gonopod conformations, yet display a number of constant differences in both promerite and posterior gonopods (Table 1). Although resembling, differences in posterior gonopods can be clearly noticeable on the rotatable models (Figs 13, 26, 41), which, in addition to the external morphological features, indicate their separate taxonomic status. The external morphological differences concern colour pattern and size. Fig. 42 illustrates the variation of the maximum vertical diameter in relation to the number of podous rings. It clearly demonstrates that males of *O. crassinigripes* have more podous rings and are generally thicker compared to males of *O. punicus* and *O. khroumiriensis* of the same development stadium (with the same number of RO). The same applies when one compares males of stadia 9 and 10 RO of *O. punicus* and *O. khroumiriensis* where the latter is clearly thicker. The three species are allopatric in Tunisia and exhibit different habitat preferences. *O. khroumiriensis* is confined to the cork-oak forests of the Khroumirie in the northwest (mainly the Aïn Draham area), *O. crassinigripes* occurs in open, semi-arid habitats of the centre, in the plain of Kairouan and mountains of the Ridge, while *O. punicus*

Table 1. Comparison of main gonopod and peripheral structures of *O. punicus*, *O. crassinigripes* and *O. khroumiriensis*.

	O. punicus **(Figs 41, 51–53)**	***O. crassinigripes*** **(Figs 7–13)**	***O. khroumiriensis*** **(Figs 20–26)**
Gonopod structures	**Similarities**		
Promerite	abruptly narrowing in the distal half-third		
	deep lateral incision		
	mesal ridge protruding in a distal process		
Mesomerite	broad, distally narrowing and hook-shaped		
Solenomerite	broad, narrowing at mid-length		
	subapical triangular process		
	apical folded lamella		
	long and curved seminal groove		
Paracoxite	lamellar, folded, marginally serrated		
	Differences		
Promerite	lateral margin well rounded	lateral margin angular	lateral margin reduced and pointed
	distal process broad and triangular	distal process laterally rounded and bulgy	distal process slender, slightly expanded laterally
Mesomerite	distally slightly broaden and bearing serrations on the lateral margin	distally broaden latero-mesad and bearing strong serrations on both margins	distally strongly constricted and narrowed
Solenomerite			
Paracoxite	broad, apical margin rounded	broader, apical margin truncate	slender, apically tapering
Non gonopod structures (males)			
Body vertical diameter (mm)	1.7–2.7	2.7–3.6	2–2.8
Podous rings	43–48	45–53	43–48
Apodous rings	1–2	1–2	1–2
Colour	ash-grey alternating with light brown, legs purple	pale grey alternating with golden brown, legs black	dark grey alternating with yellowish brown, legs yellowish brown

is mainly distributed around Tunis City, Cap Bon Peninsula and the eastern part of the Ridge *viz*. Zaghouan Mt. in the north (see Akkari et al. 2009). *O. punicus* was recorded from Aïn Draham, Tabarka and Nefza, as well as from Kairouan Plain by Akkari et al. (2009). These authors pointed out the variation observed in the material: "*Ommatoiulus punicus* as currently delimited is quite a variable taxon, and a detailed analysis may well necessitate splitting it into several (sub)species." Our renewed study has corroborated this assumption. Attems (1903, 1926) must have been looking at *O. crassinigripes* and *O. khroumiriensis* while recording and illustrating *Ommatoiulus punicus*. In fact the gonopod drawings he provided left no doubt that what he recorded from Aïn Draham (Attems 1926, figs 240–241) is *O. khroumiriensis*. On the other hand, the record of *O. punicus* from unspecified locality in Tunisia (Attems 1903: 144, figs 77–81) is here referred to as *O. crassinigripes*.

Figure 41. *Ommatoiulus punicus*, specimen from Jebel Rsas, NE Tunisia, right posterior gonopod. Interactive SEM image. [Morphbank # 831228–831245]

Intercalary males are here recorded for the species *Ommatoiulus khroumiriensis* and *O. crassinigripes*. This is of little surprise considering that postembryonic development involving periodomorphosis (regression of secondary sexual characters followed by a return to a morphologically copulatory stadium following an additional moult) is considered as particularly prevalent for schizophylline species (Enghoff et al. 1993). Characteristic morphology of intercalary stadia was directly observed on reared specimens of three schizophyllines: *O. moreleti* (Lucas, 1860), *O. sabulosus* (Linnaeus, 1758) and *Tachypodoiulus niger* (Leach, 1814) while field-collected samples provided periodomorphic specimens belonging to no less than 8 species of genus *Ommatoiulus*, including *O. punicus* (see Akkari and Enghoff 2011 for species list). The same authors discussed the particular case of the species *O. sempervirilis* for which a large hand-collected sample revealed the complete absence of intercalary stadia and presence instead of four successive stadia of adult males implying a direct copulatory-copulatory succession (Akkari and Enghoff 2011).

Colour pattern and somatic characters cannot be used reliably to distinguish the Tunisian *Ommatoiulus* species, although we have provided information about these features above in order to point out fine differences between morphologically close or syntopic taxa. In the identification key (below) we prefer to include only gonopod characters.

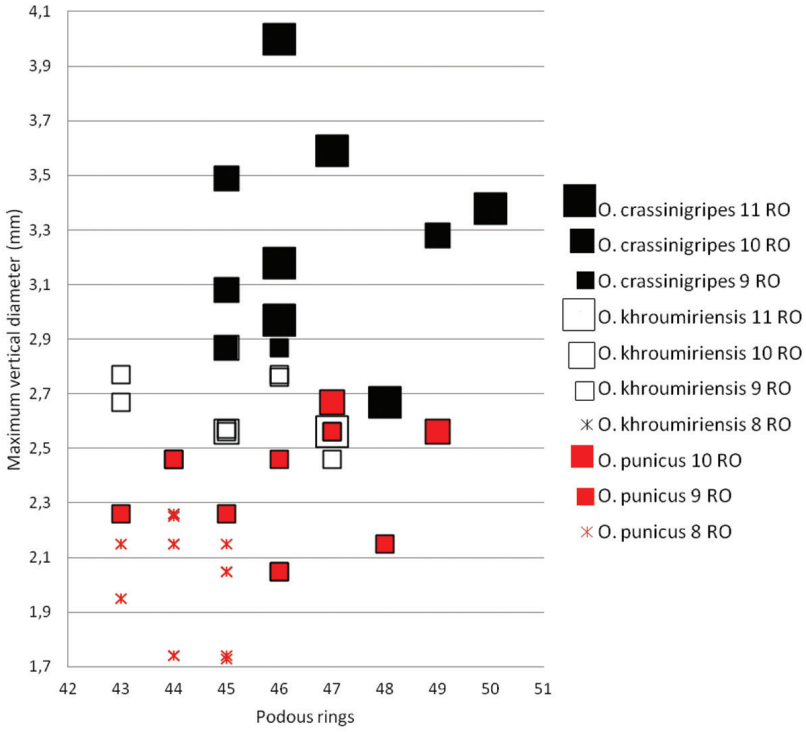

Figure 42. *O. crassinigripes* sp. n., *O. khroumiriensis* sp. n. and *O. punicus*. Scatter diagram illustrating size of adult males expressed as maximum vertical body diameter (mm) vs number of podous rings in different developmental stadia (8–11RO).

Identification key to Tunisian *Ommatoiulus* species

The key is based on characters of the male gonopods.

1 Promerite with parallel margins, apically regularly rounded, without lateral incision (Fig. 43); mesomerite distally expanded into a subrectangular apical plate, concave and mesally incised (Fig. 44) ..... ***O. sempervirilis***

– Promerite with at least one lateral or apical incision (Figs 2, 7, 14, 20, 32, 45, 47, 49, 51); mesomerite different..... **2**

2 Mesomerite (**Ms**) apically expanded and bifurcated (Figs 16, 46) **3**

– Mesomerite (**Ms**) apically narrowed and simple (Figs 3, 9, 24, 33, 48, 50, 53) **4**

3 Mesomerite (**Ms**) hammer-shaped (Fig. 46), bifurcated into long asymmetrical processes; promerite (Fig. 45) broad, with a complex distal process, apically bearing two blunt bumps, a pointed process and a lateral serrated lamella .... ***O. malleatus***

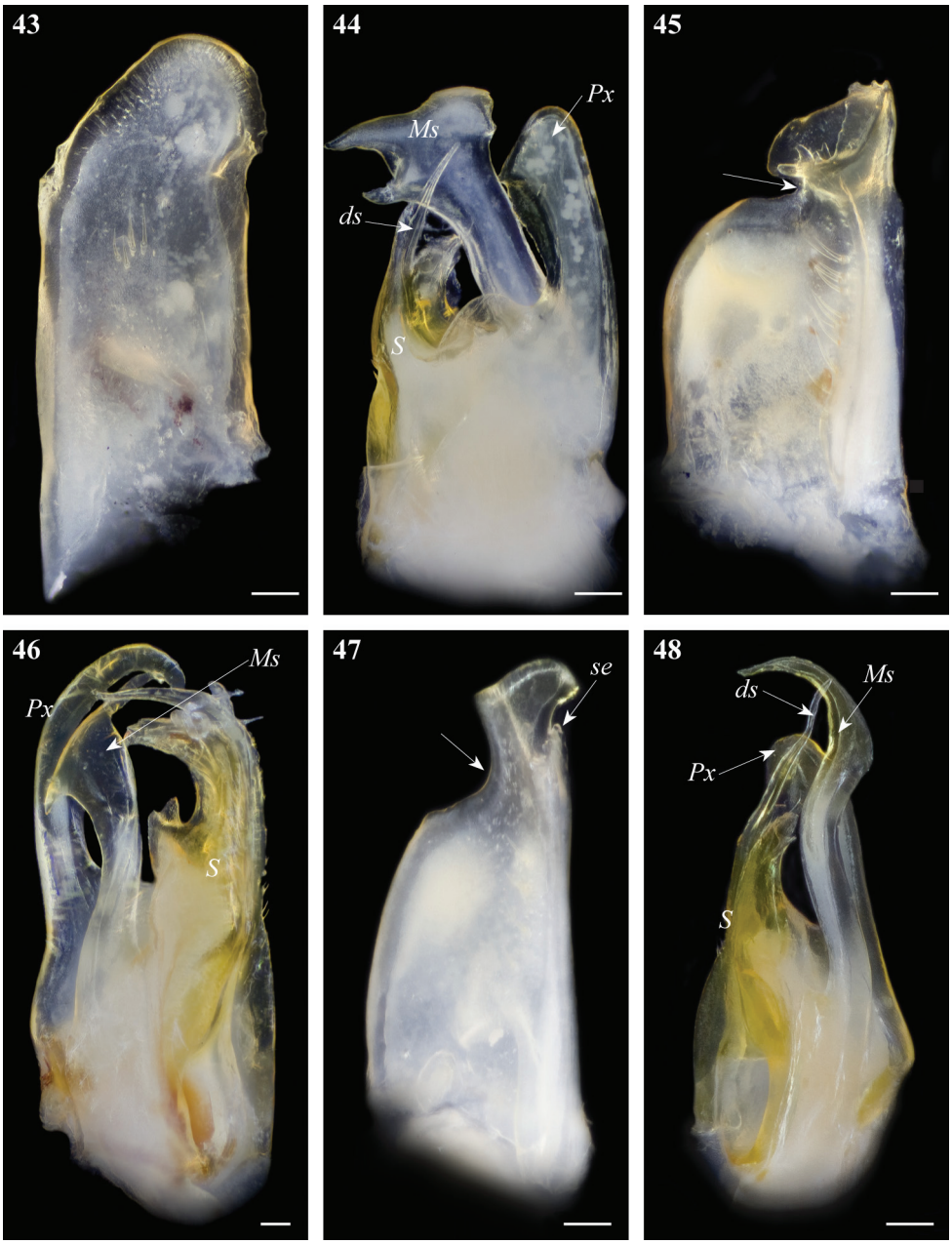

Figures 43–48. Gonopod structures of *Ommatoiulus sempervirilis*, *O. malleatus*, *O. seurati* **43** *O. sempervirilis* left promerite, posterior view **44** *O. sempervirilis*, left posterior gonopod, meso-posterior view **45** *O. malleatus*, right promerite, anterior view **46** *O. malleatus*, left posterior, mesal view **47** *O. seurati* right promerite, posterior view **48** *O. seurati*, right posterior gonopod, antero-mesal view. Abbreviations: **ds** distal process of the solenomerite, **Ms** mesomerite, **Px** paracoxite, **S** solenomerite, **se** serrations. Arrow pointing to the lateral incision of the promerite. Scale bar 0.1 mm.

– Mesomerite (**Ms**) horn-shaped (Fig. 16), bifurcated into short and curved processes; promerite (Fig. 14) apically with three lobes separated by deep incisions..... ***O. kefi* sp. n.**

4 Promerite gradually narrowing distally, lateral incision shallow to moderately deep; mesal ridge sometimes protruding in a serrated subapical process (**se**) (Figs 2, 32, 47); paracoxite (**Px**) without conspicuous marginal serrations (Figs 5, 34, 48, 50) **5**

– Promerite strongly narrowing distally, lateral incision deep; mesal ridge protruding in a blunt subapical process (Figs 7, 20, 51); paracoxite (**Px**) broad, lamellar, folded, with strong marginal serrations (Figs 8, 22, 52) **10**

5 Mesomerite (**Ms**) slender, sinuous and strongly curved distally; solenomerite (**S**) with a long distal process (**ds**) lodging the seminal groove (Fig. 48)..... ***O. seurati***

– Mesomerite (**Ms**) broad, distally narrowing; solenomerite (**S**) with a shorter distal process lodging the seminal groove (Figs 3, 33, 50) **6**

6 Mesomerite (**Ms**) with irregular margins, apically strongly narrowed and hook-shaped; solenomerite (**S**) with a short distal process (**ds**) (Figs 37, 50) **7**

– Mesomerite (**Ms**) with a regular mesal margin, distally gradually narrowed into a bent folded process; solenomerite (**S**) with a longer distal process (**ds**) (Figs 3, 33) **8**

7 Mesomerite with a subapical serrated lateral process, a truncated mesal margin, apically strongly narrowed into a small hook-shaped process (Fig. 50); promerite with a shallow lateral incision and a rounded distal process (Fig. 49)..... ***O. fuscounilineatus***

– Mesomerite with a subapical lateral process (Figs 37, 39), apically gradually narrowed in a long curved process (Fig. 39); promerite with a deeper lateral incision and a broad distal process with apical and lateral lobes (Fig. 36)..... ..... ***O. zaghouani* sp. n.**

8 Promerite straight, bearing a pointed distal process (Fig. 27); paracoxite stout and shorter (Fig. 30) ..... ***O. xenos* sp. n.**

– Promerite strongly bent anteriad, bearing a subapical serrated process (Figs 1, 31); paracoxite broad and elongate (Figs 5, 34)..... **9**

9 Solenomerite (**S**) with a rounded notch (**n**), a pointed process (**pr**) and apically a wrinkled protruding lamella (Fig. 5); promerite with a subtriangular apex (Fig. 2)..... ***O. chambiensis* sp. n.**

– Solenomerite (**S**) without such a process; wrinkled lamella not protruding (Fig. 33); promerite with a globular apex (Fig. 32) ..... ***O. xerophilus* sp. n.**

10 Lateral incision of promerite extending basad, distal process broad and triangular (Fig. 20); mesomerite (**Ms**) distally strongly narrowed, without subapical serrations on lateral margin, paracoxite (**Px**) slender (Fig. 22)..... ***O. khroumiriensis* sp. n.**

– Lateral incision of promerite not extending basad, distal process slenderer and more rounded (Figs 7, 51); mesomerite (**Ms**) with lateral subapical serrations, paracoxite (**Px**) broader (Figs 12, 53) **11**

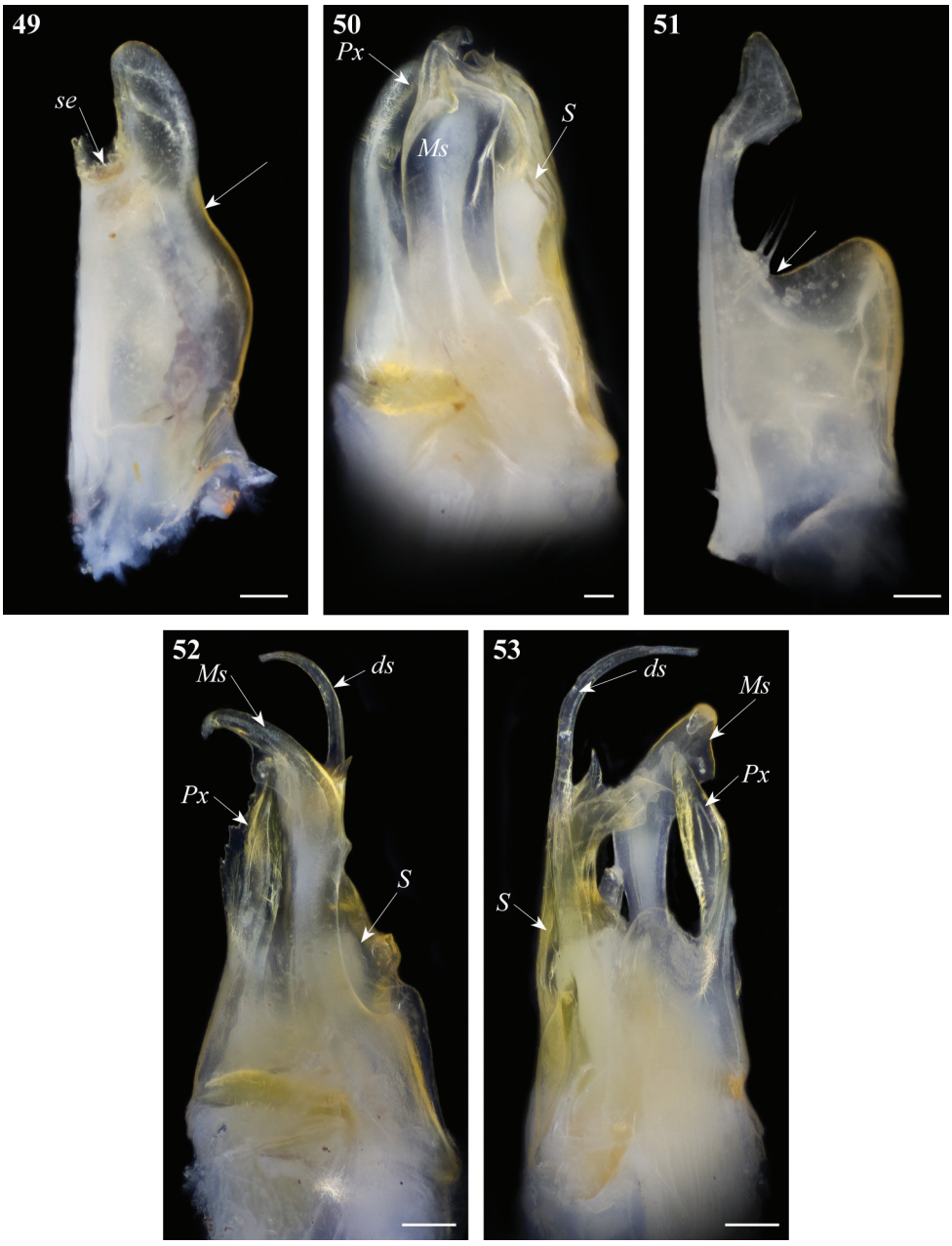

Figures 49–53. Gonopod structures of *O. fuscounilineatus*, *O. punicus*. **49** *O. fuscounilineatus*, left promerite, posterior view **50** *O. fuscounilineatus*, left posterior gonopod, anterior view **51** *O. punicus*, left promerite, posterior view **52** *O. punicus*, left posterior gonopod, lateral view **53** *O. punicus*, left posterior gonopod, posterior view. Abbreviations: **ds** distal process of the solenomerite, **Ms** mesomerite, **Px** paracoxite, **S** solenomerite, **se** serrations. Arrow pointing to the lateral incision of the promerite. Scale bar 0.1 mm.

11 Apical process of promerite (**ap**) bulgy, with a lobed process (**ap1**) on tip (Fig. 7); mesomerite (**Ms**) with strong subapical mesal serrations (Fig. 8); paracoxite (**Px**) broadened distally with truncated apex (Fig. 12) ..... ***O. crassinigripes***

– Apical process of promerite slender, without a lobed process; mesomerite (**Ms**) without mesal serrations (Fig. 52); paracoxite (**Px**) distally narrowed, with rounded apex (Fig. 53) ..... ***O. punicus***

Interactive key to Tunisian *Ommatoiulus* species

We provide an interactive key in Flash (SWF) format to the *Ommatoiulus* species known from Tunisia. The key is dichotomous and based on gonopod characters. These are illustrated with line drawings, light microscopy photographs and SEMs, and for some of the species with rotatable SEM animations. A species list and species pages are included in the key to provide additional information on species diagnostic characters, distribution and habitats. An introductory section for the first-time user provides background information of importance for applying the key.

Adobe Flash Player (version 11.2 or higher) or a browser (e.g. Internet Explorer, Firefox and Chrome) with Flash Player plug-in is required to run the key.

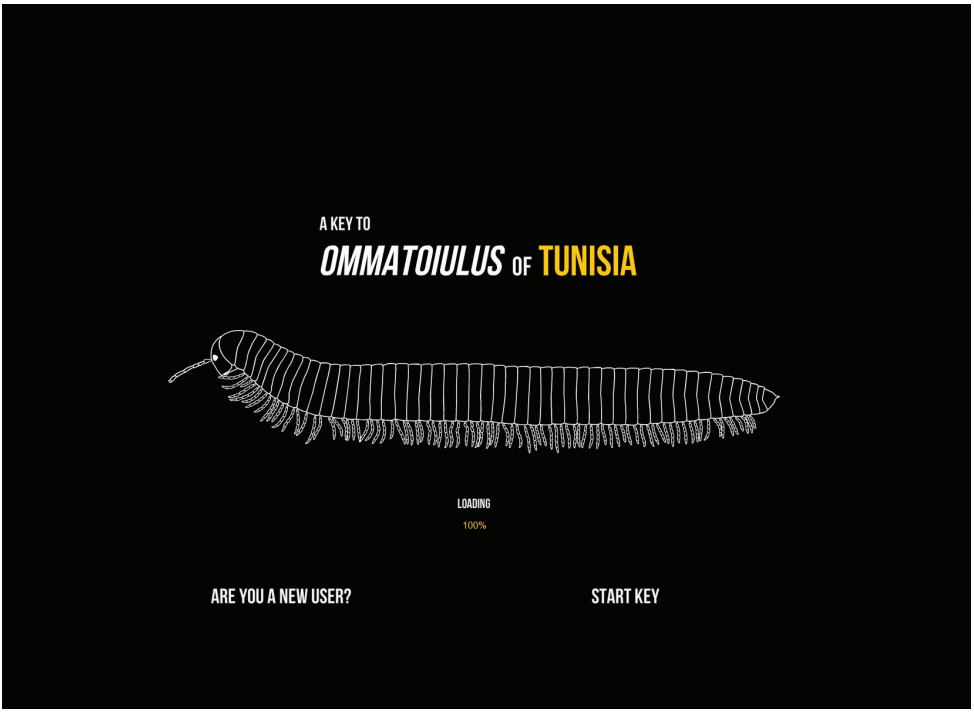

Acknowledgements

This work was financed by a Carlsberg Foundation grant to N.A. and H.E. We are most grateful to Thomas Pape (ZMUC) for his overall support and comments on the manuscript. Nikolaj Scharff (ZMUC) provided advices about the SEM mounting technique and access to the photographing equipment. Jason Dunlop (Museum für Naturkunde, Berlin), Jean-Jacques Geoffroy (MNHN) and Rosana Pisoni (MSNB) kindly arranged loans under their care. The fieldwork in Tunisia in March 2008 was financed by the Field Museum Collection Fund. N.A. and P.S. are grateful to Petra Sierwald (Chicago, USA) for the logistic help. Specimens were collected in national parks and reserves with a permit from "La direction générale des forêts, ministère d'Agriculture" of Tunisia. NA and PS are thankful to Ridha Ouni and Malek Akkari for their assistance during the filed work. N.A.'s short visit to MNHN, March 2013, was financed by the EC FP7 Project SYNTHESYS. Many thanks are also due to Bob Mesibov (Queen Victoria Museum and Art Gallery, Tasmania) and two anonymous reviewers for their useful comments on the manuscript. The publication of this article was made possible with financial support from the EC FP7 project ViBRANT (www.vbrant.eu) to P.S.

References

Akkari N (2013) On the identity of *Julus rimosus* Karsh, 1881 (Diplopoda, Julida, Julidae), the only schizophylline known from Libya (North Africa) and notes on Libyan millipedes. Zootaxa 3652(3): 392–396. doi: 10.11646/zootaxa.3652.3.7

Akkari N, Enghoff H (2011) Copulatory-copulatory male succession and male slenderness in *Ommatoiulus sempervirilis* sp. n., a new insular millipede from Tunisia (Diplopoda: Julida: Julidae). Journal of Zoological Systematics and Evolutionary Research 49(4): 285–291. doi: 10.1111/j.1439-0469.2011.00625.x

Akkari N, Enghoff H (2012) Review of the genus *Ommatoiulus* in Andalusia, Spain (Diplopoda: Julida) with description of ten new species and notes on a remarkable gonopod structure, the fovea. Zootaxa 3538: 1–53.

Akkari N, Stoev P, Enghoff H, Nouira S (2009) The millipede order Julida (Myriapoda: Diplopoda) in Tunisia, with an overview of the North African species. Soil Organisms 81 (3): 453–488.

Akkari N, Voigtländer K (2007) *Ommatoiulus malleatus* sp. n., a new Tunisian millipede, with notes on the *punicus* species group of *Ommatoiulus* (Diplopoda, Julidae). Zootaxa 1400: 59–68.

Attems C (1903) Beiträge zur Myriopodenkunde. Zoologische Jahrbücher, Abtheilung für Systematik, Ökologie und Geographie der Thiere 18 (1): 63–154.

Attems C (1926) Myriopoda. In: Kükenthal W, Krumbach T (Eds) Handbuch der Zoologie. Eine Naturgeschichte der Stämme des Tierreiches. 4(1). Progoneata, Chilopoda, Insecta I. Walter de Gruyter and Co., Berlin and Leipzig, 402 pp.

Attems C (1952) Myriopoden der Forschungsreise Dr. H. Franz in Spanien 1951 nebst Übersicht über die gesamte iberische Myriopodenfauna. EOS, Revista Espanola de Entomologia 28(4): 323–366.

Błażejowski B, Binkowski M, Bitner MA, Gieszcz P (2011) X-ray Microtomography (XMT) of Fossil Brachiopod Shell Interiors for Taxonomy. Acta Palaeontologica Polonica 56 (2): 439–440. doi: 10.4202/app.2010.0114

Bond JE, Sierwald P (2002) Cryptic speciation in the *Anadenobolus excises* millipede species complex on the island of Jamaica. Evolution 56(6): 1123–1135.

Brolemann HW (1921) Liste des Myriapodes signalés dans le nord de l'Afrique. Bulletin de la Société des Sciences Naturelles du Maroc 1(3–6): 99–110.

Brolemann HW (1924) Myriapodes du Grand Atlas Marocain. Bulletin de la Société des Sciences Naturelles du Maroc, 4(8): 184–197.

Brolemann, HW (1925a) Deux formes nouvelles de Diplopodes tunisiens. Bulletin de la Société d'Histoire Naturelle de l'Afrique du Nord 16: 61–66.

Brolemann HW (1925b) Races nouvelles de *Schizophyllum* algériens (Myriapodes-Diplopodes). Bulletin de la Société d'Histoire Naturelle de l'Afrique du Nord 16: 245–253.

Cheung DK-B, Brunke AJ, Akkari N, Souza CM, Pape T (2013) Rotational Scanning Electron Micrographs (rSEM): A novel and accessible tool to visualize and communicate complex morphology. ZooKeys 328: 47–57. doi: 10.3897/zookeys.328.5768

Costello MJ, May RM, Stork NE (2013) Can we name Earth's species before they go extinct? Science 339: 413–416. doi: 10.1126/science.1230318

Deans A, Yoder M, Balhoff J (2012) Time to change how we describe biodiversity. Trends in Ecology & Evolution 27(2): 78–84 doi: 10.1016/j.tree.2011.11.007

Enghoff H (1987) Revision of *Nepalmatoiulus* Mauriès 1983 - a Southeast Asiatic genus of millipedes (Diplopoda: Julida: Julidae). Courier Forschungsinstitut Senckenberg 93: 241–331.

Enghoff H (1992) *Dolichoiulus* - a mostly Macaronesian multitude of millipedes. With the description of a related new genus from Tenerife, Canary Islands (Diplopoda, Julida, Julidae). Entomologica Scandinavia 40: 1–158.

Enghoff H, Dohle W, Blower JG (1993) Anamorphosis in millipedes (Diplopoda) – the present state of knowledge with some developmental and phylogenetic considerations. Zoological Journal of the Linnean Society 109: 103–234. doi: 10.1111/j.1096-3642.1993.tb00305.x

Enghoff H, Seberg O (2006) A taxonomy of taxonomy and taxonomists. The Systematist, Newsletter of the Systematics Association 27: 13–15. http://www.systass.org/newsletter/TheSystematist27.pdf

Enghoff H, Petersen G, Seberg O (2011) Phylogenetic relationships in the millipede family Julidae. Cladistics 27: 606–616. doi: 10.1111/j.1096-0031.2011.00360.x

Erwin T, Penev L, Stoev P, Georgiev T (2012) Accelerating innovative publishing in taxonomy and systematics: 250 issues of ZooKeys. ZooKeys 251: 1–10. doi: 10.3897/zookeys.251.4516

Faulwetter S, Aikaterini V, Michail K, Thanos D, Arvanitidis C (2013) Micro-computed tomography: Introducing new dimensions to taxonomy. ZooKeys 263: 1–45. doi: 10.3897/zookeys.263.4261

Fontaine B, Perrard A, Bouchet P (2012) 21 years of life shelf between discovery and description of new species. Current Biology 22(22): 943–944. doi: 10.1016/j.cub.2012.10.029

Frederiksen S, Petersen G, Enghoff H (2012) How many species are there of Pachyiulus? A contribution to the taxonomy of Europe's largest millipedes (Diplopoda: Julida: Julidae). Journal of Natural History 46(9–10): 599–611. doi: 10.1080/00222933.2011.651636

Görög Á, Szinger B, Tóth E, Viszkok J (2012) Methodology of the micro-computer tomography on foraminifera. Palaeontologia Electronica 15(1/3): 1–15. palaeo-electronica.org/content/issue-1-2012-technical-articles/121-methodology-of-ct-on-forams

Hartenberger J-L (1986) Hypothèse paléontologique sur l'origine des Macroscelidea (Mammalia). Comptes Rendus de l'Académie des Sciences, Paris, 302: 247–249.

Hauser H (2000) Heterodactyly in the genus *Craspedosoma* (Diplopoda, Chordeumatida): an observation error. 11th international Congress of Myriapdology, 20–24 July 1999, Bialowieza, Poland. Fragmenta faunistica 43: 131–138.

Heim I, Nickel M (2010) Description and molecular phylogeny of *Tethya leysae* sp. nov. (Porifera, Demospongiae, Hadromerida) from the Canadian Northeast Pacific with remarks on the use of microtomography in sponge taxonomy. Zootaxa 2422: 1–21.

Highton R (2009) Two and a half centuries of Diplopod taxonomy (1758–2008): Retrospect and prospect. In: Roble SM, Mitchell JC (Eds) A Lifetime of Contributions to Myriapodology and the Natural History Museum of Virginia: A Festschrift in Honor of Richard L. Hoffman's 80th Birthday. Virginia Museum of Natural History, Special publication 16, Martensville, VA, 101–108.

Kovařík F (2006) Review of Tunisian species of the genus *Buthus* with descriptions of two new species and a discussion of Ehrenberg's types (Scorpiones: Buthidae). Euscorpius 34: 1–16.

La Salle J, Wheeler Q, Jackway P, Winterton S, Hobern D, Lovell D (2009) Accelerating taxonomic discovery through automated character extraction. Zootaxa 2217: 43–55.

Manfredi P (1939) Miriapodi della Libia. Bollettino dei Musei di Zoologia ed Anatomia Comparata della R. Università di Torino 47: 109–120.

Pimvichai P, Enghoff H, Panha S (2011a) A revision of the *Thyropygus allevatus* group. Part 3: the *T. induratus* subgroup (Diplopoda: Spirostreptida: Harpagophoridae). Zootaxa 2941: 47–68.

Pimvichai P, Enghoff H, Panha S (2011b) A revision of the *Thyropygus allevatus* group. Part 4: the *T. cuisinieri* subgroup (Diplopoda: Spirostreptida: Harpagophoridae). Zootaxa 2980: 37–48.

Schubart O (1952) Diplopoden aus Marokko, gesammelt vom Institut Scientifique Chérifien. Bulletin de la Société des sciences naturelles du Maroc 32(1): 199–225.

Schubart O (1960) Ein weiterer Beitrag zur Diplopoden-Fauna Marokkos. Bulletin de la Société des Sciences Naturelles et Physiques du Maroc 40(3): 159–232.

Schubart O (1963a) Progoneata, Opisthogoneata. In: Brohmer, Eirmann, Ulmer (Eds) Die Tierwelt Mitteleuropas, Bd. II, Leipzig, 51pp.

Schubart O (1963b) Ueber einige Diplopoden aus Algier. Bulletin de la Société des Sciences Naturelles et Physiques du Maroc 43 (1–2): 79–94.

Stoev P, Enghoff H (2011) A review of the millipede genus *Sinocallipus* Zhang, 1993 (Diplopoda, Callipodida, Sinocallipodidae), with notes on gonopods monotony vs. peripheral diversity in millipedes. ZooKeys 90: 13–34. doi: 10.3897/zookeys.90.1291

Verhoeff KW (1915) Polymorphismus bei Chilognathen und seine Abhängigkeit von äußeren Einflüssen. Zoologischer Anzeiger 45: 378–382, 385–390.

Verhoeff KW (1916) Beiträge zur Kenntnis der Gattungen *Macheiriophoron* und *Craspedosoma*. Zoologischer Jahresarbeit 39: 273–416.

Verhoeff KW (1917) Zur Kenntnis der zoogeographie Deutschlands zugleich über Diplopoden, namentlich Mitteldeutschlands und für die biologische Beurteilung der Eiszeiten. Nova Acta Leopoldina, Halle 103: 1–156.

Verhoeff KW (1939) Über Craspedosomen aus Baden und die Variationen des *Craspedosoma germanicum* Verh. Entstehung des Polymorphismus. Zoologischer Anzeiger 128: 257–270.

Appendix 1

Source image library of the interactive SEM image of *Ommatoiulus chambiensis* (doi: 10.3897/zookeys.328.5763.app1) File format: WinZip Image Archive (jpg).

Citation: Akkari N, Cheung DK-B, Enghoff H, Stoev P (2013) Revolving SEM images visualising 3D taxonomic characters: application to six species of the millipede genus *Ommatoiulus* Latzel, 1884, with description of seven new species and an interactive key to the Tunisian members of the genus (Diplopoda, Julida, Julidae). ZooKeys 328: 5–45. doi: 10.3897/zookeys.328.5763 Source image library of the interactive SEM image of Ommatoiulus *chambiensis*. *doi: 10.3897*/zookeys.328.5763.app1

Appendix 2

Source image library of the interactive SEM image of *Ommatoiulus crassinigripes* (doi: 10.3897/zookeys.328.5763.app2) File format: WinZip Image Archive (jpg).

Citation: Akkari N, Cheung DK-B, Enghoff H, Stoev P (2013) Revolving SEM images visualising 3D taxonomic characters: application to six species of the millipede genus *Ommatoiulus* Latzel, 1884, with description of seven new species and an interactive key to the Tunisian members of the genus (Diplopoda, Julida, Julidae). ZooKeys 328: 5–45. doi: 10.3897/zookeys.328.5763 Source image library of the interactive SEM image of Ommatoiulus c*rassinigripes. doi: 10.3897*/zookeys.328.5763.app2

Appendix 3

Source image library of the interactive SEM image of *Ommatoiulus kefi* (doi: 10.3897/zookeys.328.5763.app3) File format: WinZip Image Archive (jpg).

Citation: Akkari N, Cheung DK-B, Enghoff H, Stoev P (2013) Revolving SEM images visualising 3D taxonomic characters: application to six species of the millipede genus *Ommatoiulus* Latzel, 1884, with description of seven new species and an interactive key to the Tunisian members of the genus (Diplopoda, Julida, Julidae). ZooKeys 328: 5–45. doi: 10.3897/zookeys.328.5763 Source image library of the interactive SEM image of Ommatoiulus *kefi. doi: 10.3897*/zookeys.328.5763.app3

Appendix 4

Source image library of the interactive SEM image of *Ommatoiulus khroumiriensis* (doi: 10.3897/zookeys.328.5763.app4) File format: WinZip Image Archive (jpg).

Citation: Akkari N, Cheung DK-B, Enghoff H, Stoev P (2013) Revolving SEM images visualising 3D taxonomic characters: application to six species of the millipede genus *Ommatoiulus* Latzel, 1884, with description of seven new species and an interactive key to the Tunisian members of the genus (Diplopoda, Julida, Julidae). ZooKeys 328: 5–45. doi: 10.3897/zookeys.328.5763 Source image library of the interactive SEM image of Ommatoiulus *khroumiriensis. doi: 10.3897*/zookeys.328.5763.app4

Appendix 5

Source image library of the interactive SEM image of *Ommatoiulus xerophilus* (doi: 10.3897/zookeys.328.5763.app5) File format: WinZip Image Archive (jpg).

Citation: Akkari N, Cheung DK-B, Enghoff H, Stoev P (2013) Revolving SEM images visualising 3D taxonomic characters: application to six species of the millipede genus *Ommatoiulus* Latzel, 1884, with description of seven new species and an interactive key to the Tunisian members of the genus (Diplopoda, Julida, Julidae). ZooKeys 328: 5–45. doi: 10.3897/zookeys.328.5763 Source image library of the interactive SEM image of Ommatoiulus *xerophilus. doi: 10.3897*/zookeys.328.5763.app5

Appendix 6

Source image library of the interactive SEM image of O*mmatoiulus punicus* (doi: 10.3897/zookeys.328.5763.app6) File format: WinZip Image Archive (jpg).

Citation: Akkari N, Cheung DK-B, Enghoff H, Stoev P (2013) Revolving SEM images visualising 3D taxonomic characters: application to six species of the millipede genus *Ommatoiulus* Latzel, 1884, with description of seven new species and an interactive key to the Tunisian members of the genus (Diplopoda, Julida, Julidae). ZooKeys 328: 5–45. doi: 10.3897/zookeys.328.5763 Source image library of the interactive SEM image of Ommatoiulus *punicus. doi: 10.3897*/zookeys.328.5763.app6

Appendix 7

Source file library of the interractive key to genus *Ommatoiulus* in Tunisia (doi: 10.3897/zookeys.328.5763.app7) File format: WinZip Archive (zip).

Citation: Akkari N, Cheung DK-B, Enghoff H, Stoev P (2013) Revolving SEM images visualising 3D taxonomic characters: application to six species of the millipede genus *Ommatoiulus* Latzel, 1884, with description of seven new species and an interactive key to the Tunisian members of the genus (Diplopoda, Julida, Julidae). ZooKeys 328: 5–45. doi: 10.3897/zookeys.328.5763 Source file library of the interractive key to genus Ommatoiulus *in Tunisia.* doi: 10.3897/zookeys.328.5763.app7

ZooKeys 328: 47–57 (2013)
doi: 10.3897/zookeys.328.5768
www.zookeys.org

RESEARCH ARTICLE

A peer-reviewed open-access journal
ZooKeys
Launched to accelerate biodiversity research

Rotational Scanning Electron Micrographs (rSEM): A novel and accessible tool to visualize and communicate complex morphology

David K-B Cheung[1], Adam J. Brunke[1], Nesrine Akkari[1], Carina Mara Souza[2], Thomas Pape[1]

1 *Natural History Museum of Denmark, Zoological Museum, Universitetsparken 15, Copenhagen, Denmark, 2100*
2 *Department of Animal Biology, Institute of Biology, State University of Campinas (UNICAMP), Barão Geraldo, Campinas, São Paulo, Brazil, P.O.B. 6109, 13083-970*

Corresponding author: *David K-B Cheung* (David.Cheung@snm.ku.dk)

Academic editor: *Pavel Stoev* | Received 11 July 2013 | Accepted 5 August 2013 | Published 3 September 2013

Citation: Cheung DK-B, Brunke AJ, Akkari N, Souza CM, Pape T (2013) Rotational Scanning Electron Micrographs (rSEM): A novel and accessible tool to visualize and communicate complex morphology. ZooKeys 328: 47–57. doi: 10.3897/zookeys.328.5768

Abstract

An accessible workflow is presented to create interactive, rotational scanning electron micrographs (rSEM). These information-rich animations facilitate the study and communication of complex morphological structures exemplified here by male arthropod genitalia. Methods are outlined for the publication of rSEMs on the web or in journal articles as SWF files. Image components of rSEMs were archived in MorphBank to ensure future data access. rSEM represents a promising new addition to the toolkit of a new generation of digital taxonomy.

Keywords

Scanning electron microscopy, digital taxonomy, interactive animation

Introduction

In the effort to discover, describe and organize the planet's biodiversity, taxonomists are faced with the challenge of providing clear and concise diagnostic characters in species descriptions, often involving structures with complex morphology. To address this challenge, a variety of imaging methods have emerged over the past ten years to complement more traditional line drawings, which continue to play an important role

in species descriptions. Traditionally, diagnostic characters are illustrated in one or a set of standard views to facilitate the comparison of taxa within and between publications by taxonomists and other users. In this current paradigm, characters not or suboptimally visible in these conventional views are difficult for taxonomists to convey and for users to interpret, placing a constraint on the range of published morphological data. These issues are further exacerbated in the case of complex or asymmetrical male genitalia, which are challenging to clearly and accurately describe in words. Multifocal, 'stacked' images of external structures or habitus are now standard in most taxonomic descriptions and recent advances in micro-computed tomography (μCT) and magnetic resonance imaging (MRI) promise to yield exciting new character data from both external and internal morphology (i.e., Hart et al. 2003, Beutel et al. 2008, Mietchen et al. 2008); even from non-sclerotized specimens preserved in alcohol (Faulwetter et al. 2013) or living specimens (Lowe et al. 2013). Both μCT and MRI scans can be represented as rotating (Mietchen et al. 2008), even interactive (Faulwetter et al. 2013) animations and have dramatically increased the level of morphological data available to users in one 'illustration'. Raman-atomic force microscopy has revealed morphological differences in molecular surface structure between various Diptera taxa, at the nanometer level of resolution (Andersen and Gaimari 2003).

Since the early 1970s (for an early example, see Herman 1972), scanning electron microscopy (SEM) has had an increasingly important role in several taxonomic fields, especially the study of Arthropoda, in exploring the fine surface sculpture and other morphological aspects impossible to assess with a standard stereo- or compound microscope, or poorly resolved at higher magnifications using μCT and MRI (e.g., Rota 2005; Whitmore 2009, 2011; Akkari and Enghoff 2011, 2012; Grzywacz et al. 2012; Miller et al. 2012; Shear 2012). For some millipede families (i.e., Dalodesmidae Cook, 1896, Haplodesmidae Cook, 1896) characterized by minute genitalia, descriptions of new taxa are based primarily on SEM, supplemented with line drawings (e.g., Mesibov 2008, 2009). Additionally, the level of detail and magnification provided by SEMs are now commonly harnessed to facilitate the interpretation of phylogenetic character states (e.g. Edgecombe and Hollington 2005, Chani-Posse 2013).

Recently, we have sought for an accessible method to integrate and present diagnostic differences of taxa existing at non-standard and standard angles, using SEM micrographs. Here we describe an SEM image workflow that results in information-rich, rotatable animations (hereafter referred to as rSEMs – rotational scanning electron micrographs), which can be either web published or embedded in PDF articles for publication in journals accepting such media (e.g., ZooKeys). Examples of rSEM from different arthropod groups (Coleoptera, Diptera, Myriapoda) are provided.

Specimen preparation and mounting

Larger, dry specimens were mounted (see below) without special cleaning or dehydration. Specimens preserved in 70% ethanol or glycerin were first cleaned of debris and

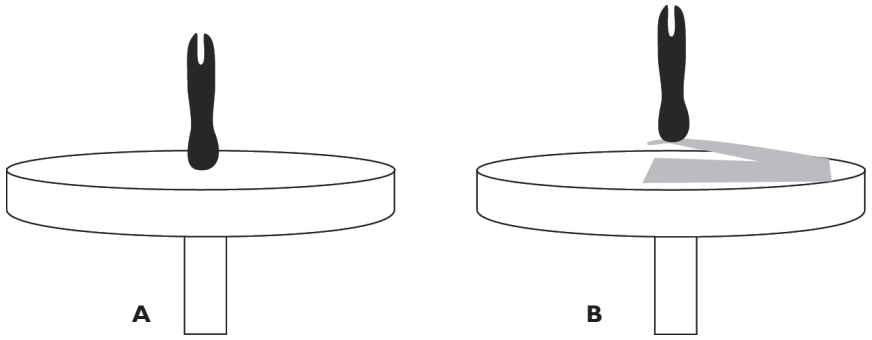

Figure 1. Specimens directly (**A**) and secondarily (**B**) mounted on an aluminum SEM stub.

then dehydrated in 96% ethanol, then acetone, and air dried before mounting. Fragile specimens (e.g. small flies, nymphs, larvae) should be dried using critical point drying to avoid shriveling or collapsing (Oster and Pollister 1966). Specimens with a broad, flattened base can be mounted directly onto the SEM stub (Fig. 1A). The majority of specimens will have a much smaller contact point with the stub and should be attached via flexible secondary mounts consisting of electrical tape or thin, aluminum wire (Fig. 1B). Specimens should be mounted as close to the center of rotation and as perpendicular to the SEM stub surface as possible (Fig. 1), to reduce image alignment difficulties and 'swaying' rSEMs. Secondary mounts allow manipulation of the specimen to the optimal position, even after coating.

Image Acquisition and processing

For users unfamiliar with the elements of this workflow, a step-by-step set of instructions is provided in Appendix I. Specimens were sputter-coated with platinum/palladium and studied with a JEOL JSM-6335F scanning electron microscope. Note that the microscope stage MUST be able to tilt to 90° in order to produce a usable animation (Fig. 2). Images were taken at fixed rotational intervals and named sequentially.

Images were then processed (adjusting the exposure, contrast, highlights, shadows, whites, blacks) and cropped to improve image quality and detail, and to ensure that all images were 'aligned', such that they form a smooth transition when browsed in sequence. Images were exported as JPG. Image processing can be accomplished using subscription based software such as Adobe® Lightroom® or Photoshop®, or open-source software such as ImageJ (http://rsbweb.nih.gov/ij/). The images can now be integrated into an animation for submission to a scientific journal or published on a website. The individual images generated for this study were archived in MorphBank under object #830913, 830920-830935, 830953-830970 and 831016-831034; they can be found together by searching for collection 'rSEM'.

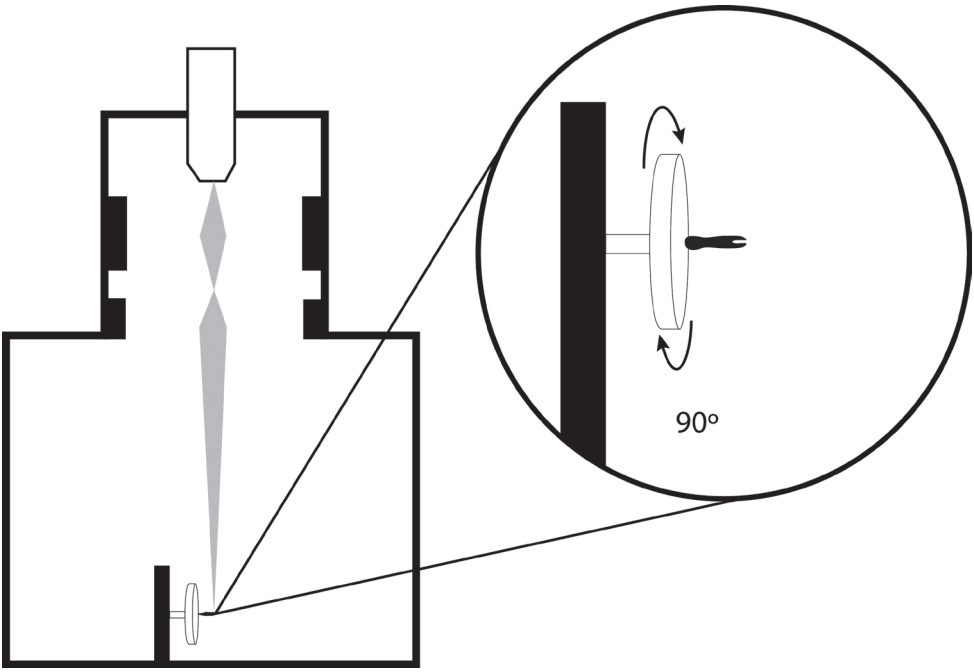

Figure 2. Schematic representation of SEM specimen and stage positioning for creation of rSEM image frames.

Creation of rSEMs for submission to a journal

rSEMs in the present article and in Akkari et al. (2013) were submitted as SWF files. These files were embedded in the PDF version of each article by the publisher and therefore instructions for this procedure are not included here. Depending on the journal, SWF files may be embedded or included as downloadable, supplementary figures (Appendix I and II). We have opted for the integrated nature of embedded files as plates rather than disjointed supplementary files. The creation of rSEMs was performed using Adobe® Flash® CS5, which were then exported as SWF files. Images were inserted as individual key frames and animated using the following Action Script in the action palette (script by 'winlwin', http://www.icodesnip.com/snippet/actionscript-3/360-degree-view):

```
import flash.events.Event;
instancename.stop();
var frameTo:Number=0;
addEventListener(Event.ENTER_FRAME,goTo);
function goTo(e:Event):void{
frameTo=int(mouseX/stage.stageWidth*instancename.totalFrames)+1;
instancename.gotoAndStop(frameTo);}
```

Figure 3. rSEM illustrating the distiphallus of *Oxysarcodexia* (*Xylocamptopsis*) *fringidea* (Curran & Walley) (Sarcophagidae, Diptera). The offline version of this rSEM can be explored by moving the mouse over the image in the x-axis and can be viewed using Adobe® Acrobat® Reader version 8 or higher, with Adobe® Flash® Player installed. Compatible with Windows and Mac OS X.6 (Snow Leopard, 2009) or newer. Image components were archived in MorphBank as objects #830953-830970.

Web publication of rSEM

To publish an rSEM on the web, a program or web plug-in is needed to integrate the images into an animation. There is a multitude of these available online of varying quality and functionality (search 'object viewer' or '360 panorama') ranging from subscription-based (Magic 360™ (http://www.magictoolbox.com/magic360/)) to free and open-source (Reel© 1.2.1 (http://jquery.vostrel.cz/reel#dict)). A set of scripts needs to be downloaded and a folder containing the sequentially numbered images should be created. We have tested the two previously mentioned options and both result in web

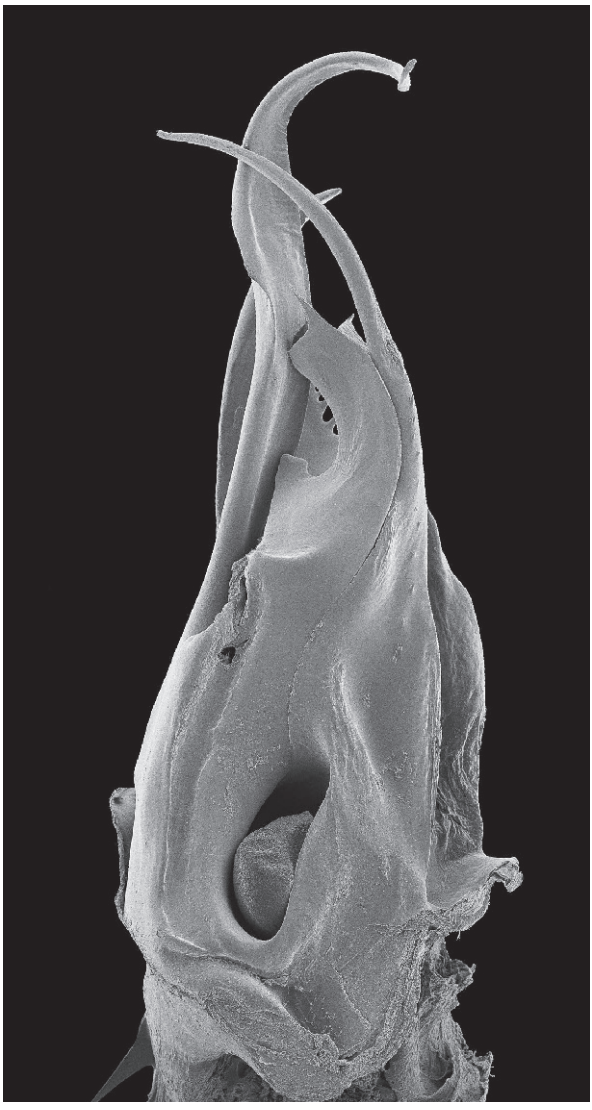

Figure 4. rSEM illustrating the posterior gonopod of *Ommatoiulus khroumiriensis* Akkari & Enghoff (Julidae, Diplopoda). The offline version of this rSEM can be explored by moving the mouse over the image in the x-axis and can be viewed using Adobe® Acrobat® Reader version 8 or higher, with Adobe® Flash® Player installed. Compatible with Windows and Mac OS X.6 (Snow Leopard, 2009) or newer. Image components were archived in MorphBank as objects #831016-831034.

animations that are compatible with all operating systems, including mobile devices. For full instructions, readers are directed to the tutorials provided by the publishers (see links above). The rSEMs included in the html version of Akkari et al. (2013) and the present paper (Figs 3–5) were created using Reel 1.2.1, and an example of Magic 360 output is given in Appendix II.

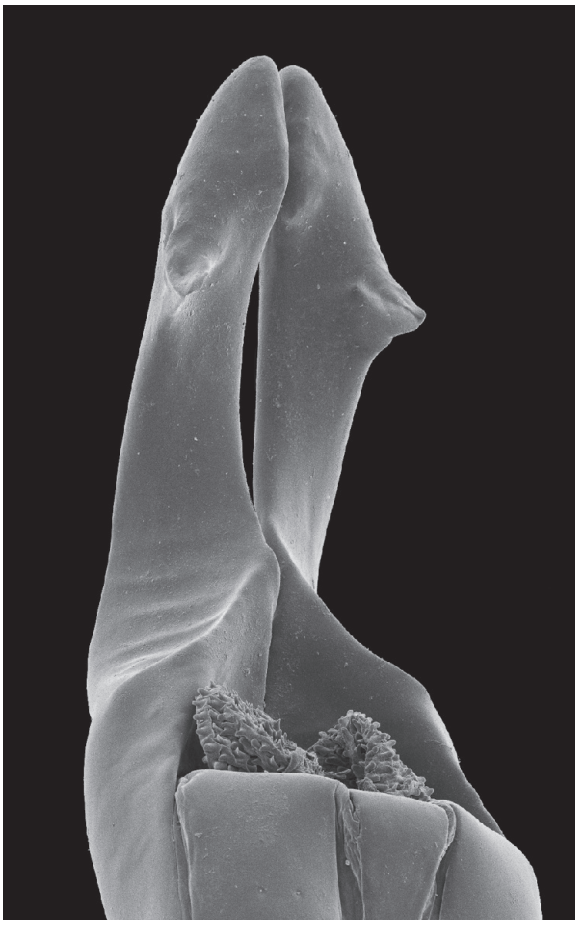

Figure 5. rSEM illustrating the median lobe (paramere removed) of *Bolitogyrus* sp. (Staphylinidae, Coleoptera). The offline version of this rSEM can be explored by moving the mouse over the image in the x-axis and can be viewed using Adobe® Acrobat® Reader version 8 or higher, with Adobe® Flash® Player installed. Compatible with Windows and Mac OS X.6 (Snow Leopard, 2009) or newer. Image components were archived in MorphBank as objects #830913, and 830920-830935.

Discussion

The workflow described herein will generate interactive, information-rich animations that facilitate both the study and communication of complex morphology in systematics (Figs 3–5). rSEMs combine sharply detailed SEM micrographs into a single, holistic representation of a structure that may even reveal diagnostic characters visible but yet unnoticed when using a light microscope. The use of SEM is not always optimal or appropriate as users may not have access to facilities or cannot image large, fragile or unique specimens. In these cases, morphological characters will still need to be illustrated by line drawings or stacked images, despite their potential complexity. Differ-

ences in color and degree of sclerotization are also lost in SEM. However, rSEMs can be created using technology and software in widespread use and provide an accessible alternative to other imaging methods such as μCT if the user is focused on structural aspects of external morphology. As HTML5 is becoming more prominent than Flash® as a media development standard, an update is planned to incorporate instructions for developing rSEM in HTML5. rSEMs are integrated into a taxonomic revision for the first time in a companion article (Akkari et al. 2013) to provide clear, accurate and user-accessible descriptions of morphological structures, which are typically difficult to interpret without taxonomic expertise.

With the development of Web 2.0 and Open Access publishing, the demand for image quality and methods for visualizing taxonomic traits has increased. Recently, publishing 3D models and embedding multimedia files in biomedical journals has become common practice (e.g. Tyzack 2008, Ziegler et al. 2011). However, the adoption of such media in taxonomy is still relatively scattered, and is mostly limited to MRI and Micro-computed Tomography (e.g. Mietchen et al. 2008, Boistel et al. 2011, Laforsch et al. 2012, Faulwetter et al. 2013). This may be due to the perception that sophisticated imaging requires special software, e-infrastructure and significant funding. The rSEM workflow provided here demonstrates this to be incorrect. The workflow does not require special equipment beyond that of a scanning electron microscope and the processing and integration of images can be accomplished using photo editing software and Adobe Flash CS5 or a plug-in such as Reel 1.2.1.

Here, additional rSEMs of arthropod genitalia were provided as examples of complex morphology. However, this approach could easily be extended to structures than other genitalia, and could be applied to the illustration of a phylogenetically important character system (e.g., a rotatable insect head capsule). So far, we have only animated rSEM in the x-axis because our test structures varied mainly along the y-axis. However, illustration of structures along both x and y-axes of rotation, while requiring many more images, may be a powerful form of data delivery in certain situations. For example, if a finely controlled, electronic stage is available, full-color, rotatable habitus images could be produced using a dissecting microscope and stacking software. There are clearly far more applications of rSEM or rSEM-like animations than we have presented here, and we encourage readers to experiment with this technique in their own scientific exploration of Earth's biodiversity.

Acknowledgements

We are grateful to Nikolaj Scharff (Copenhagen) for sharing some insights on SEM mounting techniques, Petr Vostrel for making his Reel plug-in freely available online. Daniel Mietchen, Pavel Stoev and one anonymous reviewer provided comments that greatly improved this manuscript.

References

Andersen MS, Gaimari SD (2003) Raman-atomic force microscopy of the ommatidial surfaces of Dipteran compound eyes. Journal of Structural Biology 142: 364–368. doi: 10.1016/S1047-8477(03)00026-1

Akkari N, Cheung DK-B, Enghoff H, Stoev P (2013) Revolving SEM images visualising 3D taxonomic characters: application to six species of the millipede genus Ommatoiulus Latzel, 1884, with description of seven new species and an interactive key to the Tunisian members of the genus (Diplopoda, Julida, Julidae). ZooKeys 328: 5–45. doi: 10.3897/zookeys.328.5763

Akkari N, Enghoff H (2011) On some surface structures of potential taxonomic importance in families of the suborders Polydesmidea and Dalodesmidea (Polydesmida, Diplopoda). Zookeys 156: 1–24. doi: 10.3897/zookeys.156.2134

Akkari N, Enghoff H (2012) Review of the genus *Ommatoiulus* in Andalusia, Spain (Diplopoda: Julida) with description of ten new species and notes on a remarkable gonopod structure, the fovea. Zootaxa 2528: 1–53.

Beutel R, Ge S, Hörnschemeyer T (2008) On the head morphology of *Tetraphalerus*, the phylogeny of Archostemata and the basal branching events in Coleoptera. Cladistics 24: 270–298. doi: 10.1111/j.1096-0031.2007.00186.x

Boistel R, Swoger J, Kržič U, Fernandez V, Gillet B, Reynaud EG (2011) The future of three-dimensional microscopic imaging in marine biology. Marine Ecology 32: 438–452. doi: 10.1111/j.1439-0485.2011.00442.x

Chani-Posse M (2013) Towards a natural classification of the subtribe Philonthina (Coleoptera: Staphylinidae: Staphylinini): a phylogenetic analysis of the Neotropical genera. Systematic Entomology 38: 390–406. doi: 10.1111/syen.12003

Edgecombe DG, Hollington LM (2005) Morphology and relationships of a new species of *Henicops* (Chilopoda: Lithobiomorpha) from New South Wales and Queensland, Australia. Zootaxa 961: 1–20.

Faulwetter S, Vasileiadou A, Kouratoras M, Dailianis T, Arvanitidis C (2013) Micro-computed tomography: introducing new dimensions to taxonomy. ZooKeys 263: 1–45. doi: 10.3897/zookeys.263.4261

Grzywacz A, Szpila K, Pape T (2012) Egg morphology of nine species of *Pollenia* Robineau-Desvoidy, 1830 (Diptera: Calliphoridae). Microscopy Research and Technique 75: 955–967. doi: 10.1002/jemt.22020

Hart AG, Bowtell RW, Kockenberger W, Wenseleers T, Ratnieks FLW (2003) Magnetic resonance imaging in entomology: a critical review. Journal of Insect Science 3: 1–9.

Herman LH (1972) Revision of *Bledius* and related genera. Part I. The aequatorialis, mandibularis, and semiferrugineus groups and two new genera (Coleoptera, Staphylinidae, Oxytelinae). Bulletin of the American Museum of Natural History 149: 111–254.

Laforsch C, Imhof H, Sigl R, Settles M, Heß M, Wanninger A (2012) Applications of Computational 3D–Modeling in Organismal Biology. In: Alexandru C (Ed) Modeling and Simulation in Engineering. InTech, Rijeka: 117–142. doi: 10.5772/31092

Lowe T, Garwood, RJ, Simonsen, TJ, Bradley, RS, Withers PJ (2013) Imaging inside a living chrysalis. Journal of the Royal Society Interface 10, 20130304. doi: 10.1098/rsif.2013.0304

Mesibov R (2008) The millipede genera *Gephyrodesmus* Jeekel, 1983 and *Orthorhachis* Jeekel, 1985 in southeastern Australia, a new *Lissodesmus* Chamberlin, 1920 from Victoria, and observations on male leg setae, spinnerets and metatergite sculpture (Diplopoda: Polydesmida: Dalodesmidae). Zootaxa 1790: 1–52.

Mesibov R (2009) Revision of *Agathodesmus* Silvestri, 1910 (Diplopoda, Polydesmida, Haplodesmidae). Zookeys 12: 87–110. doi: 10.3897/zookeys.12.206

Mietchen D, Aberhan M, Manz B, Hampe O, Mohr B, Neumann C, Volke F (2008) Three-dimensional magnetic resonance imaging of fossils across taxa. Biogeosciences 5: 25. doi: 10.5194/bg-5-25-2008

Miller JA, Griswold CE, Scharff N, Řezáč M, Szűts T, Marhabaie M (2012) The velvet spiders: an atlas of the Eresidae (Arachnida, Araneae). ZooKeys 195: 1–144. doi: 10.3897/zookeys.195.2342

Oster G, Pollister A (1966) Physical techniques in biological research. Academic Press, New York, 310 pp.

Rota J (2005) Larval and pupal descriptions of the Neotropical choreutid genera *Rhobonda* Walker and *Zodia* Heppner (Lepidoptera: Choreutidae). Annals of the Entomological Society of America 98: 37–47. doi: 10.1603/0013-8746(2005)098[0037:LAPDOT]2.0.CO;2

Shear W (2012) *Snoqualmia*, a new polydesmid millipede genus from the northwestern United States, with a description of two new species (Diplopoda, Polydesmida, Polydesmidae). Insecta Mundi 238: 1–13.

Tyzack JK (2008) Dragging (and zooming and rotating) publication of 3D molecular structures into the 21st century. Trends in Biochemical Sciences 33: 405–407. doi: 10.1016/j.tibs.2008.07.001

Whitmore D (2009) A review of the *Sarcophaga* (*Heteronychia*) (Diptera: Sarcophagidae) of Sardinia. Zootaxa 2318: 566–588.

Whitmore D (2011) New taxonomic and nomenclatural data on *Sarcophaga* (*Heteronychia*) (Diptera: Sarcophagidae), with description of six new species. Zootaxa 2778: 1–57.

Ziegler A, Mietchen D, Faber C, von Hausen W, Schöbel Ch, Sellerer M, Ziegler A (2011) Effectively incorporating selected multimedia content into medical publications. BMC Medicine 9: 17. doi: 10.1186/1741-7015-9-17

Appendix I

New user guide to the creation and publication of rSEM (doi: 10.3897/zookeys.328.5768.app1) File format: Microsoft Word document (doc).

Explanation note: A step-by-step style of instructions for new users, involving the software used by the authors. Note: in the future, these instructions may not correspond exactly with the interfaces of the corresponding software.

Citation: Cheung DK-B, Brunke AJ, Akkari N, Souza CM, Pape T (2013) Rotational Scanning Electron Micrographs (rSEM): A novel and accessible tool to visualize and communicate complex morphology. ZooKeys 328: 47–57. doi: 10.3897/zookeys.328.5768 New user guide to the creation and publication of rSEM. doi: 10.3897/zookeys.328.5768.app1

Appendix II

rSEM illustrating the distiphallus of *Oxysarcodexia* (*Xylocamptopsis*) *fringidea* (Curran & Walley) (Sarcophagidae, Diptera); web-published using Magic 360™ script files. Click and drag to rotate the rSEM and point click to open and close the magnification tool. (doi: 10.3897/zookeys.328.5768.app2) File format: Hypertext Markup Document, archived (zip).

Explanation note: Example of rSEM published online using Magic 360™ script.

Citation: Cheung DK-B, Brunke AJ, Akkari N, Souza CM, Pape T (2013) Rotational Scanning Electron Micrographs (rSEM): A novel and accessible tool to visualize and communicate complex morphology. ZooKeys 328: 47–57. doi: 10.3897/zookeys.328.5768 rSEM illustrating the distiphallus of O*xysarcodexia* (X*ylocamptopsis*) f*ringidea* (Curran & Walley) (Sarcophagidae, Diptera); web-published using Magic 360™ script files. doi: 10.3897/zookeys.328.5768.app2

ZooKeys 328: 59–117 (2013)
doi: 10.3897/zookeys.328.5439
www.zookeys.org

RESEARCH ARTICLE

A peer-reviewed open-access journal
ZooKeys
Launched to accelerate biodiversity research

Further revision of the genus *Megalopsalis* (Opiliones, Neopilionidae), with the description of seven new species

Christopher K. Taylor[1,†]

1 *Dept of Environment and Agriculture, Curtin University of Technology, GPO Box U1987, Perth, WA 6845, Australia*

† *http://zoobank.org/E3E5CF0B-8C80-477E-8ED6-F78242F8D06F*

Corresponding author: *Christopher K. Taylor* (Chris.Taylor@curtin.edu.au)

Academic editor: *Adriano Kury* | Received 30 April 2013 | Accepted 21 August 2013 | Published 3 September 2013

http://zoobank.org/84988008-5B6E-4FBD-8FD7-C67DB8E92F4E

Citation: Taylor CK (2013) Further revision of the genus *Megalopsalis* (Opiliones, Neopilionidae), with the description of seven new species. ZooKeys 328: 59–117. doi: 10.3897/zookeys.328.5439

Abstract

The Australian harvestmen genus *Megalopsalis* (Neopilionidae: Enantiobuninae) is recognised as a senior synonym of the genera *Spinicrus* and *Hypomegalopsalis*, and seven new species are described in *Megalopsalis*: *M. suffugiens*, *M. walpolensis*, *M. caeruleomontium*, *M. atrocidiana*, *M. coronata*, *M. puerilis* and *M. sublucens*. A morphological phylogenetic analysis of the Enantiobuninae is also conducted including the new species. Monophyly of Neopilionidae and Enantiobuninae including 'Monoscutidae' is corroborated, with the Australasian taxa as a possible sister clade to the South American *Thrasychirus*.

Keywords

Taxonomy, harvestmen, Australasia

Introduction

The Enantiobuninae (previously Monoscutidae–see Taylor 2011) are the most speciose group of long-legged harvestmen (Eupnoi) in Australasia, with over 45 described species (Taylor 2004, 2011). The taxonomy of Australasian Enantiobuninae was long based on a small number of characters of doubtful significance, such as the presence or absence of a distal apophysis on the pedipalpal patella, or a ventral tooth-row on the tarsal claw (Forster 1949). Recent reviews of the genera *Pantopsalis* Simon, 1879 (Taylor 2004) and *Megalopsalis* Roewer, 1923 (Taylor 2011) have refined the definitions of those genera and improved our understanding of enantiobunine systematics; however, the genus *Spinicrus* Forster, 1949 remained unrevised. The current paper completes the revision of genera of Australasian Enantiobuninae.

Forster (1949) established *Spinicrus* with the type species *Pantopsalis tasmanica* Hogg, 1910 from Tasmania, distinguishing it from the New Zealand genus *Pantopsalis* (Hogg, 1910) on the basis of the presence of a ventral tooth-comb on the pedipalpal claw (a character that had been accorded high significance in the artificial classification of Eupnoi used by Roewer 1923). Forster (1949) assigned two new species *S. camelus* Forster, 1949 and *S. stewarti* Forster, 1949 to the genus, and suggested that *Pantopsalis continentalis* Roewer, 1923 of Queensland might also belong to *Spinicrus*. Hickman (1957) later described two new species from Tasmania, *S. nigricans* Hickman, 1957 and *S. thrypticum* Hickman, 1957. Around the same time, Kauri (1954) assigned two species from Western Australia to the genus, *S. minimum* Kauri, 1954 and *S. porongorupense* Kauri, 1954.

Despite the small number of included species, *Spinicrus* was a morphologically heterogeneous assemblage right from its initial establishment (Forster 1949). The absence of a pedipalp apophysis (distinguishing it from *Megalopsalis*) and the presence of a toothed pedipalp claw remained the only defining characters of the genus; neither of these characters was unique to *Spinicrus* and both are likely to be plesiomorphic for Enantiobuninae as a whole (Taylor 2011). Taylor and Hunt (2009) separated *S. camelus* and *S. continentale* from *Spinicrus* as part of the morphologically distinct genus *Neopantopsalis* Taylor & Hunt, 2009 but did not consider the status of the remaining species. The possibility that some of the species, particularly *S. nigricans* and the Western Australian species, might also need to be transferred to new genera had previously been raised by Hunt (1990) after examination of their distinct spiracle morphologies. In the phylogenetic analysis of Enantiobuninae by Taylor (2011), *Spinicrus* was not identified as monophyletic. The current paper expands Taylor's (2011) analysis with the addition of seven new species that would have previously been assigned to *Spinicrus*. *Spinicrus* is identified as paraphyletic with regard to the genera *Megalopsalis* and *Hypomegalopsalis* Taylor, 2011, and all three genera are combined into a single genus *Megalopsalis*.

Material and methods

Specimens came from the collections of the Australian Museum, Sydney (AMS), Museum Victoria, Melbourne (MV), Queensland Museum, Brisbane (QM) and Western Australian Museum, Perth (WAM). Specimens were examined using a Leica MZ6 microscope, and drawings were made using a camera lucida. Photographs and measurements were taken using a Nikon SMZ1500 stereo microscope and the NIS-Elements D 4.00.03 programme, and a Leica DM2500 compound microscope. Genitalia were retained in a microvial with the original specimen. Colouration described is as preserved in alcohol. Specimens to be photographed by SEM were dried using hexamethyldisilazane (HMDS) as described by Nation (1983). The specimens were then mounted and sputter-coated with gold and examined with a Philips XL30 SEM.

Measurements were taken using a reticle. The number of specimens measured is given as "N = x" at the beginning of each description. Measurements are reported as the mean in millimetres, with total recorded range in parentheses; if no range is given, no variation was recorded. For those species in which not all available specimens were measured, the individuals measured are indicated as such in the specimen listings.

For those species in which discrete male morphs can be identified, separate descriptions are given for each form. The larger and smaller morphs are here referred to as 'major' and 'minor' males, respectively. Other sources dealing with dimorphic males have referred to the smaller morph as 'effeminate' (e.g. Forster 1954); however, this terminology is inappropriate for enantiobunines as both morphs are morphologically distinct from females.

Key to males of genera of Enantiobuninae

Thrasychiroides brasilicus Soares & Soares, 1947 has had to be omitted from the following key, as it has not been redescribed since its original description (Soares and Soares 1947) and most of the characters used in the key remain unknown for it. *Thrasychiroides* is the only genus of Enantiobuninae described from South America other than *Thrasychirus*, from which Soares and Soares (1947) distinguished it by the lack of an apophysis on the pedipalp patella. *'Megalopsalis' triascuta* Forster 1944, whose inclusion in that genus requires investigation (Taylor 2011), is keyed out separately from *Megalopsalis*.

1 Legs relatively short, femur I less than twice length of prosoma; dorsum of opisthosoma usually conspicuously ornamented **2**

– Legs long, femur I more than twice length of prosoma **5**

2 Bristle groups on right side of shaft-glans junction only; stylus conspicuously inflated (eastern Australia) ..... ***Australiscutum***

– Bristle groups on both sides of shaft-glans junction; stylus not inflated (New Zealand) **3**

3 Opisthosoma with large flanking spines on lateral margins of dorsum .... ***Acihasta salebrosa***

– Opisthosoma without such large spines **4**

4 Dorsal denticles complex, laterally extended with raised lateral lobes; chelicerae small, unarmed ..... ***Monoscutum titirangiense***

– Dorsal denticles simple, subcircular; chelicerae with second segment swollen, heavily denticulate ..... ***Templar incongruens***

5 Mobile hinge present between leg basitarsus and distitarsus; individual spines as lateral processes on penis (South America) ..... ***Thrasychirus***

– Junction between basitarsus and distitarsus fused, not hinged; bristle groups as lateral processes on penis (Australasia) **6**

6 Pedipalp patella with distinct elongate (longer than broad) prodistal apophysis **7**

– Apophysis on pedipalp patella absent or, if present, not distinctly longer than broad **9**

7 Pedipalp patella apophysis much longer than main body of patella (North Island, New Zealand) ..... ***'Megalopsalis' triascuta***

– Pedipalp patella apophysis shorter than main body of patella (Australia) **8**

8 Chelicerae with distinct frontodistal bulge; glans significantly longer than wide, bent distinctly dorsad from shaft, with vertical platelike lateral process on left side of shaft-glans junction (Western Australia) ..... ***Tercentenarium linnaei***

– Chelicerae without frontodistal bulge; glans not longer than wide, subtriangular in dorsal view, not bent significantly dorsad from shaft, no platelike lateral process ..... ***Megalopsalis*** **(in part)**

9 Glans in lateral view distinctly short and very deep, about as deep as long (New Zealand) ..... ***Mangatangi parvum***

– Glans elongate or, if relatively short, then distinctly less deep than long **10**

10 Pedipalpal claw with ventral tooth-comb; prolateral margin of pedipalpal patella not hypersetose, lacking apophysis (Australia) **11**

– Pedipalpal claw usually without a tooth-comb; if ventral teeth present, then prolateral margin of pedipalp patella densely hypersetose *or* with small distal apophysis (New Zealand) **12**

11 Dorsum of prosoma often raised in humps; proventral row of hypertrophied spines along femur I; glans in ventral view elongate, more than twice as long as wide, oval or oblong (New South Wales, Queensland) ..... ***Neopantopsalis***

– Dorsum of prosoma never raised in humps; glans in ventral view less than twice as long as wide, more or less subtriangular ..... ***Megalopsalis*** **(in part)**

12 Patella of pedipalp prolaterally densely hypersetose, entirely without apophysis; coxa of pedipalp unarmed ..... ***Pantopsalis***

– Patella of pedipalp not prolaterally hypersetose, often with small triangular prodistal apophysis; coxa of pedipalp with array of blunt tubercles on median side ..... ***Forsteropsalis***

Taxonomy

***Megalopsalis* Roewer, 1923**
http://species-id.net/wiki/Megalopsalis

Macropsalis Sørensen, 1886: 54–55 *non* Sclater 1866 – Pocock 1903: 398; Hogg 1910: 277; Roewer 1911: 102, 1912: 278.
Megalopsalis Roewer, 1923: 866 (replacement name for *Macropsalis* Sørensen) – Forster 1944: 184–185 (referring to material of *Forsteropsalis* Taylor, 2011); Crawford 1992: 28, 29; Taylor 2011: 31.
Spinicrus Forster, 1949: 63 syn. n.; Hickman 1957: 73; Crawford 1992: 43.
Hypomegalopsalis Taylor, 2011: 45 syn. n.

Type species. *Macropsalis serritarsus* Sørensen, 1886 by monotypy.

Other included species. *Megalopsalis serritarsus*-species group: *Megalopsalis epizephyros* Taylor, 2011, *Megalopsalis eremiotis* Taylor, 2011, *Megalopsalis hoggi* Pocock, 1903, *Megalopsalis pilliga* Taylor, 2011.

Megalopsalis leptekes-species group: *Megalopsalis leptekes,* 2011, *Megalopsalis tanisphyros* (Taylor, 2011) comb. n. (=*Hypomegalopsalis tanisphyros*).

Megalopsalis minima-species group: *Megalopsalis minima* (Kauri, 1954) comb. n. (=*Spinicrus minimum*), *Megalopsalis porongorupensis* (Kauri, 1954) comb. n. (=*Spinicrus porongorupense*), *Megalopsalis suffugiens* sp. n., *Megalopsalis walpolensis* sp. n..

Species not placed in species groups: *Megalopsalis atrocidiana* sp. n., *Megalopsalis caeruleomontium* sp. n., *Megalopsalis coronata* sp. n., *Megalopsalis puerilis* sp. n., *Megalopsalis stewarti* (Forster, 1949) comb. n. (=*Spinicrus stewarti*), *Megalopsalis sublucens* sp. n., *Megalopsalis tasmanica* (Hogg, 1910) comb. n. (=*Pantopsalis tasmanica*), *Megalopsalis thryptica* (Hickman, 1957) comb. n. (=*Spinicrus thrypticum*).

Diagnosis. *Megalopsalis* can be distinguished from all other genera of Enantiobuninae by its male genital morphology, with the glans being relatively short, broad, distally flattened, and more or less subtriangular in ventral view (e.g. Fig. 3d). It can be further distinguished from *Monoscutum*, *Acihasta*, *Templar* and *Australiscutum* by having the legs relatively long and thin, and the dorsum of the opisthosoma weakly sclerotised and unarmed (except *Megalopsalis atrocidiana*; Forster 1948; Taylor 2008a, 2009). *Pantopsalis*, *Forsteropsalis*, *Neopantopsalis* and *Mangatangi* differ from all *Megalopsalis* species except *M. caeruleomontium* by the presence of setae on the mobile finger of the chelicera (Taylor 2013: figs 1d, 2c). *Tercentenarium* has males with a distinct frontodistal bulge on the chelicerae (Taylor 2008b: fig. 3), and females with a 'keyhole'-like emargination at the front of the genital operculum (Taylor 2008b: fig. 10).

Description. Ozopores usually large, oblong (small, round in *Megalopsalis nigricans*). Dorsum of opisthosoma unarmed (except with transverse rows of spines in *M. atrocidiana*). Chelicera segment II denticulate or not; mobile finger usually closing tightly against finger of segment II, fingers bowed apart in larger males of *M. caeruleomontium*. Pedipalp

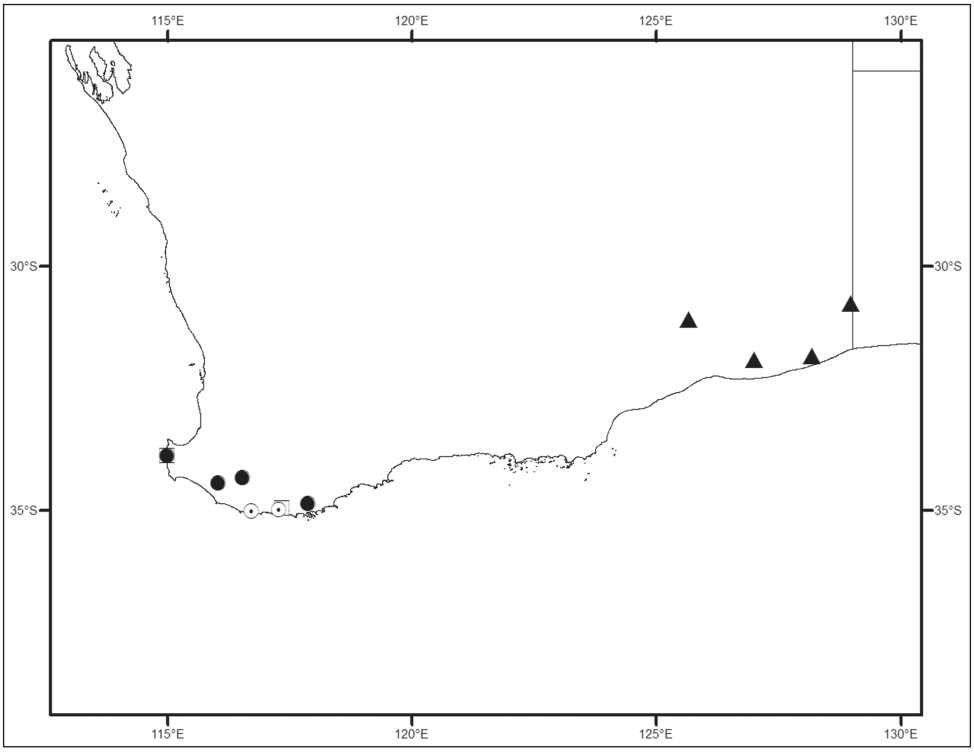

Figure 1. Locality map for *Megalopsalis minima* species-group in southern Western Australia: open square = *M. minima*; solid circle = *M. porongorupensis*; circle with dot = *M. walpolensis*; solid triangle = *M. suffugiens*.

usually with patella shorter than tibia (slightly longer in *M. nigricans*); apophysis present or absent on patella; claw with ventral tooth-row. Glans relatively short, broad, more or less subtriangular in ventral view, proximal section usually somewhat inflated dorsally (except in *M. nigricans*); distal section more or less dorsoventrally flattened. Spiracle with reticulate or partially reticulate covering spines (reduced or absent in *M. minima*-species group); lace tubercles present or absent.

Distribution (Figs 1, 7). Southern and eastern Australia.

Comments. The genus *Spinicrus* as previously defined (Forster 1949) is likely to be non-monophyletic with regard to both *Megalopsalis* and *Hypomegalopsalis*, and lacks clear synapomorphies (see phylogenetic analysis below). In contrast, the clade uniting these three genera is characterised by a distinct penis morphology, and they are hence united into a single genus *Megalopsalis*. The species groups listed above are clades that were consistently recovered in the phylogenetic analysis under varying analytical conditions; those species not placed in groups did not form consistent subgeneric clades across all analyses. Members of the *M. serritarsus*- and *M. leptekes*-groups were described by Taylor (2011).

Megalopsalis tasmanica and *M. thryptica* were described in detail by Hickman (1957), and so are not redescribed here. Both sexes of *M. tasmanica* can be distin-

guished from other Neopilionidae by their distinctive elongate opisthosoma as illustrated by Hickman (1957: fig. 29); this distinction is even more pronounced in the female. See below under *M. stewarti* for discussion of the distinction between this species and *M. thryptica*.

Key to males of species of *Megalopsalis*

1 Patella of pedipalp with elongate prodistal apophysis **2**
– Patella of pedipalp without apophysis **8**
2 Distitarsi III and IV inflated proximally, with ventral rows of brush-like bristles **3**
– Distitarsi III and IV not inflated proximally, without ventral brush-like bristles **7**
3 Distitarsus II with ventral swellings on pseudosegments..... **4**
– Distitarsus II with pseudosegments cylindrical..... ***Megalopsalis hoggi***
4 Femur II with ventral spines **5**
– Femur II unarmed ..... ***Megalopsalis pilliga***
5 Pedipalpal femur with dorsal spines ..... ***Megalopsalis epizephyros***
– Pedipalpal femur unarmed or with ventral spines only..... **6**
6 Spiracle spines relatively robust, lace tubercles short and forming more extensive field; pedipalpal femur never spinose (New South Wales) ..... ***Megalopsalis serritarsus***
– Spiracle spines more slender, lace tubercles more elongate but less extensive; pedipalpal femur may have ventral spines (Victoria, South Australia) ..... ***Megalopsalis eremiotis***
7 Pedipalpal femur with dorsal and ventral spine rows... ***Megalopsalis leptekes***
– Pedipalpal femur unarmed..... ***Megalopsalis tanisphyros***
8 Dorsum of opisthosoma with transverse rows of spines raised on mounds .... ***Megalopsalis atrocidiana***
– Dorsum of opisthosoma unarmed..... **9**
9 Ozopore openings very small, circular, not raised on lateral lobes; pedipalpal femur relatively long, more than 1.5× length of prosoma... ***Megalopsalis nigricans***
– Ozopore openings oblong, raised on lateral lobes; pedipalpal femur shorter than or subequal to prosoma..... **10**
10 Mobile finger of chelicera with ring of setae near central tooth ..... ***Megalopsalis caeruleomontium***
– Mobile finger of chelicera without setae..... **11**
11 Distitarsi III and IV with ventral rows of brush-like bristles..... **12**
– Distitarsi III and IV without ventral brush-like bristles..... **15**
12 Opisthosoma distinctly elongate, about 1.5× as long as wide ..... ***Megalopsalis tasmanica***
– Opisthosoma not elongate, not much longer than wide..... **13**
13 Dorsum of prosoma entirely unarmed ..... ***Megalopsalis sublucens***

–	Dorsum of prosoma strongly denticulate	**14**
14	Distitarsus IV inflated proximally	***Megalopsalis thryptica***
–	Distitarsus IV evenly cylindrical	***Megalopsalis stewarti***
15	Segment II of chelicera denticulate; spiracle with covering spines absent (Western Australia)	**16**
–	Segment II of chelicera unarmed; covering spines present over spiracle (eastern Australia)	**19**
16	Dorsum of prosoma strongly denticulate	***Megalopsalis minima***
–	Dorsum of prosoma unarmed or with very few denticles	**17**
17	Legs unarmed or with sparse, relatively long and slender spines; body silvery	***Megalopsalis suffugiens***
–	Legs with numerous small denticles; opisthosoma with dark transverse stripes	**18**
18	Pedipalp with numerous denticles on femur and patella	***Megalopsalis porongorupensis***
–	Pedipalp unarmed	***Megalopsalis walpolensis***
19	Ocularium spinose	***Megalopsalis coronata***
–	Ocularium unarmed	***Megalopsalis puerilis***

Megalopsalis minima **(Kauri, 1954), comb. n.**
http://species-id.net/wiki/Megalopsalis_minima
Fig. 3

Spinicrus minimus Kauri, 1954: 7–8, fig. 4a–b (incorrect original spelling).
Spinicrus minimum Kauri – Taylor 2004: 76 (spelling emended therein by W. Staręga).

Material examined. 1 minor male, Denmark, Western Australia, 34°57'S, 117°21'E, 11 November 1990, A. F. Longbottom, under granite (WAM T72865); 3 minor males, Glenbourne farm, Old Ellensbrook Rd, S of Gracetown, Western Australia, 33°53'S, 115°00'E, 27–28 October 1996, L. Marsh et al., pitfall (WAM T72171, T72184 [2 measured]); 3 major males, ditto, 28–30 June 1997, L. Marsh et al., dry pitfalls, base of cliff (WAM T72167–9; measured); 2 minor males, ditto, 13–15 September 1997, L. Marsh et al., dry pitfall traps (WAM T72176 [measured], T72186); 1 minor male, ditto, 27–29 December 1997, L. Marsh et al., dry pitfalls, site 3 (WAM T72160); 1 minor male, 33°54'28"S, 115°00'49"E, 24–26 October 1998, L. Marsh et al., dry pitfall traps (WAM T72172; measured); 2 minor males, ditto, 33°54'32"S, 115°00'24"E, 24–26 October 1998, L. Marsh et al., dry pitfall traps (WAM T72158); 2 minor males, ditto, 33°54'40"S, 115°00'34"E, 30 October–1 November 1999, L. Marsh et al., dry pitfall traps (WAM T72144; 1 measured); 1 minor male, ditto, 20–22 October 2001, L. Marsh et al., dry pitfall traps (WAM T72193; measured); 1 minor male, ditto, 33°55'08"S, 115°00'44"E, 20–23 October 2000, L. Marsh et al., dry pitfall traps (WAM T72187; measured).

Diagnosis. *Megalopsalis minima* can be distinguished from other members of the *M. minima*-species group by the heavier denticulation on the dorsal prosomal plate (Fig. 3a); the major males can also be distinguished from other species by the proportionately much longer chelicerae (Fig. 3b). It can be distinguished from *M. porongorupensis* by the absence of spines on the pedipalpal femur and patella, and from *M. suffugiens* by the heavily denticulate leg femora (Fig. 3b).

Description. MAJOR MALE (N = 3). Prosoma length 0.85 (0.78–0.90), width 1.86 (1.74–1.92); total body length 2.37 (2.18–2.56). Dorsal prosomal plate golden brown; median prosomal area strongly denticulate, fewer denticles on margins of anterior and posterior prosomal areas. Ocularium black with row of denticles along edge on each side. Ozopore large, lenticulate. Dorsum of opisthosoma with alternating tan and dark brown mottled with tan stripes, and scattered iridescent white patches. Coxae tan with medium brown distal ends; venter of opisthosoma dark brown medially; tan dusted with black laterally.

Chelicerae. Segment I 5.81 (4.78–7.00), segment II 6.83 (6.10–7.88). Chelicerae golden brown with second segment tan distad; evenly denticulate. Fingers long; mobile finger crescent-shaped (Fig. 3c).

Pedipalps. Femur 0.96 (0.89–1.00), patella 0.44 (0.43–0.46), tibia 0.55 (0.54–0.59), tarsus 1.23 (1.21–1.26). Alternating tan and brown bands; femur without denticles. Femur to proximal part of tibia with longitudinal rows of large setae, distal tibia and tarsus with large setae interspersed among small setae. Inner dorsal distal patella with swelling but no distinct apophysis. Microtrichia on distal end of tibia and tarsus; claw with ventral tooth-row.

Legs. Femora 4.27 (3.82–4.55), 7.51 (6.92–7.92), 3.72 (3.48–3.96), 5.75 (5.33–5.94); patellae 0.87 (0.80–0.98), 0.96 (0.92–1.07), 0.81 (0.76–0.86), 0.95 (0.93–1.00); tibiae 3.96 (3.62–4.28), 8.15 (7.42–8.46), 3.67 (3.44–3.84), 5.79 (5.27–5.98). Femora with strong denticles. Patella I with two longitudinal rows of spines, one on each side; rows continue on tibia, dwindling distalwards. Patellae of other legs only lightly denticulate; tibiae smooth. Tibia II with 7–9 pseudosegments, tibia IV with two pseudosegments.

Penis (Figs 3d–e). Tendon long; waist in shaft behind bristle groups; left anterior bristle group reduced. Glans short, triangular in ventral view, not strongly flattened distally; dorsal side in line with shaft, evenly convex. Deep pores.

Spiracle. Spines almost entirely absent, residual reticulate bases only towards lateral corner; dense field of lace tubercles at lateral corner.

MINOR MALE (N = 7). Prosoma length 0.73 (0.55–0.83), width 1.82 (1.39–1.68); total body length 1.83 (1.45–2.25). As above, except for following.

Chelicerae. Segment I 0.96 (0.66–2.61), segment II 1.68 (1.27–3.44).

Pedipalps. Femur 0.84 (0.78–0.90), patella 0.37 (0.34–0.39), tibia 0.48 (0.43–0.53), tarsus 1.05 (0.93–1.10).

Legs. Femora 3.48 (3.20–3.70), 6.57 (6.27–6.79), 3.34 (3.00–3.52), 4.79 (4.30–5.00); patellae 0.72 (0.63–0.80), 0.83 (0.77–0.87), 0.72 (0.69–0.76), 0.83 (0.70–0.85); tibiae 3.46 (2.84–3.80), 7.02 (6.33–7.34), 3.26 (2.72–3.52), 4.74 (4.15–5.00). Patella I lightly denticulate, without longitudinal spine rows.

Comments. Unfortunately, the type specimen(s) of *M. minima* were not available for the present study. This species has been identified based on its original description by Kauri (1954).

Females have been found in association with males of *Megalopsalis minima*, *M. porongorupensis* and *M. walpolensis* (unpublished observations, specimens in WAM). However, as no distinct morphotypes have been distinguished among the likely females, while the ranges of these species overlap, it has not been possible as yet to determine which females are assignable to which species.

***Megalopsalis porongorupensis* (Kauri, 1954), comb. n.**
http://species-id.net/wiki/Megalopsalis_porongorupensis
Figs 2a, 4

Spinicrus porongorupensis Kauri, 1954:8–9, fig. 4c (incorrect original spelling).
Spinicrus porongorupense Kauri – Taylor 2004: 76 (spelling emended therein by W. Staręga).

Material examined. 5 males, Glenbourne, Old Ellensbrook Road, S of Gracetown, Western Australia, 33°53'S, 115°00'E, 27–28 October 1996, L. Marsh et al., pitfalls (WAM T72175 [2 measured]; T72184 [1 measured]); 2 males, ditto, 27–29 December 1997, L. Marsh et al., dry pitfalls (WAM T72152–3; measured); 1 male, ditto, 33°54'50"S, 115°00'57"E, 24–26 October 1998, L. Marsh et al., dry pitfall traps (WAM T72161; measured); 1 male, ditto, 33°54'32"S, 115°00'24"E, 20–23 October 2000, L. Marsh et al., dry pitfall traps (WAM T72200); 1 male, ditto, 33°54'40"S, 115°00'34"E, 24-26 October 1998, L. Marsh et al., dry pitfall traps (WAM T72173); 1 male, ditto, 25–27 October 2003, L. Marsh et al., dry pitfall traps (WAM T72198; measured); 1 male, ditto, 33°54'35"S, 115°00'15"E, 30 October–1 November 1999, L. Marsh et al., dry pitfall traps (WAM T72155; measured); 3 males, ditto, 33°54'50"S, 115°00'57"E, 30 October–1 November 1999, L. Marsh et al., dry pitfall traps (WAM T72143; 2 measured); 1 male, Pemberton, Crowea Block, Western Australia, 240 m, 17 December 1976, S. J. Curry, pitfall trap (WAM 90/1319); 2 males, ditto, 24 October 1977, S. J. Curry, ridge site, pitfall traps (WAM 90/1321–2); 1 male, ditto, 31 October 1977, S. J. Curry, ridge site, pitfall trap (WAM 90/1335); 1 male, ditto, 11 November 1977, S. J. Curry, ridge site, pitfall trap (WAM 90/1326); 1 male, Porongurup Range, Western Australia, 20 January 1932, E. W. Bennett (WAM 32/217); 1 male, Porongurup National Park, Porongurups, Western Australia, 34°40'55.8"S, 117°51'58.6"E, 570 m, 13 June 1996, S. Barrett, wet pitfalls (WAM T72214); 3 males, Mordalup Road, Unicup, Western Australia, 34°19'01"S, 116°31'49"E, 15 Oct 1999–31 Oct 2000, P. van Heurck, wet pitfalls (WAM T73035).

Diagnosis. *Megalopsalis porongorupensis* is distinguishable from other members of the *M. minima*-species group by the presence of denticulation on the pedipalp (Kauri 1954).

Description. MALE (N = 10). Prosoma length 0.81 (0.65–0.91), width 1.55 (1.41–1.74); total body length 1.94 (1.70–2.33). Dorsal prosomal plate including

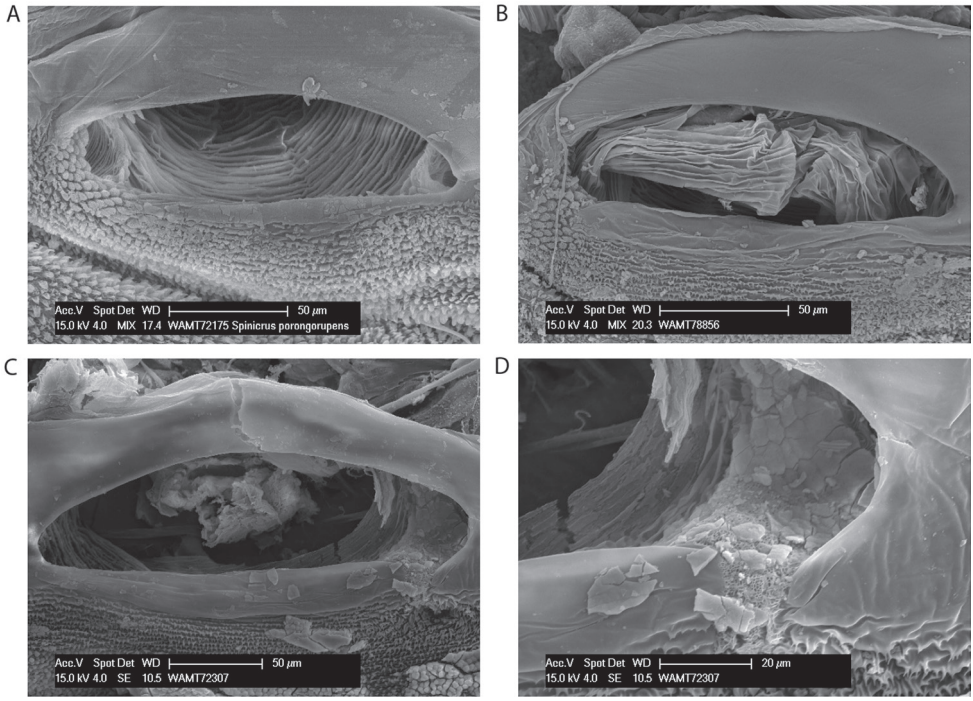

Figure 2. Spiracles of *Megalopsalis minima* species-group: **a** *M. porongorupensis* **b** *M. walpolensis* **c** *M. suffugiens* **d** same, close-up of lateral corner showing area of reticulation.

ocularium tan with dark mottling; unarmed. Ozopore large. Dorsum of opisthosoma tan with iridescent white spots and broad white median stripe.

Chelicerae. Segment I 1.35 (0.69–2.20), segment II 2.04 (1.23–3.00). Tan; heavily and uniformly denticulate. Cheliceral fingers medium length; mobile finger crescent-shaped (Fig. 4c).

Pedipalps. Femur 0.83 (0.75–1.00), patella 0.38 (0.31–0.45), tibia 0.45 (0.40–0.52), tarsus 1.05 (0.94–1.19). Tan. Femur and patella heavily denticulate, few scattered large setae only; tibia lightly denticulate proximally. Inner dorsal distal patella slightly bulging but no distinct apophysis. Microtrichia on distal part of tibia and tarsus; claw with ventral tooth row.

Legs. Femora 3.46 (3.08–3.92), 6.68 (6.00–7.34), 3.24 (2.92–3.48), 5.20 (4.65–5.67); patellae 0.73 (0.66–0.84), 0.84 (0.67–0.89), 0.66 (0.56–0.78), 0.80 (0.64–1.00); tibiae 3.16 (2.88–3.42), 7.12 (6.60–7.83), 3.03 (2.70–3.24), 4.78 (4.15–5.27).

Penis (Figs 4d–e). Glans short, dorsal edge in line with shaft; stylus at 90° to glans and shaft. Left anterior bristle group reduced; waist in shaft behind bristle groups. Deep pores.

Spiracle (Fig. 2a). Spines almost entirely absent, residual reticulate bases only towards lateral corner; dense field of lace tubercles at lateral corner.

Comments. Unfortunately, the type specimen(s) of *M. porongorupensis* were not available for the present study. This species has been identified based on its original description by Kauri (1954), who clearly figured the denticulate pedipalp.

This species shows a relatively large degree of difference in cheliceral size between the largest and smallest individuals, but there is no clear clustering into a larger and a smaller morph.

Megalopsalis suffugiens sp. n.

http://zoobank.org/EA5093FB-A854-4AE1-B512-5789F226176C
http://species-id.net/wiki/Megalopsalis_suffugiens
Figs 2c–d, 5

Material examined. *Male holotype*. Balgair Station, cave 6N–612, Western Australia, 14 September 1999, N. Poulter, from ceiling adjacent to cave entrance (WAM T72303).

Paratypes. 1 male, Balgair Station, cave 6N–1536, Western Australia, 13 September 1999, N. Poulter, walking on damp earth floor (WAM T72299); 1 male, ditto, c. 11 m below cave entrance (WAM T72307); 1 female, Balgair Station, cave 6N-1616, Western Australia, 15 September 1999, P. Devine, N. Poulter, rockhole cave (WAM T72287); 2 males, 1 female, Hampton Tableland, Mundrabilla Station, cave 6N–326, 22 September 1999, P. Devine, N. Poulter, from cave walls in dark zone, largest [female] from entrance lip at night fall (WAM T72298); 1 female, Madura Plains Station (=Moonera Station), cave 6N–1617, 17 September 1999, R. Anderson, N. Poulter, from cave ceiling in dark zone (WAM T72305); 1 female, Nullarbor area, cave 6N–481, 1 October 1994, R. Foulds, from roof of entrance squeeze (WAM T72141).

Diagnosis. *Megalopsalis suffugiens* is readily distinguished from other species of the *M. minima*-species group by its pale coloration without dark transverse bands on the opisthosoma (Fig. 5a–b). The spines on the legs (if present) are also proportionately longer and more slender than those found in other species. It can also be distinguished from *M. minima* by the lack of denticles on the ocularium and median propeltidial area (Fig. 5a) and from *M. porongorupensis* by the lack of denticles on the pedipalps.

Description. MALE (N = 5). Prosoma length 0.75 (0.68–0.83), width 1.69 (1.56–1.86); total body length 2.21 (2.08–2.30). Dorsal prosomal plate unarmed (Balgair Station specimens) or with few denticles on anterior propeltidial area (Hampton Tableland specimens); patched tan and iridescent white with scattered darker mottling. Mesopeltidium with distinct transverse row of black setae. Metapeltidium and anterior part of opisthosoma mottled tan and silver. Posterior part of opisthosoma silver with transverse bands of dark brown mottling.

Chelicerae. Segment I 1.47 (0.78–2.22), segment II 2.44 (1.56–3.28). Both segments tan; lightly denticulate with reduced denticulation distad on both segments. Segment II slightly inflated distad. Cheliceral fingers long, slender; mobile finger crescent-shaped.

Pedipalps. Femur 1.01 (0.87–1.09), patella 0.51 (0.50–0.54), tibia 0.57 (0.54–0.64), tarsus 1.27 (1.20–1.33). White with tan patches and black setae; femur with

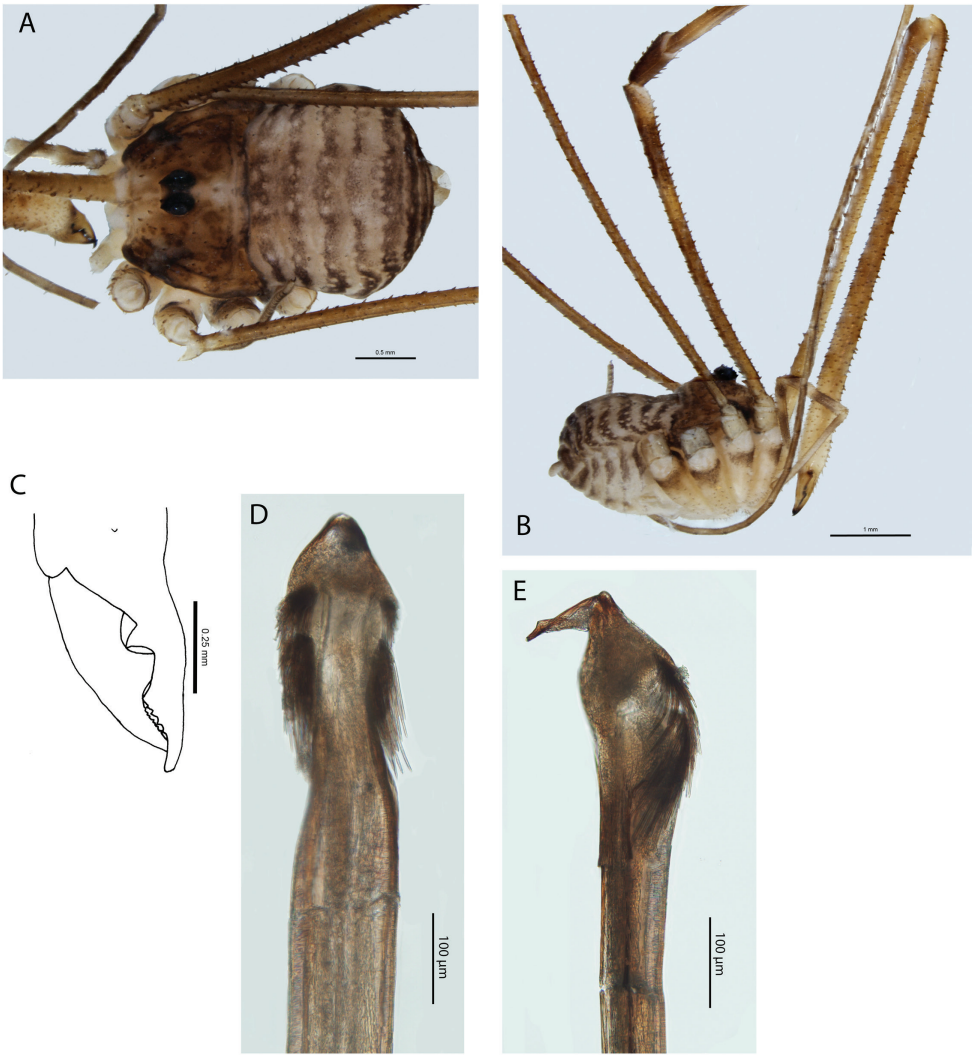

Figure 3. *Megalopsalis minima*, major male (all WAM T72169): **a** body, dorsal view **b** body, lateral view **c** right cheliceral fingers, frontal view **d** glans, ventral view **e** glans, right lateral view.

longitudinal rows of setae; patella and tibia with black setae laterally and medially, midline glabrous; no apophysis. Microtrichia over greater part of tarsus and tibia; claw with ventral tooth row.

Legs. Femora 3.83 (3.17–4.45), 7.14 (6.38–7.77), 3.10 (2.66–3.36), 4.94 (4.10–5.56); patellae 0.90 (0.83–0.99), 1.05 (0.98–1.12), 0.85 (0.78–0.94), 0.99 (0.90–1.06); tibiae 3.71 (3.34–4.00), 7.42 (6.81–7.89), 3.57 (2.90–4.05), 4.91 (4.10–5.52). Trochanters iridescent white; unarmed or with single anterior spine on trochanters I and III. Legs tan; femur I with sparse, slender spines, reduced to only a few dorsally in some specimens; femur II unarmed or with few spines near base; remaining segments

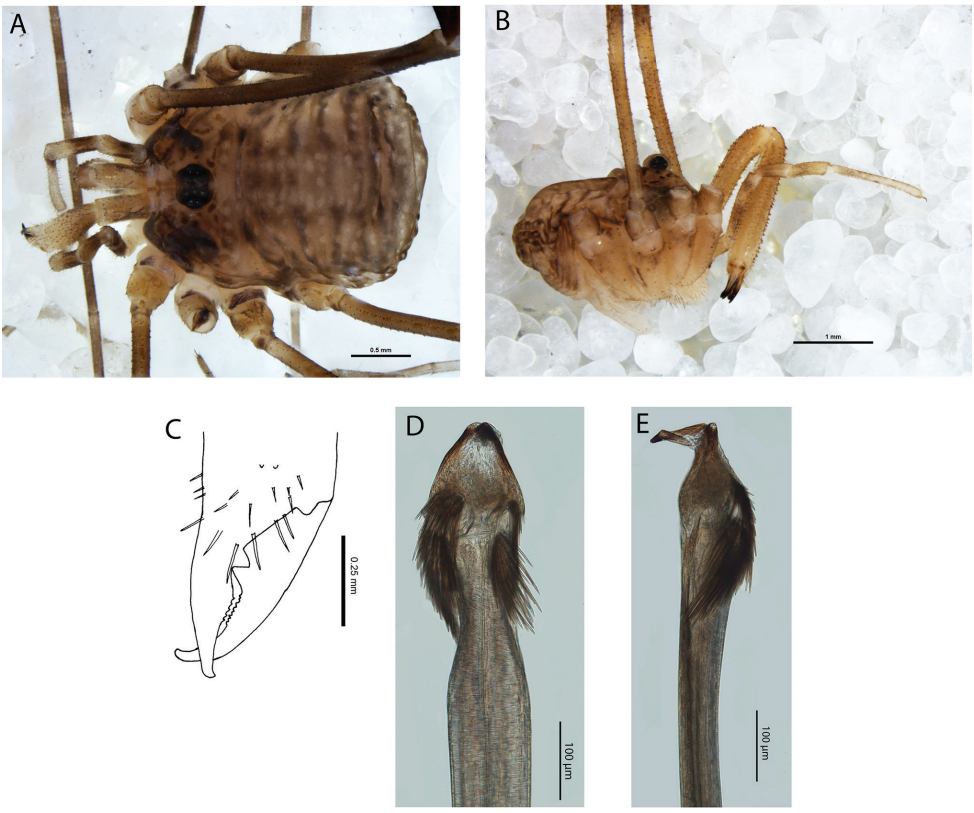

Figure 4. *Megalopsalis porongorupensis*, male: **a** body, dorsal view (WAM T72311) **b** body, lateral view (WAM T72203) **c** left cheliceral fingers, frontal view (WAM T72175) **d** glans, ventral view (WAM T72175) **e** glans, dorsolateral view (WAM T72175).

unarmed. Femora and patellae with scattered black setae; tibiae and tarsi densely covered in small setae. Tibia II with 11 to 13 pseudosegments; tibia IV with two or three pseudosegments.

Penis (Figs 5c–d). Shaft broad, tendon relatively short; bristle groups well-developed. Glans short, broad, triangular in dorsal view; in line with shaft; dorsal side evenly convex; not significantly flattened distally. Pores shallowly recessed.

Spiracle (Figs 2c–d). No occluding spines; lace tubercles at lateral corner reduced to patch of reticulation.

FEMALE (N = 4). Prosoma length 1.16 (0.61–1.45), width 2.13 (1.98–2.28); total body length 3.83 (3.40–4.40). As for male, except for following: Dorsum unarmed.

Chelicerae. Segment I 0.75 (0.66–0.81), segment II 1.58 (1.55–1.62). Unarmed.

Pedipalps. Femur 1.31 (1.28–1.34), patella 0.68 (0.65–0.71), tibia 0.78 (0.73–0.83), tarsus 1.65 (1.63–1.67). Patella and tibia more densely setose medially than male.

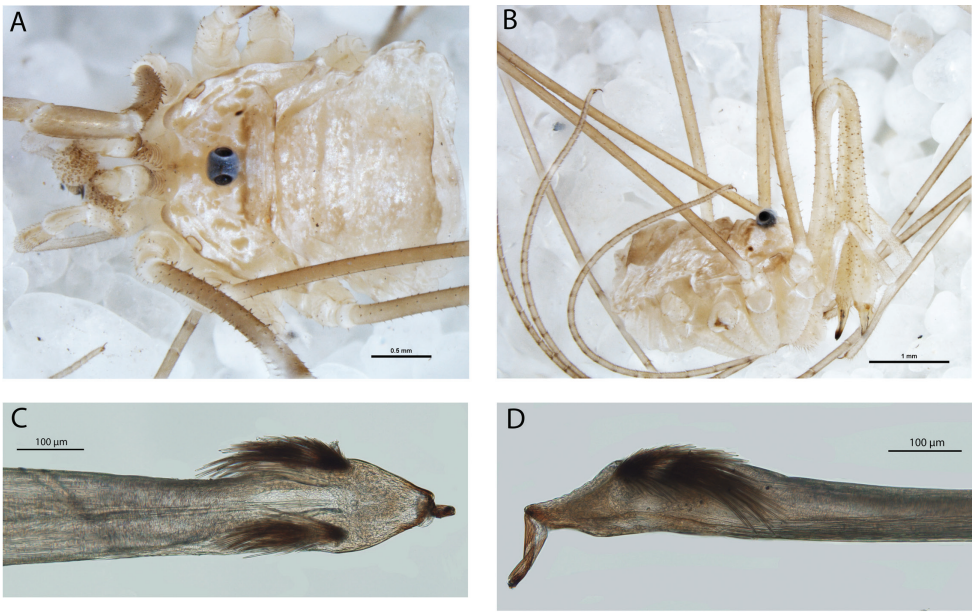

Figure 5. *Megalopsalis suffugiens*, male (all WAM T72299): **a** body, dorsal view **b** body, lateral view **c** glans, ventral view **d** Glans, right lateral view.

Legs: Femora 4.68 (4.45–4.95), 9.28 (8.73–10.23), 4.01 (3.72–4.28), 5.95 (5.63–6.16); patellae 1.18 (1.07–1.24), 1.42 (1.32–1.45), 1.11 (1.03–1.19), 1.19 (1.13–1.24); tibiae 4.79 (4.65–4.96), 9.77 (9.12–10.38), 4.44 (4.28–4.63), 6.05 (5.81–6.25). Femora and patellae with longitudinal rows of small spines.

Variation. Males show a noticeable variation in the size of the chelicerae that correlates with the development of armature on the legs; however, the variation is not as large as that found in *Megalopsalis minima*, and it is uncertain at present whether variation is continuous or a distinction occurs between major and minor males. Further specimens are also required to establish whether the difference in dorsal armature recorded above between Balgair Station and Hampton Tableland specimens indicate separate populations in these localities.

Etymology. From the Latin *suffugio*, to take shelter, to reflect the finding of specimens of this species within caves in the arid Nullarbor.

Comments. All specimens of *Megalopsalis suffugiens* recorded to date were collected in caves; however, *M. suffugiens* does not show any obvious troglobitic adaptations. The eyes remain well-developed and the legs are proportionately only slightly longer than in other *Megalopsalis* species. It seems more likely that *M. suffugiens* only uses the caves as damp refugia during the day, emerging at night to feed. This suggestion is supported by the collection of at least one specimen (WAM T72298) from a cave entrance at nightfall.

***Megalopsalis walpolensis* sp. n.**
http://zoobank.org/9ACD0DA5-BE0D-4FCB-BEB7-D2E4F195C8E9
http://species-id.net/wiki/Megalopsalis_walpolensis
Figs 2b, 6

Material examined. Male holotype. Walpole-Nornalup National Park, Knoll Drive, Walpole, Western Australia, 34°59'43"S, 116°43'12"E, 29 October 2006, M. L. Moir, A. Sampey (WAM T78848).

Paratype. 1 male, Mt Shadforth, Western Australia, 34°58'04"S, 117°16'47"E, 6 November 2006, M. L. Moir, D. Jolly, in leaf litter (WAM T78856).

Diagnosis. The features of *Megalopsalis walpolensis* appear intermediate between those of *M. minima* and *M. porongorupensis*. It differs from *M. minima* in lacking significant denticulation on the ocularium and propeltidium (Fig. 6a) and from *M. porongorupensis* in lacking denticles on the pedipalps.

Description. MALE (N = 2). Prosoma length 0.65 (0.55–0.74), width 1.44 (1.34–1.53); total body length 2.22 (2.13–2.30). Anterior propeltidial area cream, remainder of propeltidium golden-brown with mottled black patches on anterior corners of dorsal prosomal plate and lateral shelves. Prosoma mostly unarmed, except few small scattered denticles on lateral edge of dorsal prosomal plate near odoriferous glands. Odoriferous glands visible as black patches through cuticle. Ocularium dark golden-brown, with row of small low denticles around each eye. Mesopeltidium, metapeltidium and opisthosoma with transverse band of mottled black across golden-brown background of each segment, broken by tan or iridescent white spots. Coxae cream with mottled purple patches at distal ends; venter of opisthosoma cream dusted with purple, condensing to more solid patches laterally.

Chelicerae. Segment I 0.73 (0.67–0.79), segment II 1.42 (1.25–1.59). Segment I mottled purple on cream background with purple mottling more solid laterally than medially; scattered denticles dorsally. Segment II cream, mottled with purple proximally, densely denticulate proximally with denticles thinning until distal third is unarmed. Cheliceral fingers short, lateral margin evenly rounded.

Pedipalps. Femur 0.90 (0.89–0.91), patella 0.42 (0.40–0.44), tibia 0.50 (0.48–0.52), tarsus 1.11 (1.07–1.14). Cream banded with purple, with cream stripe down dorsal midline; unarmed. No patellar apophysis; black setae denser on medial side of patella but not hypersetose. Microtrichia on tarsus, except for proximal third, and distalmost end of tibia. Tooth-comb on claw.

Legs. Femora 3.48 (3.44–3.52), 6.20 (6.15–6.24), 3.33 (3.32–3.34), 5.05 (4.98–5.11); patellae 0.81 (0.78–0.83), 1.05 (1.03–1.06), 0.82 (0.81–0.83), 0.95; tibiae 3.42 (3.40–3.44), 6.95 (6.93–6.96), 3.16 (3.13–3.19), 4.90 (4.84–4.96). Trochanters white-cream mottled with purple, unarmed. Femora golden-brown proximally, with cream band beginning distad of halfway, followed by purple band, then cream distal end. Patellae dark cream dusted with black, tibiae and metatarsi banded cream and dusty black, tarsi cream. Femora and distal ends of patellae with broken rows of dorsal denticles, remaining segments unarmed. Tibia II with seven pseudosegments, tibia IV undivided.

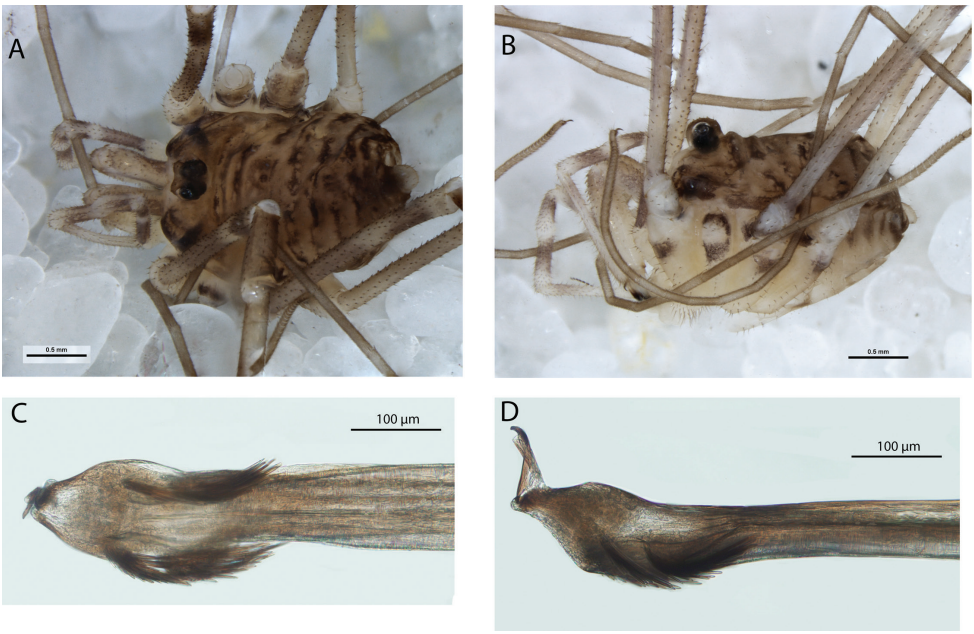

Figure 6. *Megalopsalis walpolensis*, male (all WAM T78848): **a** body, dorsal view **b** body, lateral view **c** glans, ventral view **d** glans, left lateral view.

Penis (Figs 6c–d). Left anterior bristle group somewhat reduced, remaining bristle groups well-developed. Glans short, broad, triangular in dorsal view; roughly in line with shaft; dorsal side evenly convex; not significantly flattened distally. Deep pores.

Spiracle (Fig. 2b). Spines entirely absent; dense patch of lace tubercles at lateral corner.

Etymology. From the type locality, Walpole, with the suffix *–ensis* indicating geographic origin.

***Megalopsalis atrocidiana* sp. n.**
http://zoobank.org/10CF153B-F43C-4FFE-9511-EC6BE7320776
http://species-id.net/wiki/Megalopsalis_atrocidiana
Figs 8, 9a–c

Material examined. *Male holotype*. Central Queensland, Mt Dalrymple, 21°03'S, 148°38'E, 1200 m, 21 December 1992–10 January 1993, ANZSES Expedition, flight intercept trap (QM S35935).

Paratype. 1 female, ditto (QM S35935).

Diagnosis. *Megalopsalis atrocidiana* differs from all other long-legged Enantiobuninae in the presence of transverse rows of spines on the opisthosoma (Fig. 8a); these are present in reduced form in the females as well as the males.

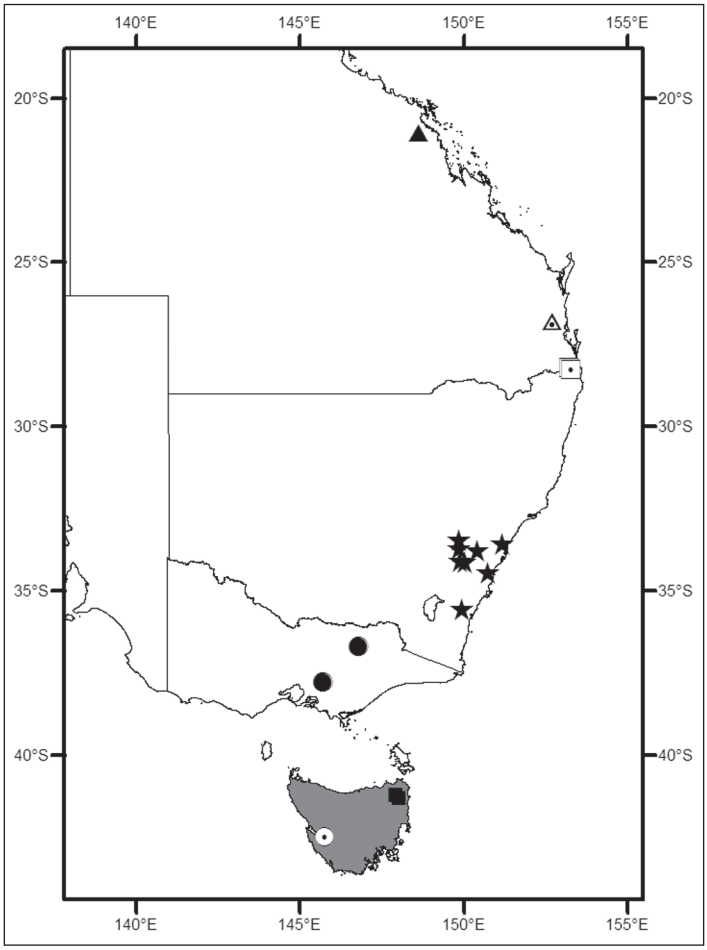

Figure 7. Locality map for *Megalopsalis* species (excluding *M. serritarsus*-group) in eastern Australia: grey shading = *Megalopsalis tasmanica* and *M. nigricans*; circle with dot = *M. sublucens*; solid square = *M. thryptica*; solid circle = *M. stewarti*; solid star = *M. caeruleomontium*; square with dot = *M. coronata*, triangle with dot = *M. puerilis*, solid triangle = *M. atrocidiana*.

Description. MALE (N = 1). Prosoma length 2.18, width 1.26; total body length 2.66. Body medium brown; darker mottling on prosoma. Dorsal prosomal plate sharply denticulate; denticles along posterior margins of prosomal segments. Lateral spines on each side of metapeltidium. Ocularium with high spines. Ozopore large. Opisthosoma with transverse rows of spines on raised mounds along midlines of first four segments. Coxae golden brown with dark brown patches distally; venter of opisthosoma light grey-brown.

Chelicerae. Segment I 1.40, segment II 2.53. Segment II darker than segment I; distal end of segment I white. Both segments evenly denticulate. Cheliceral fingers long, mobile finger angular crescent-shaped.

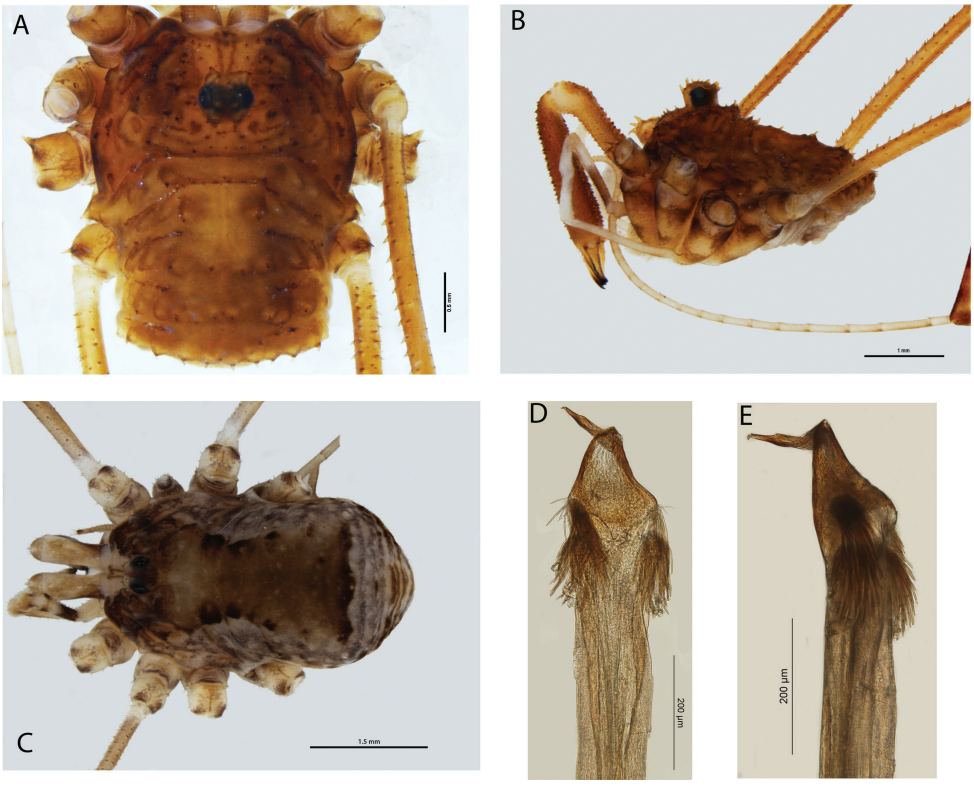

Figure 8. *Megalopsalis atrocidiana* (all QM S35935): **a** body of male, dorsal view **b** body of male, lateral view **c** body of female, dorsal view **d** glans, ventral view **e** glans, right lateral view.

Pedipalps. Femur 1.15, patella 0.53, tibia 0.63, tarsus 1.42. Proximal half of femur brown, distal half of femur to tibia white, tarsus tan. Unarmed; no apophysis on patella. Plumose setae present medially (Fig. 9c). Microtrichia on distal three-quarters of tarsus; claw with ventral tooth-row.

Legs. Femora –, 6.77, 3.48, 5.41; patellae –, 1.19, 1.01, 1.11; tibiae –, 7.89, 3.24, 5.03. Golden brown. Trochanters with robust spines on prolateral face. Leg I not preserved. Femora of remaining legs denticulate; patellae with longitudinal rows of small denticles; remaining segments unarmed. Tibia II with seven or eight pseudosegments; tibia IV undivided.

Penis (Figs 8d–e). Left anterior bristle group slightly reduced, remaining bristle groups well developed. Glans of medium length, edges converging in ventral view.

Spiracle (Figs 9a–b). Dense curtain of robust reticulate spines extending partway across spiracle; terminations of spines multifurcate but not palmate; lace tubercles in lateral corner, with small number of reticulate spines at lateral end of posterior margin.

FEMALE (Fig. 8c; N = 1). Prosoma length 1.5, width 2.3; total body length 3.48. Anterior propeltidial area tan, remainder of propeltidium mottled medium brown. Ocularium with row of denticles on each side. Mesopeltidium medially medium

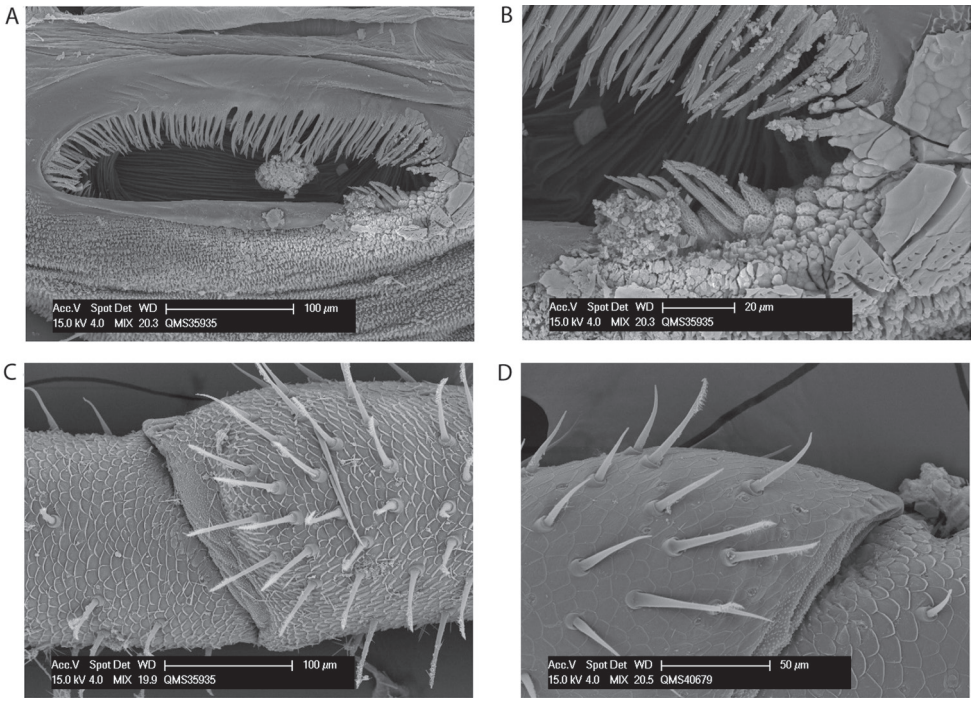

Figure 9. *Megalopsalis atrocidiana* and *M. coronata*, SEM images: **a** *M. atrocidiana*, spiracle **b** same, close-up of lateral corner **c** *M. atrocidiana*, right pedipalp, medial view of patella and tibia, showing plumose setae **d** *M. coronata*, left pedipalp, medial view of distal end of patella, showing mixture of plumose and non-plumose setae.

brown, laterally tan with black mottling; small denticles medially. Metapeltidium and first three segments of opisthosoma medially medium brown with black patches on edge of medial area, laterally tan mottled with black. Metapeltidium and first four segments of opisthosoma with transverse rows of small denticles. Posterior part of opisthosoma tan mottled with black. Coxae patched tan and dark brown; venter of opisthosoma grey with longitudinal rows of dark brown patches.

Chelicerae. Segment I 0.77, segment II 1.65. Segment I tan with dark brown lateral patches proximodorsally; segment II golden brown with tan fingers. Unarmed.

Pedipalps. Femur 1.28; patella 0.59; tibia 0.72; tarsus 1.60. Femur dark brown on proximal half, tan on distal half with golden brown patch on distalmost end; patella and tibia each golden brown proximally, tan distally; tarsus tan. Unarmed; no apophysis on patella.

Legs: Femora 3.56, 6.77, 3.40, –; patellae 1.17, 1.23, 1.11, –; tibiae 3.84, 7.69, 3.24, –. Banded tan and medium brown; longitudinal dorsal rows of denticles on femora and patellae. Tibia II with eight pseudosegments; leg IV not preserved.

Etymology. From the Latin *atrox*, cruel, and the goddess Diana. The transverse rows of mounds on the opisthosoma are reminiscent of the figure known as Diana of Ephesus, while the epithet 'cruel' refers to the addition of a spine on each of the mounds.

***Megalopsalis caeruleomontium* sp. n.**
http://zoobank.org/F531E2F7-3799-4970-AA4A-26F53A9F95B3
http://species-id.net/wiki/Megalopsalis_caeruleomontium
Figs 10–11

Material examined. *Male holotype*. Mt Kembla, Sydney Catchment Authority Reserve, New South Wales, 34°26'33"S, 150°44'24"E, 11–15 December 1998, L. Gibson, pitfall traps (AMS KS63019; measured).

Paratypes. 2 males, 1 female, Blue Mountains road to Ingar picnic area, New South Wales, 33°46'03"S, 150°24'30"E, 3 October 1996, pitfall trap (AMS KS57166, KS57168; all measured); 3 males, Clyde Mountain, 35°33'S, 149°57'E, 24 October 1968, G. B. M[illedge] (AMS KS65018; measured); 3 males, 2 females, Kirkconnell, 28 May 1972, G. S. Hunt (AMS KS21480; 2 females measured); 1 male, Mt Shivering (near pluviometer), E of Oberon, New South Wales, 23 September 1972, G. S. Hunt (AMS KS21484; measured); 4 males, 6 females, Mt Werong (near pluviometer), New South Wales, 3 July 1972, G. S. Hunt (AMS KS23117; 2 males, 5 females measured); 4 males, 3 females, Muogamarra Nature Reserve, Pacific Highway, 0.7 km SE of Bird Gully Swamp, New South Wales, 33°33'42"S, 151°11'15"E, 2-16 December 1999, M. Gray, G. Milledge, H. Smith, pitfall traps (AMS KS62256; 2 females measured); 1 male, hill NE of Oberon, 10 June 1972, G. S. Hunt (AMS KS21483; measured); 1 male, "Scalloway" pool, Geringong, New South Wales, 23 November 1986, G. Wishart, found 'walking on water' (AMS KS17413, measured).

Diagnosis. *Megalopsalis caeruleomontium* differs from other species of *Megalopsalis* in the presence of setae on the mobile finger of the chelicerae (Fig. 10b). Most males (except the smallest) can also be distinguished by the inflated second segment of the chelicerae (Fig. 10b). *Megalopsalis caeruleomontium* has a relatively flattened penis compared to other *Megalopsalis* species except *M. nigricans*; the glans is rather short, with the sides becoming subparallel distally (Figs 10d–e).

Description. MALE (N = 10). Prosoma length 1.17 (0.88–1.46), width 2.34 (1.98–2.50); total body length 3.25 (2.81–3.88). Propeltidium light orange-brown spotted with white and dark brown patches. Anterior propeltidial area pinkish-brown, with diverging dark-brown lines from ocularium to anterior margin, and dark-brown area around short supracheliceral groove on sharply downturned face. Prosoma unarmed. Ocularium bright white with light orange-brown base and behind eyes; postocularium bright white. Mesopeltidium, metapeltidium and first four segments of opisthosoma grey-brown with slightly lighter median band and distinctive transverse row of black setae in lighter spots across each segment. Posterior part of opisthosoma yellow-brown dusted with dark-brown; anal operculum silver. Coxae pinkish-brown with median white areas proximally; venter of opisthosoma grey-brown.

Chelicerae. Segment I 2.26 (0.57–3.26), segment II 3.36 (1.24–4.55). Segment I medium-brown dorsally and on proximal two-thirds laterally, peach-coloured ventrally and distolaterally, white patch at distolateralmost end with ventrolateral medium-brown patch directly underneath it; denticulate dorsally and on ventrolateral and

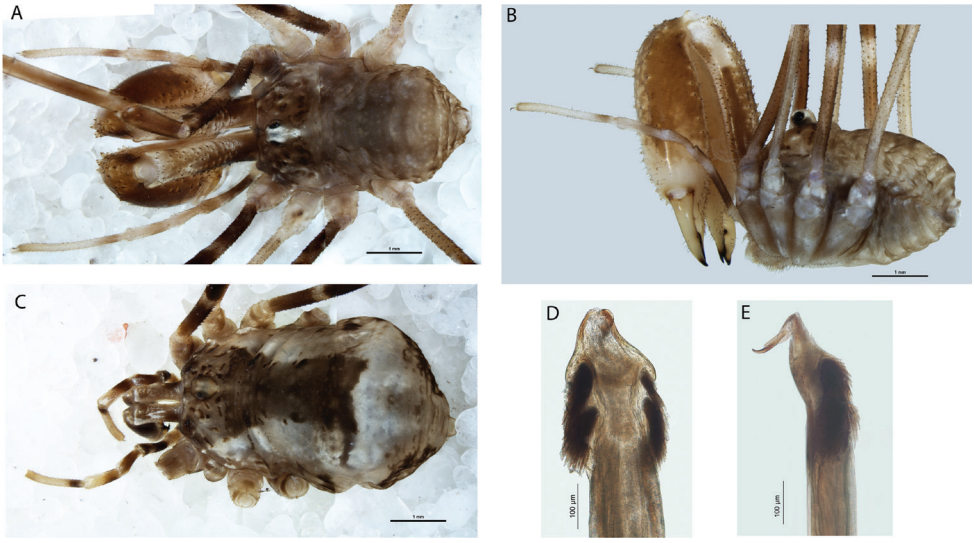

Figure 10. *Megalopsalis caeruleomontium*: **a** body of male, dorsal view (AMS KS63019) **b** body of male, lateral view (AMS KS63019) **c** body of female, dorsal view (AMS KS57168) **d** glans, ventral view (AMS KS63019) **e** glans, right lateral view (AMS KS63019).

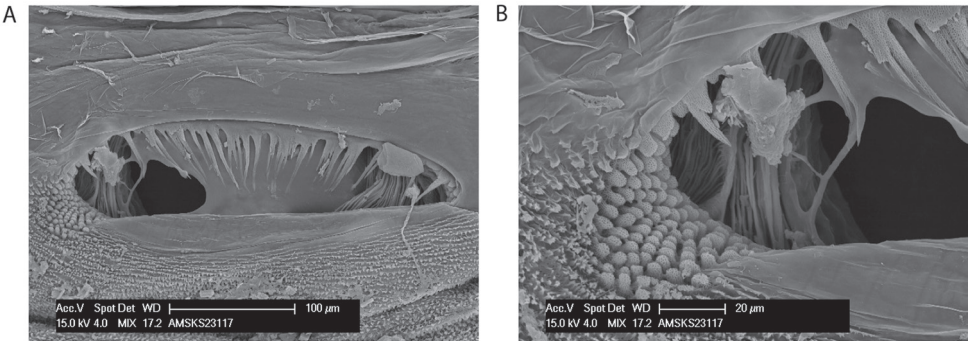

Figure 11. *Megalopsalis caeruleomontium*: **a** spiracle **b** same, close-up of lateral corner.

ventromedial edges. Segment II strongly inflated in larger specimens to not inflated in smallest specimens, proximally mottled medium-brown and pink dorsally, medium-brown laterally, peach ventrally; distally pink-cream, fingers yellow-cream; denticulate dorsally and ventrolaterally. Cheliceral fingers bowed apart proximally in larger specimens, less or not bowed in smaller specimens.

Pedipalps. Femur 1.29 (0–1.46), patella 0.55 (0.37–0.64), tibia 0.78 (0.48–0.95), tarsus 1.63 (1.08–1.91). Trochanter and proximalmost part of femur cream; proximal two-thirds of femur medium-brown, then peach band, then light-brown band; patella pink-brown; tibia pink-brown proximally, cream distally; tarsus pink-brown at proximalmost end, remainder cream. No patellar apophysis. Microtrichia on tarsus and distal third of tibia; tooth-comb on claw.

Legs. Femora 4.26 (3.72–4.65), 7.29 (6.50–8.15), 3.97 (3.60–4.25), 5.90 (5.31–6.28); patellae 1.11 (0.91–1.23), 1.26 (1.06–1.44), 1.08 (0.80–1.30), 1.23 (0.97–1.37); tibiae 3.96 (3.31–4.28), 7.35 (6.50–8.00), 3.81 (3.14–4.10), 5.48 (4.67–6.00). Trochanters pinkish-cream, unarmed. Legs I and III medium-brown with cream bands, legs II and IV yellow-brown. Femora denticulate, with larger denticles dorsally than ventrally; fewer denticles dorsally on patellae, remaining segments unarmed.

Penis (Fig. 10d–e). Tendon long; bristle groups well-developed. Glans in line with shaft; dorsoventrally flattened for entire length with bases of bristle groups (especially left) consequently more ventral than lateral; glans short, sides converging in ventral view. Deep pores.

Spiracle (Fig. 11). Sparse curtain of slender reticulate spines extending only partway across spiracle; terminations of spines multifurcate; dense patch of lace tubercles at lateral corner.

FEMALE (Fig. 10c; N = 10). Prosoma length 1.30 (1.03–1.74), width 2.29 (2.08–2.59); total body length 4.60 (3.88–6.13). Propeltidium medium-grey-brown with dark-brown patches; prosoma unarmed. Ocularium grey-brown, unarmed. Mesopeltidium, metapeltidium and first three segments of opisthosoma medially dark-grey-brown, laterally whitish-grey with dark-brown patches on lateral margins. Posterior part of opisthosoma whitish-grey with mottled dark-brown patches laterally. Coxae light-brown mottled with white proximally followed by central cream band, medium-brown distally darkening to dark-brown pro- and retrolaterally. Mouthparts and genital operculum light tan. Venter of opisthosoma medium-orange-brown densely mottled with silver-white.

Chelicerae. Segment I 0.84 (0.72–0.95), segment II 1.66 (1.49–1.79). Dark orange-brown reticulated with silver dorsally and large silver-white patch distolaterally on first segment; unarmed.

Pedipalps. Femur 1.21 (1.14–1.38), patella 0.55 (0.50–0.59), tibia 0.78 (0.70–0.84), tarsus 1.55 (1.42–1.67). Femur light tan at proximalmost end, remainder medium brown; patella medium brown with small silver patches distolaterally; tibia and tarsus each proximally medium brown, distally light tan silvered dorsally. No apophysis or hypersetose areas; microtrichia over entire length of tibia and tarsus.

Legs. Femora 3.57 (3.38–3.92), 6.30 (5.97–7.23), 3.37 (3.17–3.86), 5.20 (4.94–5.63); patellae 1.10 (1.00–1.15), 1.22 (1.15–1.31), 1.06 (0.95–1.15), 1.18 (1.03–1.26); tibiae 3.40 (3.22–3.76), 6.31 (6.07–6.85), 3.26 (3.06–3.60), 4.84 (4.45–5.06). Trochanters grey-tan mottled with white, unarmed. Legs banded medium brown and light tan, with tan bands overlain by silver from distalmost end of femur to tibia. Femora and patellae with longitudinal rows of small denticles.

Etymology. From the Latin words *caeruleus*, blue, and *mons*, mountain: "of the Blue Mountains", in reference to the distribution of this species.

Comments. Males of this species vary significantly between the largest and smallest individuals in the development of the chelicerae, from inflated with bowed fingers in the largest specimens to slender with unbowed fingers in the smallest. However, variation appears to be more or less continuous (albeit with large individuals distinctly more numerous than small individuals) without a clear division between morphs.

***Megalopsalis coronata* sp. n.**
http://zoobank.org/ACE42F7E-1AB9-48CE-A102-39E2530A452F
http://species-id.net/wiki/Megalopsalis_coronata
Figs 9d, 12, 13a–b

Material examined. *Male holotype*. Queensland, Sunday Creek, 18 December 1996–20 January 1997, G. Monteith, rainforest intercept (QM S40679).

Paratypes. 1 male, ditto (QM S40679); 1 male, ditto, Conondale Range, 900 m, 2 March–12 April 1992, D. J. Cook, rainforest pitfall (QM S74237).

Diagnosis. *Megalopsalis coronata* is distinguished from all other *Megalopsalis* species except *M. tanisphyros*, *M. puerilis* and *M. sublucens* by its small, unarmed chelicerae. It is distinguished from *M. tanisphyros* by the absence of a pedipalpal patellar apophysis, from *M. puerilis* by the presence of denticles on the ocularium, and from *M. sublucens* by the absence of ventral brush-like bristles on distitarsi III and IV. The glans of *M. coronata* is relatively long compared to other *Megalopsalis* species, with a lower angle of convergence between the sides in ventral view (Fig. 12c).

Description. MALE (N = 3). Prosoma length 0.97 (0.93–1.04), width 1.79 (1.74–1.86); total body length 1.94 (1.78–2.13). Propeltidium golden-brown reticulated with iridescent white, anterior propeltidial area mottled with black; prosoma unarmed. Lateral shelves mostly iridescent white. Mesopeltidium and metapeltidium medially light golden-brown with transverse rows of iridescent white spots, laterally iridescent gold-white. First three segments of opisthosoma medially yellow-brown with iridescent white spots, median area broadening posteriorly; laterally solid gold-white, fading posteriorly, with medium brown edges medially and along boundary of segments I and II. Posterior part of opisthosoma patched white and mottled purple. Coxae I-III yellow-cream; coxae IV and venter of opisthosoma orange.

Chelicerae. Segment I 0.48 (0.36–0.57), segment II 1.09 (1.06–1.11). Iridescent white articular membranes between prosoma and chelicerae. Chelicerae white-cream reticulated with iridescent white; unarmed. Fingers long, closing tightly against each other.

Pedipalps. Femur 0.89 (0.89–0.90), patella 0.44 (0.42–0.45), tibia 0.53 (0.51–0.55), tarsus 1.09 (1.05–1.12). White-cream, unarmed. Patella with angular mediodistal bulge, but no apophysis; medial side not hypersetose. Small number of plumose setae on mediodistal end of patella only (Fig. 9d). Microtrichia along most of tarsus; claw with ventral tooth row.

Legs. Femora 3.60, 6.70 (6.46–6.93), 3.48 (3.36–3.70), 5.45 (5.13–5.94); patellae 0.88, 0.97 (0.95–0.98), 0.80 (0.75–0.85), 0.93 (0.88–0.95); tibiae 3.36, 7.40 (7.38–7.42), 3.06 (2.84–3.36), 4.91 (4.63–5.25). Trochanters medium-brown, unarmed. Legs banded medium-brown and golden-brown; legs I and III predominantly medium-brown, legs II and IV predominantly golden-brown. Femora with scattered denticles, remaining segments unarmed.

Penis (Figs 12c–d). Tendon relatively short; bristle groups well-developed. Glans of medium length; sides in ventral view subparallel, converging only slightly; dorsal side angled only slightly dorsad from shaft. Pores with surrounding rim, not raised.

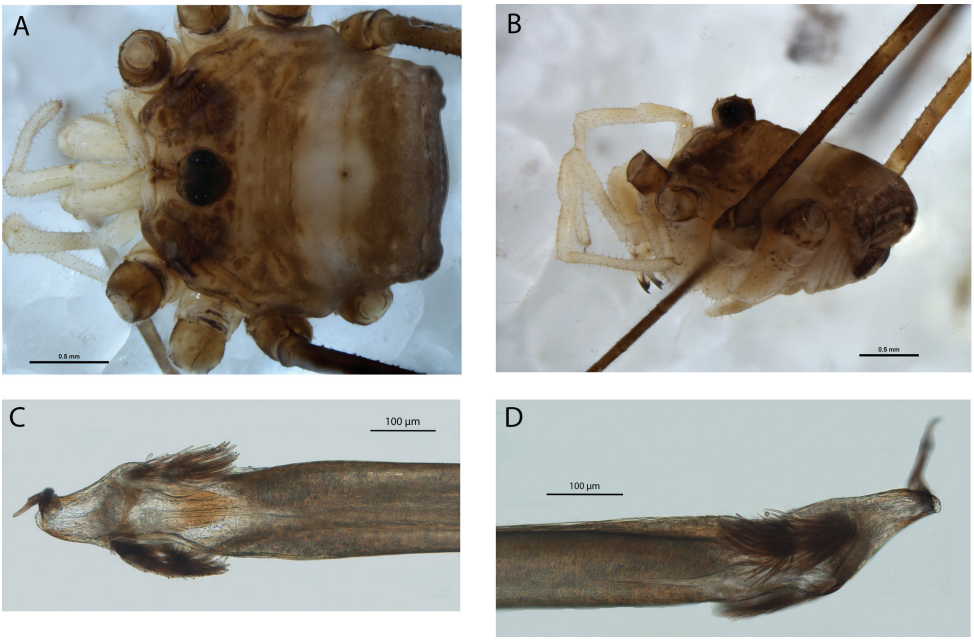

Figure 12. *Megalopsalis coronata*, male (all QM S74237): **a** body, dorsal view **b** body, lateral view **c** glans, ventral view **d** glans, right lateral view.

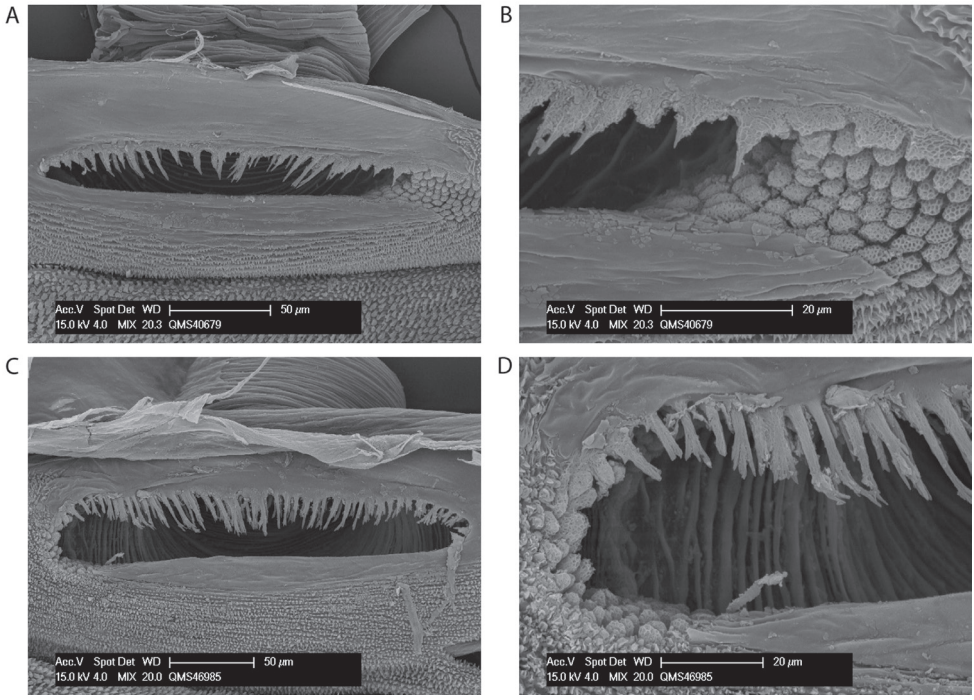

Figure 13. Spiracles of *Megalopsalis* species: **a** *M. coronata*, spiracle **b** same, close-up of lateral corner **c** *M. puerilis*, spiracle **d** same, close-up of lateral corner.

Spiracle (Figs 13a–b). Sparse curtain of reticulate spines extending partway across spiracle; spines basally much broader than terminally; terminations of spines simple, pointed, some larger central spines multifurcate; dense patch of lace tubercles at lateral corner.

Variation. The paratype specimens differ in coloration from the holotype, but this may be due to preservation. QM S74237 has the prosoma golden-brown mottled with orange-brown patches, while both QM S74237 and the paratype QM S40679 have a brown transverse band, cream in the former and iridescent white in the latter, across the anterior part of the opisthosoma.

Etymology. From the Latin *coronatus*, crowned, referring to the denticulate ocularium.

Comments. Leg I was only preserved in the holotype.

Megalopsalis nigricans (Hickman 1957), comb. n.

http://species-id.net/wiki/Megalopsalis_nigricans
Fig. 14

Spinicrus nigricans Hickman, 1957: 77, figs 34–40.

Material examined. 1 major male, Tasmania, Mount Wellington, 4 January 1969, J. L. Hickman, under logs (AMS KS23719); 1 major male, Tasmania, V. V. Hickman (AMS KS23737); 1 female, SW Tasmania, 12 February 1977, C. Howard, C. Johnson (AMS KS24747); 1 minor male, ditto (AMS KS24749); 2 minor males, NE Tasmania, August 1993 (QM C3.2, C5.1); 1 minor male, 1 female, SW Tasmania, Mount Rufus track, 42°07'S, 146°07'E, 29 April 1987, R. Raven, T. Churchill, open forest, pyrethrum knockdown (QM S1707).

Description. MALE. As for Hickman (1957), except minor male (Fig. 14a): As for major male, except chelicerae not enlarged relative to female. Armature of chelicerae reduced: segment I mostly unarmed with ventral spur, segment II with dorsal longitudinal row of denticles only, with long black seta on each denticle.

Spiracle (Taylor 2011: fig. 25). Curtain of partially reticulate spines (reticulation reduced basally) extending partway across spiracle; spines broad, terminations palmate; dense patch of lace tubercles at lateral corner, outer lace tubercles terminally anastomosing.

Comments. This species has already been described in detail by Hickman (1957). As noted above in the discussion of the phylogenetic analysis, this is the most divergent species here assigned to *Megalopsalis*. Its genital morphology is unique: the shaft of the penis is distinctly short and broad (Fig. 14b), in contrast to the elongate shaft of other *Megalopsalis* species (see figures in Taylor 2011). The glans is strongly flattened, not proximally inflated as in other species, and the overall shape is less distinctly subtriangular than in other *Megalopsalis* species, being rather more oblong over the greater part. The ozopores of *M. nigricans* are small and round, and not raised on lateral lobes like the larger ozopores of other Enantiobuninae.

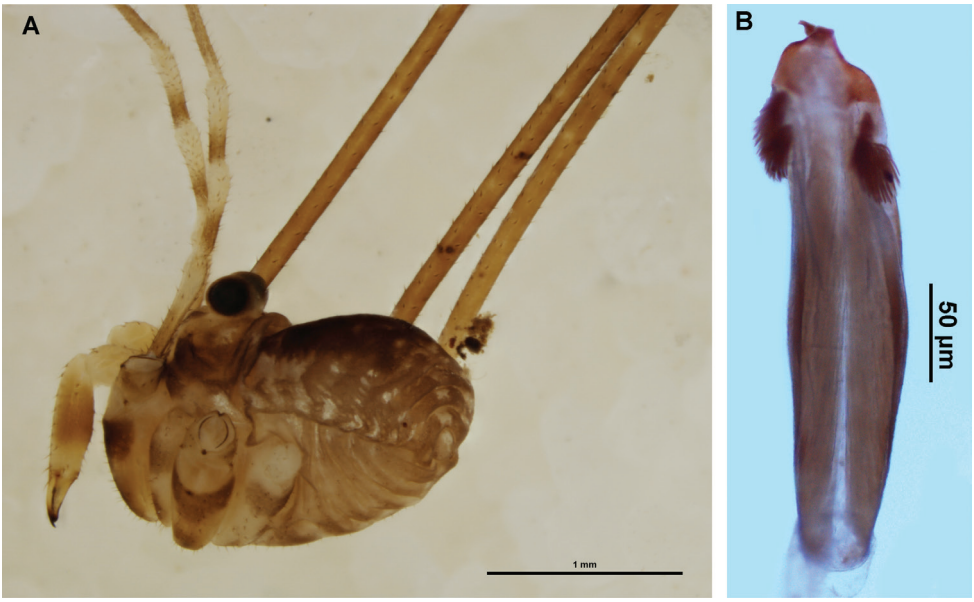

Figure 14. *Megalopsalis nigricans*: **a** minor male, lateral view (AMS KS24749) **b** penis, ventral view (AMS KS23719).

Despite Hickman (1957) describing only the major male of this species, collections of this species in AMS and QM indicate that minor males are more abundant and majors relatively uncommon.

***Megalopsalis puerilis* sp. n.**
http://zoobank.org/6ED54D80-108C-4AFC-BB79-E9B5B92CB5E4
http://species-id.net/wiki/Megalopsalis_puerilis
Figs 13c–d, 15

Material examined. *Male holotype*. SE Queensland, Binna Burra, 27 March 1976, R. Raven, VED, night collection (QM S2835).

Paratype. 1 male, Springbrook Repeater, SE Queensland, 1000 m, 28°15'S, 153°16'E, 9 January–19 February 1995, G. B. Monteith, intercept traps (QM S46985).

Diagnosis. *Megalopsalis puerilis* is distinguished from all other *Megalopsalis* species except *M. tanisphyros*, *M. coronata* and *M. sublucens* by its small, unarmed chelicerae. It is distinguished from *M. tanisphyros* by the absence of a pedipalpal patellar apophysis, from *M. coronata* by the absence of denticles on the ocularium, and from *M. sublucens* by the absence of ventral brush-like bristles on distitarsi III and IV. The glans of *M. puerilis* is less triangular in overall shape than most other *Megalopsalis* species, with the sides distally subparallel in ventral view (Fig. 15c).

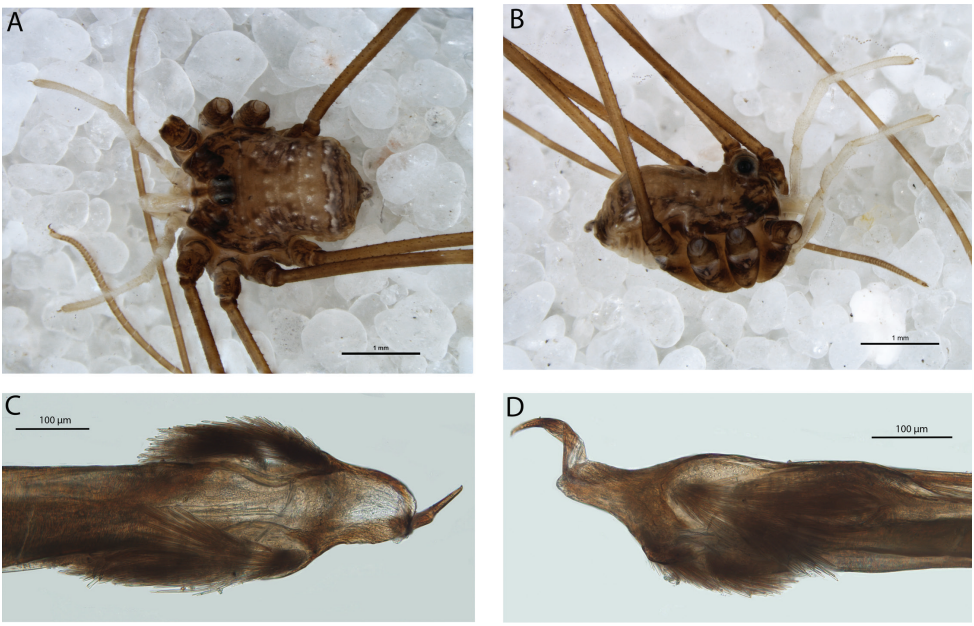

Figure 15. *Megalopsalis puerilis*, male (all QM S2835): **a** body, dorsal view **b** body, lateral view **c** glans, ventral view **d** glans, left ventrolateral view.

Description. MALE (N = 2). Prosoma length 0.89 (0.83–0.94), width 1.72 (1.56–1.88); total body length 2.37 (2.35–2.38). Dorsum entirely unarmed. Anterior propeltidial area with central stripe of light orange-brown between ocularium and anterior margin of prosoma, flanked by two yellow stripes; remainder of anterior and median propeltidial areas mottled black and dark orange-brown with broad iridescent dark silver patches between ocularium and ozopores. Ocularium iridescent white with dark grey stripe down central groove. Mesopeltidium, metapeltidium and first four segments of opisthosoma orange-yellow medially and along segment boundaries with blackish brown patches laterally; fifth opisthosomal segment with transverse iridescent white stripe bordered by mottled black; remaining segments mottled black with yellow segment boundaries. Mouthparts brown-cream. Coxae dull orange proximally, mottled black distally; venter of opisthosoma iridescent white.

Chelicerae. Segment I 0.53 (0.52–0.54), segment II 1.07 (1.00–1.14). Cream; segment I with iridescent white reticulation dorsally. Both segments unarmed. Fingers long; mobile finger closes tightly with segment II.

Pedipalps. Femur 0.94 (0.90–0.97), patella 0.45 (0.44–0.45), tibia 0.58 (0.57–0.59), tarsus 1.15 (1.14–1.15). Cream; unarmed. Patella with distomedial bulge, but no true apophysis. Microtrichia on distal three-quarters of tarsus; claw with ventral tooth-comb. *Legs*: Femora 4.16 (3.86–4.45), 7.20 (6.08–8.31), 4.00 (3.76–4.23), 5.65 (5.10–6.19); patellae 0.91 (0.87–0.94), 1.13, 0.87 (0.84–0.89), 1.00 (0.98–1.02); tibiae 4.10 (3.64–4.55), 7.50 (6.46–8.54), 3.74 (3.46–4.02), 5.46 (4.98–5.94). Trochanters mottled black

on orange, remaining segments orange-yellow, with widely-spaced mottled black transverse stripes. Femora with scattered denticles, mostly dorsal; other segments unarmed.

Penis (Figs 15c–d). Bristle groups well-developed on both sides, left groups set slightly back and longer than right groups. Glans short, sides in ventral view subparallel, dorso-ventrally flattened distally, dorsal surface in plane with shaft. Deep pores.

Spiracle (Figs 13c–d). Curtain of robust reticulate spines extending only partway across spiracle; terminations of spines multifurcate but not palmate; lace tubercles on margin of lateral corner only.

Etymology. From the Latin *puerilis*, childish, referring to the lack of ornamentation or significant secondary sexual characteristics in the adult male.

***Megalopsalis stewarti* (Forster 1949), comb. n.**
http://species-id.net/wiki/Megalopsalis_stewarti
Figs 16, 18a

Spinicrus stewarti Forster, 1949: 68–70, figs 11–16.

Material examined. *Paratypes*. 1 female, Victoria, Mount Buffalo, 30–31 December 1947, ex bole of snow gum (*Eucalyptus pauciflora*) (NMV K-8910); 8 males, ditto (NMV K-8911–8919).

Other material examined. 1 male, Victoria, Lala Falls, near Warburton, 37°46'S, 145°42'E, 22 December 2002, M. S. Harvey, M. E. Blosfelds, under bark of *Eucalyptus regnans* (WAM T72315).

Description. MALE. Description as in Forster (1949), except following.

Legs. Leg I with anterior longitudinal row of enlarged denticles from proximal end of femur to distal end of tibia (males with smaller chelicerae with reduced denticle row on femur only), scattered denticles on basitarsus I; smaller row on femora and patellae of other legs.

Penis (Fig. 16). Shaft and tendon elongate; all four bristle-groups well-developed. Distinct lateral protrusion of glans above left anterior bristle group. Glans short, broad, triangular in dorsal view, dorsoventrally flattened at distal end. Pores shallowly recessed.

Spiracle (Fig. 18a). Reticulate spines extending only partway across spiracle; terminations of spines palmate; small group of lace tubercles in lateral corner.

FEMALE. Description as in Forster (1949), except all legs with dorsal longitudinal row of small denticles along femora.

Comments. Forster (1949) stated that the holotype and female paratype had been deposited in NMV, while the remaining male paratypes (of unspecified number) had been deposited in the Canterbury Museum, Christchurch, New Zealand (CMNZ). However, as indicated above, NMV holds eight male specimens of this species labelled as paratypes. Because these specimens share the same collection data as the female paratype, it seems likely that these correspond to the specimens that Forster (1949) intended to place in CMNZ.

Figure 16. *Megalopsalis stewarti*, male, glans (all WAM T72315): **a** ventral view **b** right lateral view **c** dorsal view.

M. thryptica is very similar to *M. stewarti*, from which it can be distinguished by having distitarsus IV basally swollen. Hickman (1957) initially distinguished *Megalopsalis stewarti* from *M. thryptica* by the presence of denticles on tibia I in males of *M. thryptica*, compared to their supposed absence in *M. stewarti* as described by Forster (1949). However, specimens of *M. stewarti* with longer chelicerae also have more extensive denticulation on leg I, extending as far as the basitarsus in some specimens. There is insufficient data as yet to determine whether this indicates a division between major and minor males or whether variation is continuous. *Megalopsalis thryptica* may still be distinguished from *M. stewarti* by the male of the former having distitarsus IV basally inflated (personal examination of holotype, AMS).

***Megalopsalis sublucens* sp. n.**
http://zoobank.org/7EAD50EE-61F4-40AB-9EFE-B6164D1596A1
http://species-id.net/wiki/Megalopsalis_sublucens
Figs 17, 18b–c

Material examined. *Male holotype*. SW Tasmania, Franklin River, below Goodwin's Peak, January 1983, ANZSS Expedition (QM S2857).

Paratypes. 1 male, 1 female, as above (QM S2857).

Diagnosis. *Megalopsalis sublucens* can be readily distinguished from other *Megalopsalis* species by the absence of a pedipalpal patellar apophysis or enlarged chelicerae, in combination with the presence of ventral brush-like bristles on distitarsi III and IV. It can also be distinguished from other species except *M. stewarti* by the presence of a lateral protrusion on the left side of the glans near the shaft-glans junction (Fig. 17c).

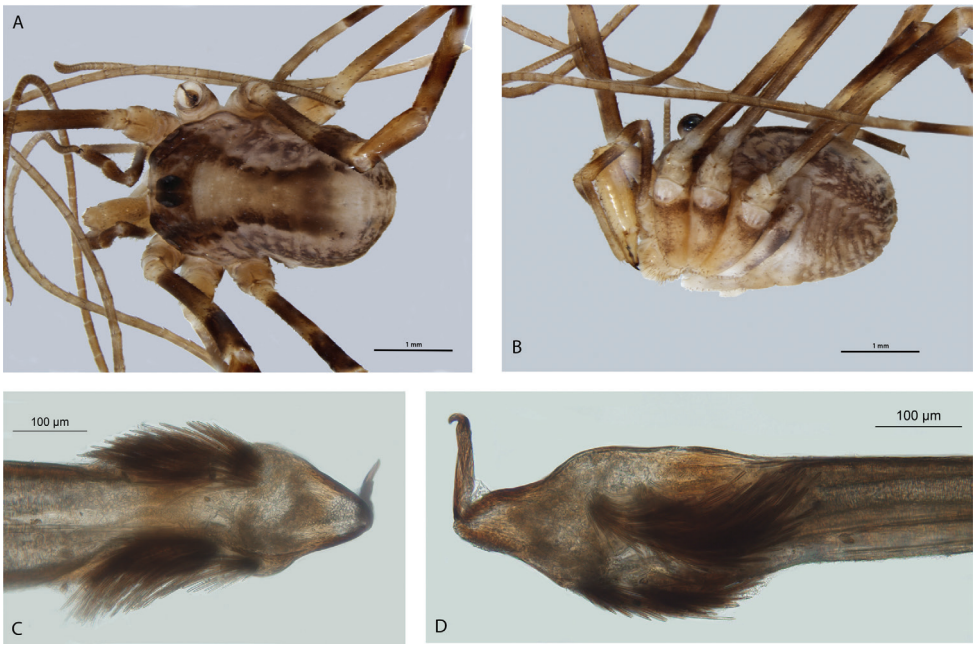

Figure 17. *Megalopsalis sublucens*, male (all QM S2857): **a** body, dorsal view **b** body, lateral view **c** glans, ventral view **d** glans, left ventrolateral view.

Description. MALE (N = 2). Prosoma length 1.34 (1.33–1.34), width 1.99 (1.98–2.00); total body length 2.66 (2.59–2.72). Dorsum entirely unarmed. Dark tan stripes from ocularium to anterior margin, remainder of anterior iridescent white. Median propeltidial area white with dark brown patches. Posterior propeltidial area mottled dark brown. Lateral shelves dark brown anteriorly, iridescent white around and posterior to ozopores. Ocularium golden-brown with anterior face silver. Mesopeltidium, metapeltidium and first four segments of opisthosoma medially yellow-brown edged with dark brown with medial iridescent white spots; laterally iridescent white with dark purple mottling. Posterior of opisthosoma white with purple mottling. Venter of prosoma cream, coxae mottled black distally; opisthosoma purple-brown with transverse rows of iridescent white spots.

Chelicerae. Segment I 0.68, segment II 1.65 (1.57–1.73). Yellow-cream with tan mottling; not particularly enlarged compared to female. Segment I unarmed, segment II with proximodorsal denticles only. Fingers long, apotele closely opposed to finger of segment II.

Pedipalp. Femur 1.13 (1.11–1.15), patella 0.54 (0.50–0.58), tibia 0.70, tarsus 1.35 (1.32–1.38). Banded dark brown and yellow-brown; unarmed; no apophyses. Tooth-comb on apotele.

Legs. Femora 3.50 (3.42–3.58), 6.26 (6.13–6.38), 3.28, 5.44 (5.19–5.69); patellae 1.17 (1.13–1.20), 1.27, 1.02, 1.13 (1.06–1.20); tibiae 3.15 (3.07–3.22), 5.48, 3.08, 4.70 (4.50–4.90). Banded dark brown and yellow-brown, with prominent iridescent white spots around accessory spiracles on tibiae. No denticles, but robust spinose setae

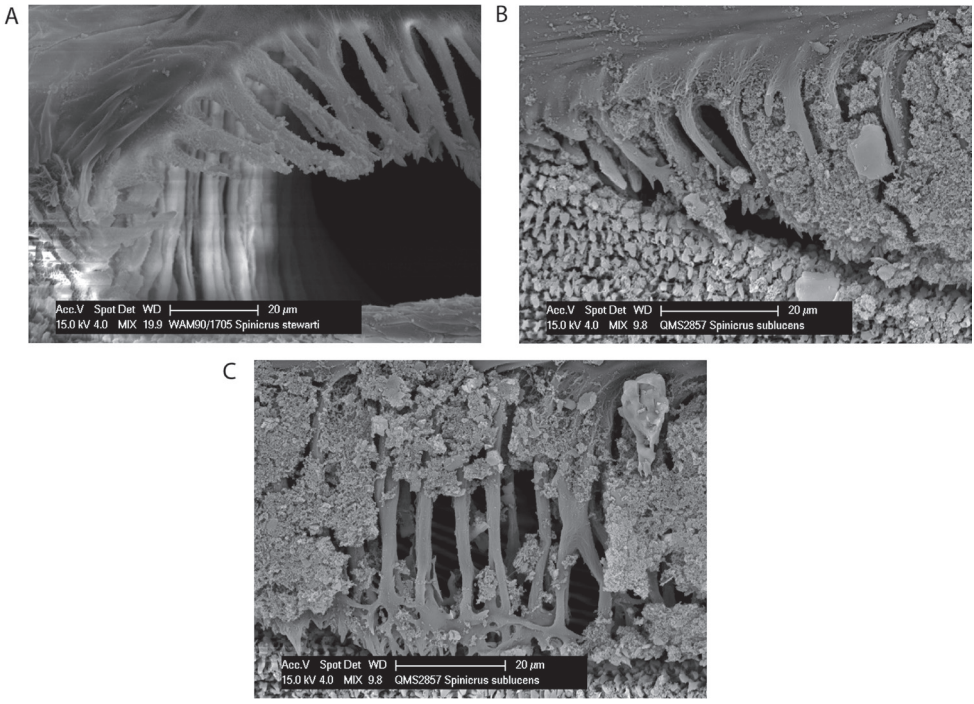

Figure 18. Spiracles of *Megalopsalis* species: **a** *M. stewarti*, lateral corner **b** *M. sublucens*, lateral corner **c** same, showing anastomosing ends of median spines.

on all legs to tibiae. Brush-like bristles intermittently present on ventral side of distitarsi III and IV. Femur II not pseudosegmented, tibia II with six pseudosegments, tibia IV with two pseudosegments.

Penis (Figs 17c–d). Left anterior bristle group reduced, but left posterior group well-developed. Glans short, triangular in dorsal view, dorsoventrally flattened, dorsal edge in plane with shaft.

Spiracle (Figs 18b–c). Sparse spines, reticulate basally with reticulations fading terminally, extending across spiracle; terminations of spines palmate, anastomosing; no lateral lace tubercles.

FEMALE (N = 1). Prosoma length 1.40, width 2.03; total body length 4.45. As for male except for following. Ocularium iridescent white. Venter of opisthosoma duller.

Chelicerae. Segment I 0.75, segment II 1.32. Unarmed.

Pedipalps. Femur 1.01, patella 0.50, tibia 0.64, tarsus 1.27.

Legs. Femora 2.32, 4.45, 2.28, 3.56; patellae 0.82, 1.01, 0.93, 0.95; tibiae 2.43, 4.30, 2.35, 3.44. Tibia IV undivided.

Etymology. From the Latin *sublucens*, gleaming faintly, in reference to the iridescent patches covering part of the dorsum.

Comments. Those measurements for which a range is not given in the description of the male were only preserved in the holotype.

While *Megalopsalis sublucens* possesses brush-like bristles on distitarsi III and IV as found in *M. stewarti*, *M. tasmanica* and species of the *M. serritarsus*-group, the number of bristles is reduced and they are proportionately more widely spaced and less regular. This may be related to *M. sublucens*' smaller size.

Phylogenetic analysis

A maximum parsimony analysis was conducted using the programme TNT (Goloboff et al. 2008); apomorphies were mapped onto the resulting trees using the programme Winclada (Nixon 1999). An initial analysis was conducted with all characters given equal weight, followed by successive implied weighting analyses with *k* varying in values of 1.0 from 1.0 to 6.0. Heuristic ("traditional") searches were conducted using a Wagner-tree random seed, 10 replicates holding 10 trees per replication and constructing trees using a tree bisection-reconnection (TBR) swapping algorithm. Changes from an unambiguous character state to a polymorphic character are counted by TNT as a step, even if the ancestral character state is included in the polymorphism. Jack-knife resampling analysis was conducted with a 36% removal probability over 1000 replications. The character matrix was based on that used in Taylor (2011); see therein for descriptions and discussion of characters not elaborated on below, and for specimen details of outgroup taxa (note that the name *Pantopsalis luna* [Forster, 1944] has been replaced by *Pantopsalis listeri* [White, 1849] as per Taylor 2013). As the monophyly of Eupnoi is well supported (Shultz 1998; Giribet et al. 2002, 2009), representatives of Dyspnoi were excluded in order to reduce the effects of possible homoplasy. The recently described *Mangatangi parvum* Taylor, 2013 was also added to the matrix; see Taylor (2013) for specimen details for this taxon. *Americovibone lanfrancoae* Hunt & Cokendolpher, 1991 was coded based on the description given by Hunt and Cokendolpher (1991). Characters with more than two states have been treated as additive in the order given in initial analyses unless otherwise specified; a further set of analyses was conducted with all characters unordered. The characters used in the analysis are as follows:

1: *Elongate anterior propeltidial area, sloping downwards anteriorly*: (0) absent; (1) present.
2: *Ozopore position*: (0) flush with lateral margin of prosoma; (1) raised on protruding lobes.
3: *Ozopore shape*: (0) small and circular; (1) large and oval or oblong.
4: *Raised humps on either side of ocularium*: (0) absent; (1) present.
5: *Raised postocularial hump*: (0) absent; (1) present.
6: *Mesopeltidium*: (0) distinct; (1) merged with propeltidium.
7: *Position of anterior margin of mesopeltidium relative to ocularium*: (0) mesopeltidium immediately behind ocularium; (1) distinct space between ocularium and anterior margin of mesopeltidium.
8: *Metapeltidium*: (0) non-sclerotised; (1) sclerotised.

9: *Dorsal junction between prosoma and opisthosoma*: (0) free; (1) fused.
10: *Dorsum of opisthosoma*: (0) non-sclerotised; (1) sclerotised.
11: *Penis tendon*: (0) long; (1) short.
12: *Angular ventral junction between shaft and glans*: (0) absent; (1) present.
13: *Lateral processes behind shaft-glans articulation*: (0) absent; (1) present.
14: *Bristle groups as lateral processes of penis*: (0) absent; (1) present.
15: *Asymmetry of penis bristle groups*: (0) both sides present; (1) left bristle groups absent in ventral view.
16: *Fused base of lateral bristles on penis*: (0) absent; (1) present.
17: *Dorsal edge of glans*: (0) in same plane as shaft; (1) directed dorsad relative to shaft.
18: *Lateral extension on left side of glans*: (0) absent; (1) present. In *Megalopsalis stewarti* and *M. sublucens*, the left side of the glans protrudes outwards above the anterior bristle group (Figs 16c, 17d).
19: *Setae or bristles on glans*: (0) absent; (1) single lateral setae; (2) numerous setae or bristles.
20: *Deeply recessed pores on glans*: (0) absent; (1) present.
21: *Raised pore-bearing papillae on glans*: (0) absent; (1) present. These last two characters were treated as separate states of a single character in Taylor (2011; character 25 therein). This was probably inappropriate: there is no *a priori* reason to believe that a single species could not possess both pore morphologies, and they are here treated separately. Taylor (2011) also differentiated character states for shallowly recessed or shallowly raised genital pores; upon re-examination of the electron micrographs used in coding these states, I am not convinced that they are not artefactual (possibly related to the preservation of the specimen used). I have therefore not included these states in the current analysis.
22: *Glans length*: (0) short; (1) long.
23: *Glans depth*: (0) shallow in lateral view; (1) distinctly deep. In *Pantopsalis albipalpis*, the glans is surmounted by a relatively high, narrow dorsal keel, but the main body of the glans is still recognisable a narrow triangular shape in lateral view, contrasting with the more uniformly deep glans in *Tercentenarium linnaei* (Taylor 2008b) and *Australiscutum* species (Taylor 2009). *Pantopsalis albipalpis* is therefore coded as lacking this character.
24: *Glans shape in ventral view*: (0) subtriangular; (1) parabolic; (2) narrow or constricted. This character replaces character 19 in Taylor (2011), in which the alternate character states were poorly distinguished. A subtriangular glans characterises the species discussed in the current paper (as well as those attributed to *Megalopsalis* in Taylor 2011), in which the sides converge along the greater length of the relatively broad glans. Species of genera such as *Pantopsalis* (Taylor 2004, 2013) and *Australiscutum* (Taylor 2009) have a parabolic glans shape, in which the glans is relatively longer and the rate of convergence of the sides less rapid. Species of outgroup taxa such as Ballarrinae (Hunt and Cokendolpher 1991), as well as *Monoscutum titirangiense* (Taylor 2008a) have a very narrow, elongate glans.
25: *Central concavity on ventral face of glans*: (0) absent; (1) present.

26: *Dorsal side of glans basally inflated*: (0) absent; (1) present (e.g. Figs 3e, 4e).
27: *Shape of distal end of glans*: (0) not dorsoventrally flattened; (1) distinctly dorsoventrally flattened.
28: *Protruding distal end of glans*: (0) absent; (1) present. In species exhibiting this character, the glans is essentially subtriangular in overall shape, but the distal end of the glans has become extended, with the lateral margins becoming more subparallel distally after converging in the proximal part of the glans (Figs 10d, 15c).
29: *Triangular dorsolateral keel on glans*: (0) absent; (1) present.
30: *Sharp dorsal papillae on glans*: (0) absent; (1) present.
31: *Longitudinal membrane on stylus*: (0) absent; (1) present; (2) enlarged. Species of Neopilionidae have a longitudinal membranous banner running along the stylus, and often wrapped around it. This membrane has become particularly large in *Australiscutum*. *Ballarra longipalpus* is coded as lacking this character, though its presence in *Americovibone lanfrancoae* suggests its absence may be secondary for the former species; small membranous flanges at the base of the stylus in *Ballarra* species (Hunt and Cokendolpher 1991) may represent the remnants of a reduced banner.
32: *Number of seminal receptacles*: (0) two; (1) four.
33: *Microsculpture anterior to spiracle*: (0) unornamented; (1) ornamented.
34: *Spiracular entapophysis*: (0) absent; (1) present.
35: *Anterior spines at spiracular aperture*: (0) absent; (1) Dyspnoi-form spines; (2) *Thrasychirus*-form spines or lace tubercles. This character has not been treated as additive. See Taylor (2011) for a discussion of the potential homology or otherwise between the spiracular spines present in Enantiobuninae and those present in Dyspnoi and *Caddo*. *Ballarra longipalpus* was coded by Taylor (2011) as exhibiting a fourth state of this character; however, as illustrated by Taylor (2011: fig. 15), the spiracular spines of *B. longipalpus* are derived from hypertrophy of the micro-ornamentation covering the broader venter, and are almost certainly not directly homologous with the spines present in Enantiobuninae, which are restricted to the spiracle and differ from the surrounding micro-ornamentation. The character state '*Ballarra*-form spines' has therefore been removed from the current analysis, and *B. longipalpus* has been coded as lacking this character. *Neopilio australis*, previously coded as unknown for this character, has been re-coded as possessing *Thrasychirus*-form spines on the basis of the figure provided by Hunt and Cokendolpher (1991).
36: *Reticulate anterior spiracular spines*: (0) absent; (1) present.
37: *Extent of anterior spines over spiracle*: (0) absent; (1) halfway; (2) entire spiracle.
38: *Terminations of anterior spiracular spines*: (0) simple; (1) palmate.
39: *Lace tubercles at corner of spiracle*: (0) absent; (1) present. *Megalopsalis suffugiens* possesses a patch of lace-like reticulation marking the position occupied by the lace tubercles in other taxa, and has been coded as possessing this character.
40: *Posterior margin of spiracle*: (0) unornamented; (1) short ornamentation; (2) elongate spines.
41: *Ventral spur at base of cheliceral segment I*: (0) absent; (1) present.

42: *Ventrolateral row of enlarged denticles on cheliceral segment I*: (0) absent; (1) present.
43: *Cheliceral segment II compared to segment I*: (0) not significantly inflated; (1) inflated.
44: *Cheliceral finger length*: (0) short; (1) long.
45: *Mobile finger of chelicera*: (0) closes tightly against immobile finger of segment II; (1) bows away from immobile finger proximally.
46: *Setae on mobile finger of chelicera*: (0) absent; (1) present.
47: *Medial side of pedipalpal coxae*: (0) unarmed; (1) with covering of blunt denticles.
48: *Plumose setae on pedipalp*: (0) absent; (1) present.
49: *Length of pedipalpal femur*: (0) shorter than or subequal to prosoma length; (1) more than 1.5 × as long as prosoma.
50: *Pedipalpal patella vs tibia*: (0) patella shorter than tibia; (1) patella longer than tibia.
51: *Medial side of pedipalpal patella*: (0) sparsely setose; (1) hypersetose.
52: *Apophysis on pedipalpal patella*: (0) absent; (1) poorly developed (less than one-third of patella length); (2) well-developed (about one-half of patella length). In Taylor (2011), the presence of a pedipalpal patellar apophysis was coded separately for males and females; this risked inappropriately weighting the significance of the patellar apophysis as the two characters are closely correlated. Instead, the presence of a pedipalpal patellar apophysis has here been coded as a single character, with a second character (character 53 below) coded only for species possessing the apophysis to account for the reduction of the apophysis in the male of *Pantopsalis* species relative to the females.
53: *Pedipalpal patellar apophysis in male*: (0) reduced relative to female apophysis; (1) fully developed as in female.
54: *Shape of apophysis on pedipalpal patella*: (0) rounded; (1) triangular. As with character 52, this character has been coded for both males and females rather than the two being coded separately as in Taylor (2011). The only species in which males and females are known to differ in apophysis shape, *Forsteropsalis grimmetti*, has been coded as polymorphic for this character.
55: *Pedipalp with reflexed tibia relative to patella*: (0) absent; (1) present. A dorsally reflexed pedipalpal tibia is characteristic of the Ballarrinae (Hunt and Cokendolpher 1991).
56: *Shape of pedipalpal tibia*: (0) straight; (1) bent mediad from patella.
57: *Distribution of microtrichia on pedipalp*: (0) absent; (1) distal half to third of tarsus only; (2) full length of tarsus; (3) tibia and tarsus.
58: *Pedipalpal claw*: (0) reduced or absent; (1) present. *Neopilio australis* has been coded as possessing a reduced pedipalpal claw, as per Hunt and Cokendolpher (1991).
59: *Teeth on pedipalpal claw*: (0) absent or only one or two teeth; (1) tooth-comb.
60: *Armature of coxa I*: (0) absent; (1) present.
61: *Armature of trochanter I*: (0) absent; (1) present in the form of prolateral denticles only; (2) present in the form of prolateral and retrolateral denticles; (3) present in the form of retrolateral denticles only. This character has not been treated as additive.
62: *Leg I length and shape*: (0) long and slender; (1) short and sturdy.
63: *Leg I armature in male*: (0) absent; (1) present on femur; (2) present on femur to patella; (3) present on femur to tibia; (4) present on femur to basitarsus; (5) present on femur to distitarsus.

64: *Arrangement of denticles on leg I*: (0) scattered; (1) sublinear; (2) linear.
65: *Prolateral longitudinal row of hypertrophied spines on leg I*: (0) absent; (1) present.
66: *Pseudoarticulations in femur II*: (0) absent; (1) present.
67: *Accessory tracheal stigmata in tibiae*: (0) absent; (1) present.
68: *Tibia II shape*: (0) cylindrical; (1) swollen.
69: *Pseudoarticulations in tibia II*: (0) absent; (1) present.
70: *Pseudoarticulations in tibia IV*: (0) absent; (1) present.
71: *Pseudoarticulations in basitarsi*: (0) absent; (1) present.
72: *Ventrodistal spines on basitarsal pseudosegments*: (0) absent; (1) present.
73: *Mobile hinge between basitarsus and distitarsus*: (0) absent; (1) present.
74: *Ventrodistal spines on the junction of the basitarsus and distitarsus*: (0) absent; (1) present.
75: *Ventrodistal swelling on pseudosegments of distitarsus II*: (0) absent; (1) present.
76: *Ventral double row of brush-like bristles on distitarsi III and IV*: (0) absent; (1) present.
77: *Ventrodistal spines on distitarsal pseudosegments*: (0) absent; (1) present.
78: *Proximal part of distitarsi III and IV*: (0) not swollen; (1) swollen.

Results and discussion

The analysis with all characters given equal weight, and multistate characters treated as ordered, produced two equally supported trees of 321 steps (CI = 0.290, RI = 0.626), the consensus of which is shown in Fig. 19. Bremer support for most clades was low, and very few can be regarded as numerically well supported. Nevertheless, monophyly was recovered for Neopilionidae (including Ballarrinae) and Enantiobuninae *sensu* Taylor (2011). Enantiobuninae was placed as sister to a clade of *Neopilio australis* and Ballarrinae. All implied weights analyses returned a single best tree, agreeing with the equal weight analysis on the monophyly of Neopilionidae and Enantiobuninae. Figure 20 shows the majority-rule consensus for all trees recovered under various weighting schemes with ordered characters; Table 1 shows support for selected clades under individual weighting schemes.

A second round of analyses was also conducted with multistate characters treated as unordered. When all characters were given equal weight, this analysis produced two equally supported trees of 309 steps (CI = 0.301, RI = 0.633), the consensus of which is shown in Fig. 21. Though Neopilionidae was recovered as monophyletic in both trees, Enantiobuninae was only recovered in one tree, in which *Neopilio australis* and Ballarrinae were sister taxa as in the analyses with ordered characters. In the other best tree, *Neopilio australis* alone was sister to the remaining Neopilionidae, while *Tercentenarium linnaei* was placed outside a clade of Ballarrinae and the remaining Enantiobuninae. All implied weights analyses with unordered characters recovered a single best tree in which both Neopilionidae and Enantiobuninae were monophyletic. Figure 22 shows the majority-rule consensus for all analyses with unordered characters, with

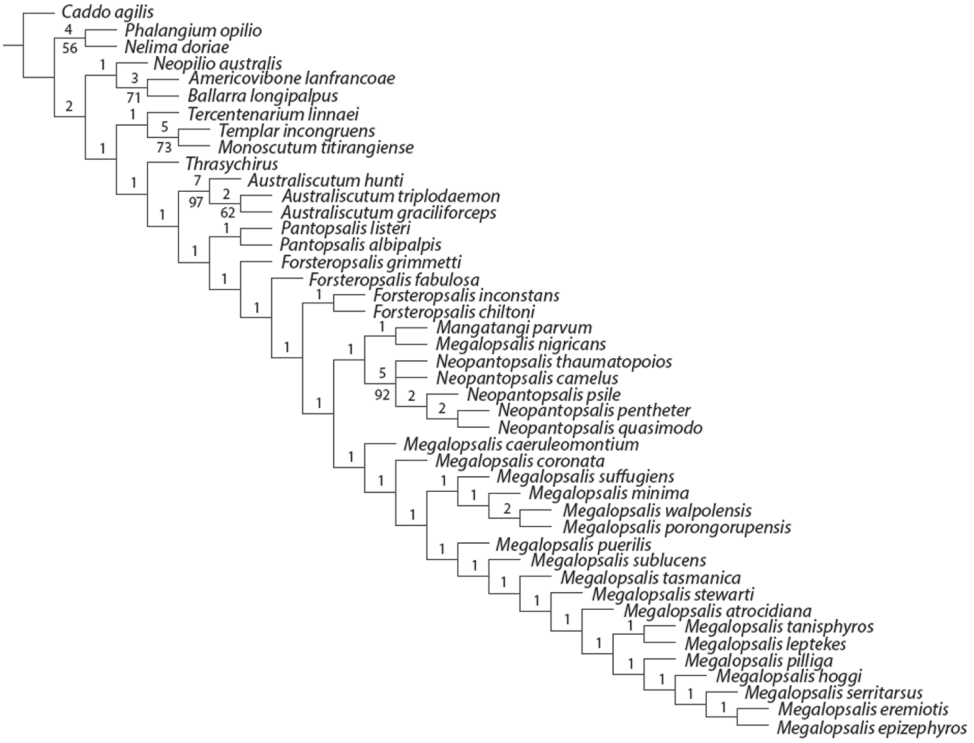

Figure 19. Consensus from equal weights analysis with multistate characters ordered. Numbers above branches indicate Bremer support values; numbers below branches indicate jack-knife support. Those branches without lower numbers received less than 50% jack-knife support.

Table 1. Plot of recovery for selected clades under varying weight analyses with ordered characters. Gray fill indicates monophyly; white fill indicates para- or polyphyly. Abbreviations used: *Mang.* = *Mangatangi*; *Pant.* = *Pantopsalis*; *Forst.* = *Forsteropsalis*; *M.* = *Megalopsalis*. See text for definition of *M. minima*- and *M. serritarsus*-groups.

***k* value**	**0.0**	**1.0**	**2.0**	**3.0**	**4.0**	**5.0**	**6.0**
Neopilionidae							
Enantiobuninae							
Australasian Enantiobuninae							
Australiscutum							
Mang. + *Pant.* + *Forst.*							
Pantopsalis + *Forsteropsalis*							
Pantopsalis							
Forsteropsalis							
Neopantopsalis							
Megalopsalis							
Megalopsalis excl. *M. nigricans*							
M. minima-group							
M. serritarsus-group							

Figure 20. 50% majority rule consensus of trees resulting from equal and implied weights analyses with multistate characters ordered. Numbers on branches indicate percentage of trees in which the given clade was recovered.

support for selected clades under individual weighting schemes shown in Table 2. Figure 23 shows the strict consensus of clades recovered under all analytical conditions, with a total majority-rule consensus shown in Fig. 24. Figure 25 shows the distribution of apomorphies when mapped onto the consensus tree in Fig. 24; some of these apomorphies are discussed below.

Neopilionidae is potentially supported by the absence of setae on the glans itself (char. 19), and by the presence of a longitudinal banner on the stylus (char. 31: lost within Ballarrinae, unknown for *Thrasychirus*). Reduction of the number of seminal receptacles to two (char. 32) is also mapped as a potential synapomorphy, but this character is reversed in *Australiscutum* and *Pantopsalis* + *Forsteropsalis*. Within Neopilionidae, most analyses supported a basal split between Enantiobuninae on one side and *Neopilio* + Ballarrinae on the other. The relationship between the latter two taxa is supported by one unique synapomorphy, the reduction in the pedipalpal claw (char. 58; Hunt and Cokendolpher 1991). None of the potential synapomorphies of Enantiobuninae are unique to that clade; they include the presence of large oblong

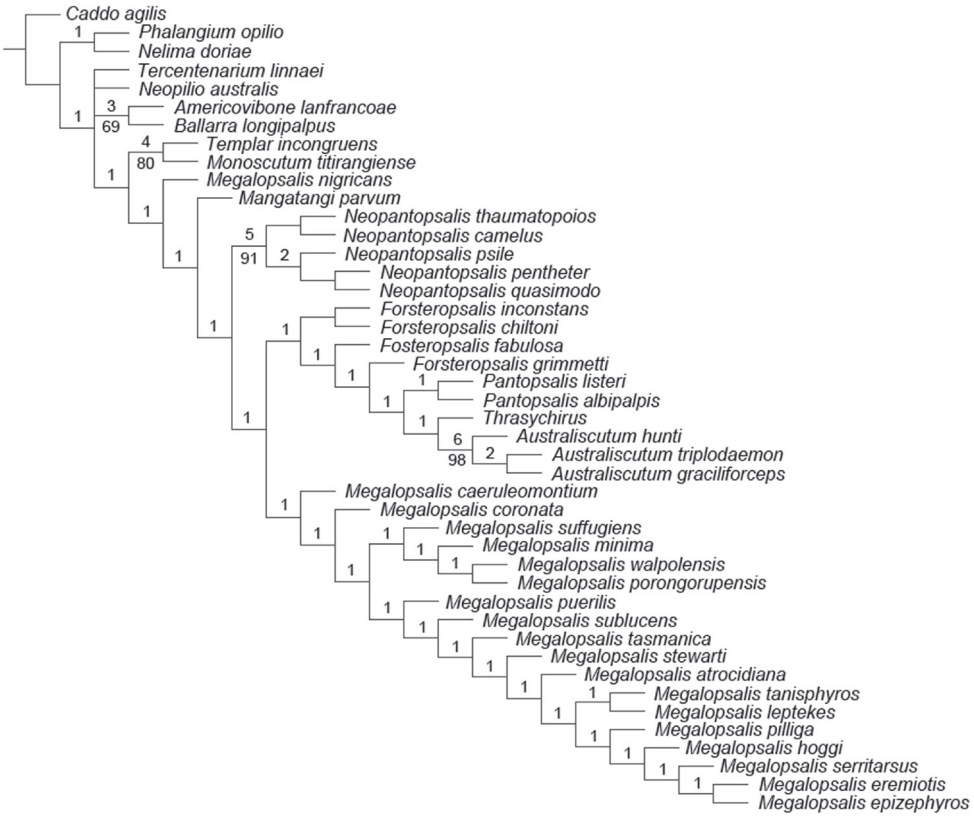

Figure 21. Consensus from equal weights analysis with multistate characters unordered. Numbers above branches indicate Bremer support values; numbers below branches indicate jack-knife support. Those branches without lower numbers received less than 50% jack-knife support.

ozopores on raised lateral lobes (chars 2, 3; reversed in *Megalopsalis nigricans*) and the presence of lateral processes behind the shaft-glans junction on the penis (char. 15; possibly homologous with the barbed process found in Australian Ballarrinae). Other potential synapomorphies, the presence of a distinct space between the ocularium and mesopeltidium (char. 7) and the presence of a pedipalpal patellar apophysis (char. 52) are both commonly reversed within Enantiobuninae.

The current analysis is, admittedly, limited in its ability to test neopilionid monophyly by the low number of outgroup taxa included. Members of all other families of Phalangioidea possess setae on the glans (Cokendolpher et al. 2007), as do males of *Caddo agilis* (Gruber, 1974). Males of Caddidae have been recorded on only rare occasions; other than *Caddo agilis*, males of Acropsopilioninae have genitalia that are highly modified relative to other Eupnoi (Shear 1975), making homologisation difficult. The lateral processes on the penis of Enantiobuninae (bristles or bristle groups) differ from the penile setae of other Palpatores in lacking a basal socket (Taylor 2011). Hedin et al. (2012) recovered a relationship between *Thrasychirus* and '*Megalopsalis*' (probably

Figure 22. 50% majority rule consensus of trees resulting from equal and implied weights analyses with multistate characters unordered. Numbers on branches indicate percentage of trees in which the given clade was recovered.

Forsteropsalis, as the original specimen was collected in New Zealand) under most analytical conditions in a molecular phylogeny focused on Sclerosomatidae, but did not include *Neopilio* or Ballarrinae.

Many of the relationships within the Enantiobuninae are sensitive to weighting regimes, but the results are more stable than those found by Taylor (2011). Major clades supported by all analyses include *Australiscutum*, a clade of *Templar* + *Monoscutum* (henceforth referred to as the '*Monoscutum* clade'), *Pantopsalis*, *Neopantopsalis*, and a clade containing all species assigned herein to *Megalopsalis* except *M. nigricans*. Implied weights analyses consistently placed *Thrasychirus* and *Australiscutum* outside a clade of the remaining Enantiobuninae; *Australiscutum* was sister taxon to the remaining Australasian Enantiobuninae when multistate characters were ordered, but was placed as sister to *Thrasychirus* in some analyses with multistate characters unordered. The equal weights analyses, in contrast, did not support monophyly of the Australasian Enantiobuninae. When multistate characters were ordered, a clade of *Tercentenarium* + the *Monoscutum* clade was positioned basalmost within the Enantiobuninae. When multistate characters were unordered, the equal weights analysis placed *Thrasychirus*

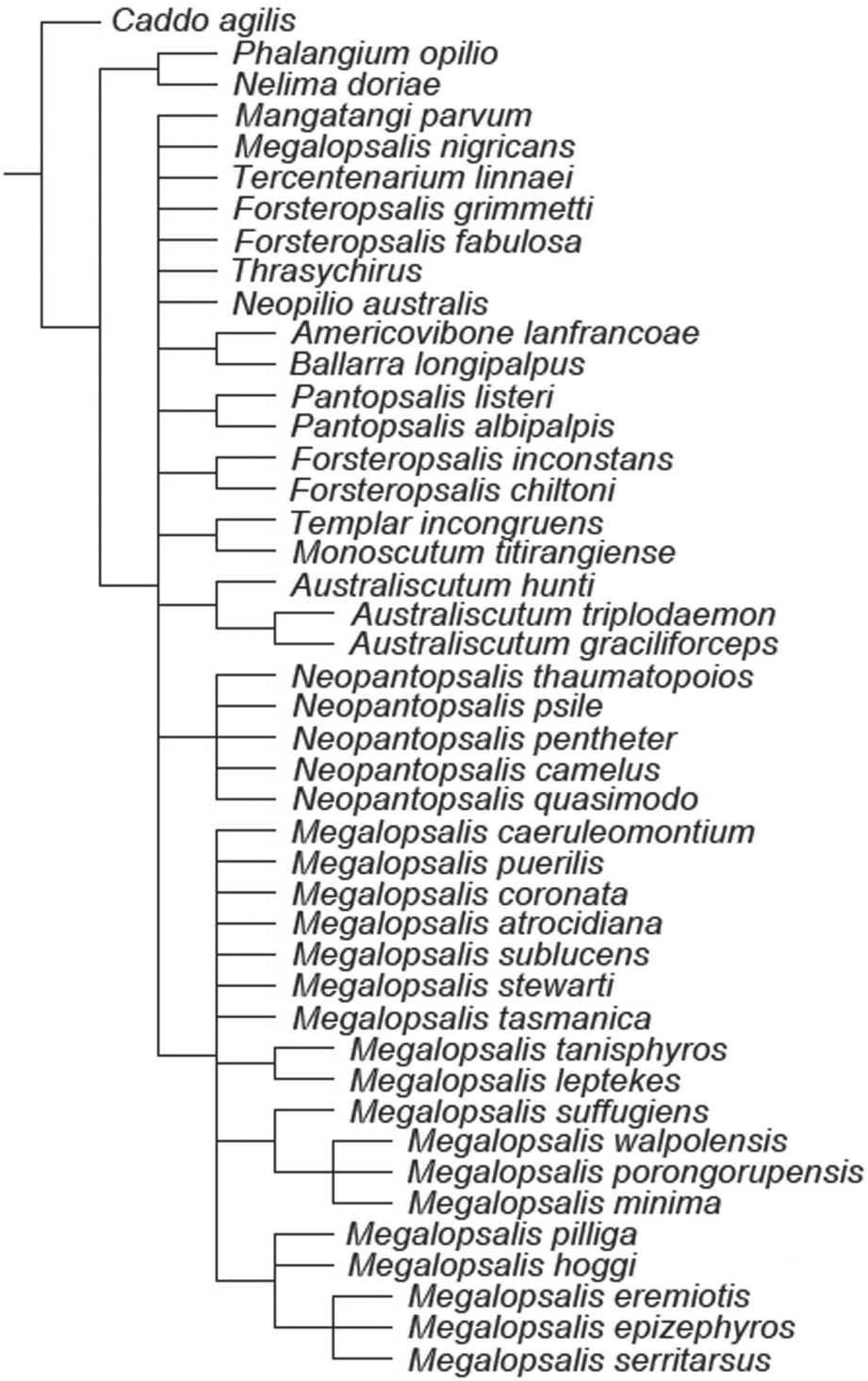

Figure 23. Strict consensus of all trees recovered under all analytical conditions.

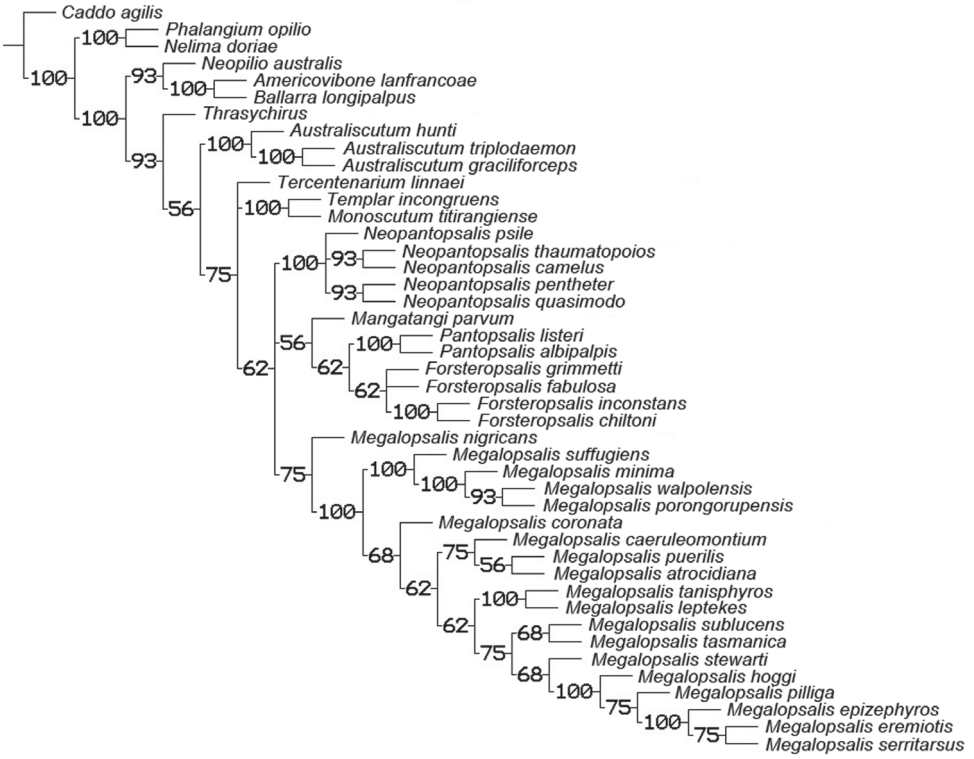

Figure 24. 50% majority rule consensus of all trees resulting from all analyses. Numbers on branches indicate percentage of trees in which the given clade was recovered.

Table 2. Plot of recovery for selected clades under varying weight analyses with unordered characters. Grey fill indicates monophyly; black fill indicates monophyly in only one of two best trees; white fill indicates para- or polyphyly. Abbreviations as for Table 1.

***k* value**	**0.0**	**1.0**	**2.0**	**3.0**	**4.0**	**5.0**	**6.0**
Neopilionidae							
Enantiobuninae							
Australasian Enantiobuninae							
Australiscutum							
Mang. + *Pant.* + *Forst.*							
Pantopsalis + *Forsteropsalis*							
Pantopsalis							
Forsteropsalis							
Neopantopsalis							
Megalopsalis							
Megalopsalis excl. *M. nigricans*							
M. minima-group							
M. serritarsus-group							

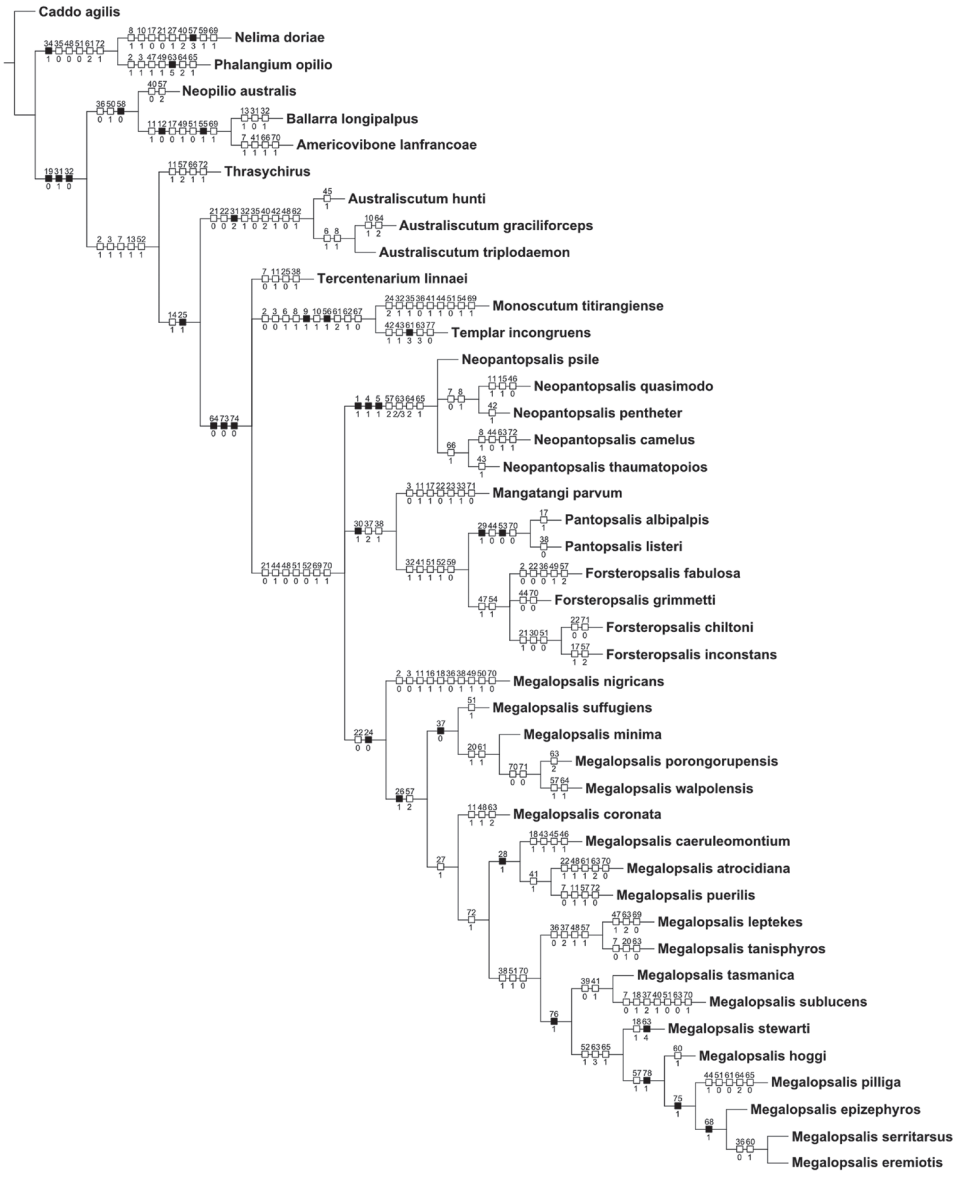

Figure 25. Character distribution mapped onto tree topology shown in Figure 24. Numbers above squares indicate character, numbers below squares indicate character state. Filled squares represent unique apomorphies, hollow squares represent homoplasious apomorphies.

and *Australiscutum* as a clade in a more nested position close to *Pantopsalis*, similar to the results found by Taylor (2011). However, as noted by Taylor (2011), *Thrasychirus* and *Australiscutum* differ from the remaining Enantiobuninae in their retention of a plesiomorphic mobile junction between the basitarsus and distitarsus (char. 73), and such a nested position would require that this character be reversed in these two taxa.

Separation of *Thrasychirus* from the Australasian Enantiobuninae also aligns with the presence of bristle groups rather than isolated bristles at the shaft-glans junction in the latter (char. 14). Within *Australiscutum*, all analyses agree with Taylor (2011) in placing *A. triplodaemon* and *A. graciliforceps* closer to each other than *A. hunti*.

For the most part, the remaining relationships between genera in Enantiobuninae were not robust to analytical conditions. Analyses with multistate characters ordered supported a relationship between *Tercentenarium* and the *Monoscutum* clade, but this was not supported when multistate characters were unordered. Most analyses placed these taxa towards the base of the enantiobunines, which accords with their morphological distinctiveness. The New Zealand *Templar incongruens* and *Monoscutum titirangiense* (together with *Acihasta salebrosa*, not included in the current analysis but expected to be closely related to these two taxa) are short-legged, heavily sclerotised species previously classified as their own subfamily Monoscutinae (Forster 1948, Crawford 1992, Taylor 2008a). *Tercentenarium linnaei* possesses a number of features unique within the Neopilionidae, including a unilateral process on the left side of the penis at the shaft-glans junction, and a 'keyhole' emargination on the anterior margin of the female genital operculum (Taylor 2008b, 2011).

Implied weights analyses supported a relationship between the New Zealand genera *Pantopsalis* and *Forsteropsalis* as found by Taylor (2011), though this clade was not recovered in equal weights analyses. The genus *Forsteropsalis* formed a paraphyletic series in the equal weights analyses, but was returned to monophyly in implied weights analyses at *k* values of 2.0 and above. Implied weights analyses at a *k* value of 1.0 supported a clade of the New Zealand genera *Forsteropsalis*, *Pantopsalis* and *Mangatangi*, but *Pantopsalis* and *Mangatangi* were both nested within *Forsteropsalis*. *Forsteropsalis* species share two distinctive characters within the Enantiobuninae, a small triangular pedipalpal patellar apophysis (except in the female only of *F. grimmetti*) and an array of blunt denticles on the inner margin of the pedipalpal coxa (Taylor 2011). Taylor (2013) suggested that the newly described *Mangatangi parvum* might be the sister taxon to *Pantopsalis* + *Forsteropsalis*, but its position was variable depending on analysis conditions. At higher *k* values with multistate characters ordered, it was placed as sister to the eastern Australian genus *Neopantopsalis*.

Neopantopsalis was supported as monophyletic in all analyses, though its internal topology was sensitive to analysis conditions. Varying analyses placed it closer to either *Megalopsalis* or *Pantopsalis* + *Forsteropsalis*.

Phylogeny of *Megalopsalis*

As found by Taylor (2011), the genus *Spinicrus* as hitherto recognised (Forster 1949, Hickman 1957, Kauri 1954) was not monophyletic, even with the segregation of *Neopantopsalis* (Taylor & Hunt, 2009). Instead, '*Spinicrus*' species were placed as paraphyletic to *Megalopsalis* in sense of Taylor (2011). Members of *Megalopsalis* and *Spinicrus* are united by penis morphology, possessing a relatively short, broad, shallow glans that

is more or less subtriangular in ventral view (char. 24). With the exception of *'Spinicrus' nigricans*, the glans is also dorsally inflated near the shaft-glans junction, becoming distally narrower in lateral view, giving the glans a 'bellied' profile (char. 26; Figs 3e, 4e). In members of other enantiobunine genera, the glans is relatively much longer and/or deeper (Taylor 2004, 2008a, 2008b, 2009, 2011, 2013, Taylor and Hunt 2009).

Spinicrus and *Megalopsalis* were distinguished by the presence in the latter of a lateral apophysis on the patella of the pedipalp (Forster 1949). However, this feature is not unique to *Megalopsalis*, being also found in the *Monoscutum* clade, *Forsteropsalis* and females of *Pantopsalis*, and has probably appeared within the Enantiobuninae on multiple occasions. Even within the clade of *Spinicrus* and *Megalopsalis*, the presence of a pedipalpal apophysis may be homoplasious. While species with this character form a single clade in the equal weights analyses, the implied weights analyses all separate the *M. leptekes*-group from the *M. serritarsus*-group (see below for group definitions), placing the latter as sister to *'Spinicrus' stewarti*. As the distinction between *Megalopsalis* and *Spinicrus* thus appears less reliable phylogenetically than the synapomorphies connecting them, the two genera are here synonymised. *Hypomegalopsalis tanisphyros*, described by Taylor (2011) in its own genus owing to its then phylogenetically uncertain position, shares these synapomorphies and is also placed within *Megalopsalis*. In this broadened sense, *Megalopsalis* admittedly encompasses a higher morphological diversity than most other genera in Enantiobuninae (with the possible exception of *Forsteropsalis*: Taylor 2011). Nevertheless, a broadened *Megalopsalis* represents a far more practical solution to the apparent paraphyly of *'Spinicrus'* than division of the latter between a number of small genera that would have to be distinguished by relatively small-scale and difficult characters.

For the most part, this expanded *Megalopsalis* forms a distinct clade in all analyses. The only exception is *M. nigricans*, which is placed as the basalmost species of *Megalopsalis* in the implied weights analyses but does not form a clade with *Megalopsalis* in the equal weights analyses. The glans of *Megalopsalis nigricans* lacks the bellied profile of other *Megalopsalis* species, and is less regularly subtriangular than most other species. *Megalopsalis nigricans* also possesses a distinctly short and broad shaft to the penis compared to the relatively elongate and narrow shaft of other *Megalopsalis* species (Fig. 14b). Nevertheless, *M. nigricans* is more similar in genital morphology to *Megalopsalis* species than to other Enantiobuninae. Compared to other species of Enantiobuninae, *M. nigricans* is a particularly small taxon with reduced armature, and it is possible that its position is being distorted in the equal weights analyses by homoplasy with similarly small-bodied taxa such as *Mangatangi parvum*. Rather than creating a new monotypic genus for this species, *M. nigricans* is here provisionally assigned to *Megalopsalis*.

Within the clade of *Megalopsalis* species other than *M. nigricans*, a small number of clades are recovered in all analyses, treated here as the *M. leptekes*-, *M. minima*- and *M. serritarsus*-species groups. The *M. leptekes*-group includes the two Western Australian species *M. leptekes* and *M. tanisphyros*. Though a number of potential synapomorphies are identified for these two species in Fig. 25, none are unique to this clade; these include the presence of an elongate, hypersetose pedipalpal patellar apophysis, and an

opisthosomal spiracle with relatively long, non-reticulate covering spines extending across the entire breadth of the spiracle rather than only partway as in other *Megalopsalis* species (Taylor 2011).

The species of the *Megalopsalis minima*-group are similarly Western Australian in distribution, comprising *M. minima*, *M. porongorupensis*, *M. suffugiens* and *M. walpolensis*. Members of this group are also united by spiracle morphology, with the covering spines being mostly lost (char. 37) though remnant lace tubercles are retained except in *M. suffugiens* (in which they have been reduced to a patch of reticulate ornamentation only). All analyses also agree in placing *M. suffugiens*, found in the Nullarbor in south-east Western Australia, as the sister taxon to the remaining species found in the south-west corner of Western Australia.

The *Megalopsalis serritarsus*-group corresponds to the 'core *Megalopsalis* clade' of Taylor (2011). Members of this group possess an elongate pedipalpal patellar apophysis, and males have specialised brush-like setae in a ventral double row on basally inflated distitarsi III and IV (Taylor 2011). With the exception of *M. hoggi*, males of the *M. serritarsus*-group also have modified second tarsi with ventrodistal swellings on the basal pseudosegments (Taylor 2011), and the majority of analyses agree with Taylor (2011) in placing *M. hoggi* as sister to the remaining species. The brush-like setae on distitarsi III and IV are shared with four further species: *M. stewarti*, *M. sublucens*, *M. tasmanica* and *M. thryptica*. For the most part, these species do not also have the distitarsi inflated as in the *M. serritarsus*-group, though *M. thryptica* has distitarsus IV only basally inflated (Hickman 1957; *M. thryptica* was omitted from the phylogenetic analysis owing to the unavailability of specimens). In the implied weights analyses, all species with brush-like setae are placed in a single clade; as this character is not found elsewhere in the Enantiobuninae, this result seems more credible than that of the equal weights analysis which unites the *M. serritarsus*-group with the *M. leptekes*-group on the basis of the probably homoplasious pedipalpal patellar apophysis.

Relationships between the remaining species of *Megalopsalis* are not consistently recovered by all analyses, and they are left unplaced in species groups. Clades recovered by implied weights analyses but not by the equal weights analyses include a sister relationship between the Tasmanian species *M. tasmanica* and *M. sublucens*, and a clade including *M. atrocidiana*, *M. caeruleomontium* and *M. puerilis*. The latter three species share a genital morphology with the sides of the glans closer to parallel in ventral view than in other *Megalopsalis* species (char. 28).

Biogeography and male variation

Though neither Australian nor New Zealand Enantiobuninae are identified as monophyletic, there is an overall separation between the fauna of the two land masses. New Zealand taxa may belong to as few as two separate clades (depending on the position of *Mangatangi parvum*). A relatively low level of interchange is also indicated between the western and eastern sides of the Australian continent, with the Western Australian

species of *Megalopsalis* mostly assignable to the endemic clades of the *M. minima*- and *M. leptekes*-groups. *Megalopsalis epizephyros* is a member of the otherwise eastern Australian *M. serritarsus*-group and may represent a more recent immigration; it is notable in this regard that the only Enantiobuninae known to date from South Australia are representatives of the *M. serritarsus*-group (Forster 1949, Taylor 2011). In general, members of the *M. leptekes*- and *M. serritarsus*-groups tend to be found in more inland, and presumably drier, localities than other *Megalopsalis* species (Taylor 2011).

The feature of Australasian Enantiobuninae that has perhaps caused the most comment is the presence in males of most species of greatly enlarged chelicerae relative to the females. Though this has been cited as a diagnostic characteristic of the group (e.g. Dunlop and Mammitzsch 2010), many species also exhibit minor males with chelicerae that are less exaggerated than those of majors (Taylor and Hunt 2009). For a number of species of *Megalopsalis* (*M. coronata*, *M. puerilis*, *M. sublucens*, *M. tanisphyros* and *M. walpolensis*), the males appear to lack enlarged chelicerae (Taylor 2011 and below), though the possibility cannot be excluded that major males of these species remain to be discovered. The ratios of major to minor males in a population may vary between species: in *Neopantopsalis* species, for instance, the majority of specimens in collections are majors, while in *M. minima* and *M. nigricans*, majors are relatively rare and greatly outnumbered by minors (personal observations).

Variation in male cheliceral development has been identified for species of *Megalopsalis*, *Neopantopsalis* and *Pantopsalis* (Taylor 2004, 2013, Taylor and Hunt 2009; as noted by Taylor 2013, the 'effeminate' males described by Forster 1964 and Taylor 2004 for certain *Pantopsalis* species probably represent young specimens that have yet to complete cuticular hardening). Specimens of *Forsteropsalis chiltoni* vary in the degree of inflation of the second cheliceral segment, though they are not divisible between discrete morphs (Taylor 2011). In *Pantopsalis*, broad- and slender-chelicerate males differ in cheliceral length and inflation of the second segment, but males otherwise do not differ significantly in body size (Taylor 2004). In *Neopantopsalis* and *Megalopsalis*, major and minor males distinctly differ in body size as well as cheliceral size. It seems likely that discrete male dimorphism has developed independently in *Pantopsalis* versus *Neopantopsalis* + *Megalopsalis*, though it is possible that a more general variability as seen in *Forsteropsalis chiltoni* may be ancestral for the larger clade containing all three genera.

Within the Australian taxa, discrete major and minor morphs (i.e. without intermediate-sized individuals) are identifiable in *Neopantopsalis* species, *Megalopsalis minima* and *M. nigricans*. However, *M. caeruleomontium*, *M. porongorupensis* and *M. stewarti* exhibit more continual variation without clearly discrete morphs (variation is also present in *M. suffugiens*, but sample size is not large enough to identify whether it is discrete or continuous). Most other *Megalopsalis* species are known from too few specimens to discount the possibility of male variation, with the possible exception of *M. epizephyros* (Taylor 2011). It seems likely that at least some degree of male variation is ancestral for *Megalopsalis*, though we cannot say whether it was discrete or continuous.

Acknowledgements

Thanks are due to Mark Harvey and Julianne Waldock (WAM), Owen Seeman (QM), Graham Milledge (AMS) and Peter Lilywhite (MV) for arranging the loan of specimens used in this study. Thank you also to Mark Harvey and Jonathan Majer (Curtin University) for guidance and criticism in preparing this manuscript. Research towards this manuscript was conducted as part of a PhD programme at Curtin University.

References

Crawford RL (1992) Catalogue of the genera and type species of the harvestman superfamily Phalangioidea (Arachnida). Burke Museum Contributions in Anthropology and Natural History 8: 1–60.

Dunlop JA, Mammitzsch L (2010) A new genus and species of harvestman from Baltic amber. Palaeodiversity 3: 23–32.

Forster RR (1944) The genus *Megalopsalis* Roewer in New Zealand with keys to the New Zealand genera of Opiliones. Records of the Dominion Museum 1(1): 183–192.

Forster RR (1948) A new sub-family and species of New Zealand Opiliones. Records of the Auckland Institute and Museum 3: 313–318.

Forster RR (1949) Australian Opiliones. Memoirs of the National Museum of Victoria 16: 59–89.

Forster RR (1954) The New Zealand harvestmen (sub-order Laniatores). Canterbury Museum Bulletin 2: 1–329.

Forster RR (1964) The Araneae and Opiliones of the subantarctic islands of New Zealand. Pacific Insects Monograph 7: 58–115.

Giribet G, Edgecombe GD, Wheeler WC, Babbitt V (2002) Phylogeny and systematic position of Opiliones: a combined analysis of chelicerate relationships using morphological and molecular data. Cladistics 19: 5–70.

Giribet G, Vogt L, Pérez González A, Sharma P, Kury AB (2009) A multilocus approach to harvestman (Arachnida: Opiliones) phylogeny with emphasis on biogeography and the systematics of Laniatores. Cladistics 26: 408–437.

Goloboff PA, Farris JS, Nixon K (2008) TNT: Tree Analysis Using New Technology. Version 1.0. Program and documentation available at http://www.zmuc.dk/public/phylogeny/TNT/

Gruber J (1954) Bemerkungen zur Morphologie und systematischen Stellung von *Caddo*, *Acropsopilio* und verwandter Formen (Opiliones, Arachnida). Annalen des Naturhistorischen Museums in Wiens 78: 237–259.

Hedin M, Tsurusaki N, Macías-Ordóñez R, Shultz JW (2012) Molecular systematics of sclerosomatid harvestmen (Opiliones, Phalangioidea, Sclerosomatidae): geography is better than taxonomy in predicting phylogeny. Molecular Phylogenetics and Evolution 62: 224–236. doi: 10.1016/j.ympev.2011.09.017

Hickman VV (1957) Some Tasmanian harvestmen of the sub-order Palpatores. Papers and Proceedings of the Royal Society of Tasmania 91: 65–79.

Hogg HR (1910) Some New Zealand and Tasmanian Arachnidae. Transactions and Proceedings of the New Zealand Institute 42: 273–283.

Hunt GS (1990) Taxonomic value of spiracle microstructure in the Megalopsalididae (Opiliones, Phalangioidea). In: Koponen S, Lehtinen PT, Rinne V (Eds) Proceedings of the XI International Congress of Arachnology, Turku, Finland, 7–12 August 1989. Acta Zoologica Fennica 190: 187–194.

Hunt GS, Cokendolpher JC (1991) Ballarrinae, a new subfamily of harvestmen from the Southern Hemisphere (Arachnida, Opiliones, Neopilionidae). Records of the Australian Museum 43(2): 131–169. doi: 10.3853/j.0067-1975.43.1991.45

Kauri H (1954) Report from Professor T. Gislén's expedition to Australia in 1951–1952. 9. Harvest-spiders from S. W. Australia. Lunds Universitets Årsskrift Ny Fjöld, Avd. 2, 50 (11): 1–10.

Nation JL (1983) A new method using hexamethyldisilazane for preparation of soft insect tissues for scanning electron microscopy. Stain Technology 58: 347–351.

Nixon KC (1999–2002) Winclada ver. 1.00.08. Program available at http://www.cladistics.com/about_winc.htm

Cokendolpher JC, Tsurusaki N, Tourinho AL, Taylor CK, Gruber J, Pinto-da-Rocha R (2007) Eupnoi. In: Pinto-da-Rocha R, Machado G, Giribet G (Eds) Harvestmen: The Biology of Opiliones. Harvard University Press, Cambridge, USA, 108–131.

Pocock RI (1903) On some new harvest-spiders of the order Opiliones from the southern continents. Proceedings of the Zoological Society of London 1902(2): 392–413.

Roewer CF (1911) Übersicht der Genera der Subfamilie der Phalangiini der Opiliones Palpatores nebst Beschreibung einiger neuer Gattungen und Arten. Archiv für Naturgeschichte, part I 77 (suppl. 2): 1–106, pl. 1–3.

Roewer CF (1912) Revision der Opiliones Palpatores (=Opiliones Plagiostethi). II. Teil: Familie der Phalangiidae. (Subfamilien: Sclerosomini, Oligolophini, Phalangiini). Abhandlungen aus dem Gebiete der Naturwissenschaften, herausgegeben von Naturwissenschaftlichen Verein in Hamburg 20(1): 1–295, pl. 1–4.

Roewer CF (1923) Die Weberknechte der Erde: Systematisches Bearbeitung der bisher bekannten Opiliones. Gustav Fischer, Jena, Germany, v + 1116 pp.

Shear WA (1975) The opilionid family Caddidae in North America, with notes on species from other regions (Opiliones, Palpatores, Caddoidea). Journal of Arachnology 2: 65–88.

Shultz JW (1998) Phylogeny of the Opiliones (Arachnida): an assessment of the "Cyphopalpatores" concept. Journal of Arachnology 26: 257–272.

Simon E (1879) Descriptions d'Opiliones nouveaux. Annales de la Société Entomologique de Belgique 22 (Comptes-Rendus): lxx–lxxv.

Soares BAM, Soares HEM (1947) Alótipos e formas novas de Opiliões Paranaenses (Opiliones–Gonyleptidae, Phalangiidae). Papéis Avulsos do Departamento de Zoologia 8(5): 63–84.

Sørensen W (1886) Opiliones descripsit W. Sörensen. In: Koch L, Keyserling E von (Eds) Die Arachniden Australiens nach der natur beschrieben und abgebildet, vol. 2. Bauer und Raspe, Nürnberg, 53–86, pls 5–6.

Taylor CK (2004) New Zealand harvestmen of the subfamily Megalopsalidinae (Opiliones: Monoscutidae) – the genus *Pantopsalis*. Tuhinga 15: 53–76.

Taylor CK (2008a) A new species of Monoscutinae (Arachnida, Opiliones, Monoscutidae) from New Zealand, with a redescription of *Monoscutum titirangiense*. Journal of Arachnology 36: 176–179. doi: 10.1636/H07-10SC.1

Taylor CK (2008b) A new species of Monoscutidae (Arachnida, Opiliones) from the wheatbelt of Western Australia. Records of the Western Australian Museum 24(4): 375–380.

Taylor CK (2009) *Australiscutum*, a new genus of Monoscutidae (Arachnida: Opiliones) from eastern Australia, with the first record of asymmetrical chelicerae in Opiliones. Insect Systematics and Evolution 40: 319–332. doi: 10.1163/187631209X458367

Taylor CK (2011) Revision of the genus *Megalopsalis* (Arachnida: Opiliones: Phalangioidea) in Australia and New Zealand and implications for phalangioid classification. Zootaxa 2773: 1–65.

Taylor CK (2013) Further notes on New Zealand Enantiobuninae (Opiliones, Neopilionidae), with the description of a new genus and two new species. ZooKeys 263: 59–73. doi: 10.3897/zookeys.263.4158

Taylor CK, Hunt GS (2009) New genus of Megalopsalidinae (Arachnida: Opiliones: Monoscutidae) from north-eastern Australia. Zootaxa 2130: 41–59.

White A (1849) Descriptions of apparently new species of Aptera from New Zealand. Proceedings of the Zoological Society of London 17: 3–6 (reprinted 1850, Annals and Magazine of Natural History, series 2, 5: 50–53).

Appendix

Character state matrix for phylogenetic analysis

Caddo_agilis

0 0 0 0 0 0 0 0 0 0 0 1 0 0 ? ?
1 0 1 ? ? 1 1 1 0 0 0 0 0 0 0 1
0 0 1 1 ? ? ? 0 0 0 0 0 0 0 0 1
0 0 1 0 ? ? 0 0 0 1 0 0 0 0 ? ?
0 0 0 ? 0 0 1 0 1 1 ? ? 0 ?

Nelima_doriae

0 0 0 0 0 0 0 1 0 1 0 1 0 0 ? ?
0 0 1 0 0 1 0 2 0 0 1 0 0 0 0 1
0 1 0 ? ? ? ? 2 0 0 0 0 0 0 0 0
0 0 0 0 ? ? 0 0 3 1 1 0 2 0 2 1
0 0 1 0 1 0 1 1 1 1 0 0 1 0

Phalangium_opilio

0 1 1 0 0 0 0 0 0 0 0 1 0 0 ? ?
1 0 1 0 1 1 1 2 0 0 0 0 0 0 0 ?
? 1 0 ? ? ? ? 1 0 0 0 0 0 0 1 0
1 0 0 ? ? ? 0 0 1 1 0 0 2 0 5 2
1 0 1 0 0 0 1 1 1 1 0 0 1 0

Neopilio_australis

0 ? ? 0 0 0 0 0 0 0 0 1 0 0 ? ?
1 0 0 ? ? 1 ? 2 0 0 0 0 0 ? 1 0
1 0 2 0 ? ? ? 0 0 0 0 0 0 ? ? 1
0 1 1 0 ? ? 0 0 2 0 0 0 0 0 0 ?
0 0 1 ? 0 0 ? ? ? ? 0 0 ? 0

Ballarra_longipalpus

0 0 0 0 0 0 0 0 0 0 1 0 1 1 ? 1
0 0 0 0 1 1 0 2 0 0 0 0 0 0 0 1
1 0 0 0 ? ? ? 2 0 0 0 0 0 0 0 1
1 1 0 0 ? ? 1 0 0 0 ? 0 0 0 0 ?
0 0 1 0 1 0 1 0 1 1 0 0 1 0

Americovibone_lanfrancoae

0	0	0	0	0	0	1	0	0	0	1	0	0	?	?	?
0	0	0	?	?	1	0	2	0	0	0	0	0	0	1	0
?	?	?	?	?	?	?	?	1	0	0	0	0	0	0	1
1	1	0	0	?	?	1	0	?	0	?	0	0	0	0	?
?	1	1	0	1	1	?	?	?	?	?	?	?	?		

Thrasychirus

0	1	1	0	0	0	1	?	0	0	1	?	1	0	?	?
?	0	0	?	?	1	?	1	0	0	0	0	?	?	?	0
1	0	2	1	2	0	0	1	1	0	1	?	?	0	?	1
0	0	1	1	?	?	0	0	2	1	1	?	?	0	?	?
?	1	1	?	?	?	1	1	1	1	?	?	1	?		

Australiscutum_hunti

0	1	1	0	0	0	1	0	0	0	0	1	1	1	1	0
1	0	0	0	0	0	1	1	1	0	0	0	0	0	2	1
0	0	0	?	?	?	?	2	1	1	1	0	1	0	0	0
0	0	1	1	?	?	0	0	1	1	1	0	0	1	0	?
0	0	1	0	0	0	0	?	1	1	0	0	1	0		

Australiscutum_graciliforceps

0	1	1	0	0	1	1	1	0	1	0	1	1	1	1	0
1	0	0	0	0	0	1	1	1	0	0	0	0	0	2	1
0	0	0	?	?	?	?	2	1	1	1	0	0	0	0	0
0	0	1	1	1	0	0	0	1	1	1	0	0	1	1	2
0	0	1	0	0	0	0	?	1	1	0	0	1	0		

Australiscutum_triplodaemon

0	1	1	0	0	1	1	1	0	0	0	1	1	1	1	0
1	0	0	0	0	0	1	1	1	0	0	0	0	0	2	?
0	0	0	?	?	?	?	2	?	1	1	0	[01]0		0	0
0	0	1	?	1	0	0	0	1	1	1	0	0	1	1	1
0	0	1	0	0	0	0	?	1	1	0	0	1	0		

Monoscutum_titirangiense

0	0	0	0	0	1	?	1	1	1	0	1	1	1	0	0
0	0	0	0	1	1	0	2	1	0	0	0	0	0	1	1
0	0	1	0	?	?	?	1	1	0	0	1	0	0	0	1
0	0	0	2	1	1	0	1	1	1	0	0	2	1	0	?
0	0	0	0	1	0	1	0	0	0	0	0	1	0		

Templar_incongruens

0 0 0 0 0 1 ? 1 1 1 ? 1 1 1 0 ?
0 0 0 ? ? 1 0 1 1 0 0 0 0 ? 1 0
0 0 2 1 1 0 ? 1 0 1 1 0 0 0 0 ?
0 0 1 2 1 0 0 1 1 1 0 0 3 1 3 0
0 0 0 0 0 0 0 ? 0 0 0 0 0 0

Tercentenarium_linnaei

0 1 1 0 0 0 0 0 0 0 1 1 1 1 0 0
1 0 0 0 1 1 1 1 0 0 0 0 0 0 1 0
0 0 2 1 1 1 1 0 0 0 0 0 0 0 0 1
0 0 1 2 1 0 0 0 1 1 0 0 0 0 0 ?
0 0 1 0 0 0 0 ? 0 0 0 0 1 0

Forsteropsalis_chiltoni

0 1 1 0 0 0 1 0 0 0 0 1 1 1 0 0
0 0 0 0 1 0 0 1 1 0 0 0 0 0 1 1
0 0 2 1 2 1 0 1 ? 0 0 1 1 1 1 0
0 0 0 1 1 1 0 0 1 1 0 0 0 0 1 0
0 0 1 0 1 1 0 1 0 0 0 0 1 0

Forsteropsalis_fabulosa

0 0 1 0 0 0 1 0 0 0 0 1 1 1 0 0
0 0 0 0 0 0 0 1 1 0 0 0 0 1 1 ?
0 0 2 0 2 1 0 1 1 0 1 1 1 1 1 0
1 0 1 1 1 1 0 0 2 1 0 0 0 0 1 0
0 0 1 0 1 1[01] 1 0 0 0 0 1 0

Forsteropsalis_grimmetti

0 1 1 0 0 0 1 0 0 0 0 1 1 1 0 0
0 0 0 0 0 1 0 1 1 0 0 0 0 1 1 1
0 0 2 1 2 1 0 1 1 0 1 0 1 1 1 0
0 0 1 1 1 [01]0 0 1 1 0 0 0 0 1 0 0
0 1 0 1 0 1 1 0 0 0 0 1 0

Forsteropsalis_inconstans

0 1 1 0 0 0 1 0 0 0 0 1 1 1 0 0
1 0 0 0 1 1 0 1 1 0 0 0 0 0 1 ?
0 0 2 1 2 ? 0 1 0 0 0 1 1 1 1 0
0 0 0 1 1 1 0 0 2 1 0 0 0 0 1 0
0 0 1 0 1 1 1 1 0 0 0 0 1 0

Pantopsalis_albipalpis

0	1	1	0	0	0	1	0	0	0	0	1	1	1	0	0
1	0	0	0	0	1	0	1	1	0	0	0	1	1	1	1
0	0	2	1	2	1	1	0	1	0	[01]	0	0	1	0	0
0	0	1	1	0	0	0	0	1	1	0	0	0	0	1	0
0	0	1	0	1	0	1	1	0	0	0	0	1	0		

Pantopsalis_listeri

0	1	1	0	0	0	1	0	0	0	0	1	1	1	0	0
0	0	0	0	0	1	0	1	1	0	0	0	1	1	1	1
0	0	2	1	2	0	0	1	1	0	0	0	0	1	0	0
0	0	1	1	0	0	0	0	1	1	0	0	0	0	1	0
0	0	1	0	1	0	1	1	0	0	0	0	1	0		

Mangatangi_parvum

0	1	0	0	0	0	1	0	0	0	1	1	1	1	0	?
1	0	0	?	?	0	1	1	1	0	0	0	0	1	1	0
1	0	2	?	2	1	1	0	0	0	1	1	1	1	0	0
0	0	0	0	?	?	0	0	1	1	1	0	0	0	0	?
?	?	1	?	?	1	0	?	0	0	?	0	1	0		

Neopantopsalis_quasimodo

1	1	1	1	1	0	0	1	0	0	1	1	1	1	1	0
0	0	0	0	0	1	0	1	1	0	0	0	0	0	1	?
0	0	2	0	1	0	?	0	?	0	0	1	1	0	0	0
0	0	0	?	?	?	0	0	2	1	1	0	1	0	3	2
1	0	1	0	1	1	1	0	0	0	0	0	1	0		

Neopantopsalis_camelus

1	1	1	1	1	1	1	1	0	0	0	1	1	1	0	?
0	0	0	?	?	1	0	1	1	0	0	0	0	0	1	?
0	0	2	?	1	1	?	?	?	0	0	0	1	1	0	?
0	0	0	?	?	?	0	0	2	1	1	0	0	0	1	2
1	1	1	0	1	1	1	1	0	0	0	0	1	0		

Neopantopsalis_pentheter

1	1	1	1	1	0	0	1	0	0	0	1	1	1	0	0
0	0	0	0	0	1	0	1	1	0	0	0	0	0	1	0
0	0	2	1	1	0	1	0	0	1	0	1	1	1	0	0
0	0	0	0	?	?	0	0	2	1	1	0	1	0	3	2
1	0	1	0	1	1	1	0	0	0	0	0	1	0		

Neopantopsalis_psile

1 1 1 1 1 1 1 0 0 0 0 1 1 1 0 0
0 0 0 0 0 1 0 1 1 0 0 0 0 0 1 0
0 0 2 0 1 0 1 0 0 0 0 1 1 1 0 0
0 0 0 0 ? ? 0 0 2 1 1 0 1 0 3 2
1 0 1 0 1 1 1 0 0 0 0 0 1 0

Neopantopsalis_thaumatopoios

1 1 1 1 1 1 1 0 0 0 0 1 1 1 0 ?
0 0 0 ? ? 1 0 1 1 0 0 0 0 0 1 ?
? ? ? ? ? ? ? ? ? 0 1 1 1 1 0 ?
0 0 0 ? ? ? 0 0 2 1 1 0 0 0 2 2
1 1 1 0 1 ? 1 0 0 0 0 ? 1 ?

Megalopsalis_serritarsus

0 1 1 0 0 0 1 0 0 0 0 1 1 1 0 ?
0 0 0 ? ? 0 0 0 1 1 1 0 0 0 1 ?
0 0 2 0 1 1 1 0 ? 0 0 0 0 0 0 1
0 0 1 ? 1 0 0 0 1 1 1 1 1 0 3 1
1 0 1 1 1 0 0 ? 0 0 1 1 1 1

Megalopsalis_epizephyros

0 1 1 0 0 0 1 0 0 0 0 1 1 1 0 0
0 0 0 0 0 0 0 0 1 1 1 0 0 0 1 0
0 0 2 1 1 0 1 0 0 0 0 0 0 0 0 1
0 0 1 2 1 0 0 0 1 1 1 0 1 0 3 1
1 0 1 1 1 0 0 ? 0 0 1 1 1 1

Megalopsalis_eremiotis

0 1 1 0 0 0 1 0 0 0 0 1 1 1 0 0
0 0 0 1 0 0 0 0 1 1 1 0 0 0 1 0
0 0 2 0 1 0 1 0 0 0 0 0 0 0 0 1
0 0 1 2 1 0 0 0 1 1 1 1 1 0 3 1
1 0 1 1 1 0 0 ? 0 0 1 1 1 1

Megalopsalis_hoggi

0 1 1 0 0 0 1 0 0 0 0 1 1 1 0 ?
0 0 0 ? ? 0 0 0 1 1 1 0 0 0 1 ?
? ? ? ? ? ? ? ? ? 0 0 0 0 0 0 ?
0 0 1 ? 1 0 0 0 1 1 1 1 1 0 3 1
1 0 1 0 1 0 0 ? 0 0 0 1 1 1

Megalopsalis_leptekes

0	1	1	0	0	0	1	0	0	0	0	1	1	1	0	0
0	0	0	0	0	0	0	0	1	1	1	0	0	0	1	?
0	0	2	0	2	1	?	0	?	0	0	0	0	0	1	1
0	0	1	?	1	0	0	0	1	1	1	0	0	0	2	1
0	0	1	0	0	0	0	?	0	0	0	0	1	0		

Megalopsalis_pilliga

0	1	1	0	0	0	1	0	0	0	0	1	1	1	0	0
0	0	0	0	0	0	0	0	1	1	1	0	0	0	1	?
?	?	?	?	?	?	?	?	?	0	0	1	0	0	0	1
0	0	0	?	1	0	0	0	1	1	1	0	0	0	3	2
0	0	1	0	1	0	0	?	0	0	1	1	1	1		

Megalopsalis_tanisphyros

0	1	1	0	0	0	0	0	0	0	0	1	1	1	0	0
0	0	0	1	0	0	0	0	1	1	1	0	0	0	1	?
0	0	2	0	2	1	1	0	0	0	0	1	0	0	0	1
0	0	1	?	1	0	0	0	1	1	1	0	0	0	0	?
0	0	1	0	1	0	0	?	0	0	0	0	1	0		

Megalopsalis_tasmanica

0	1	1	0	0	0	1	0	0	0	0	1	1	1	0	0
0	0	0	1	0	0	0	0	1	1	1	0	0	0	1	1
0	0	2	1	1	1	0	0	1	0	0	0	0	0	0	0
0	0	1	0	?	?	0	0	2	1	1	0	1	0	1	1
0	0	1	0	1	0	1	1	0	0	0	1	1	0		

Megalopsalis_minima

0	1	1	0	0	0	0	0	0	0	0	1	1	1	0	0
0	0	0	1	0	0	0	0	1	1	0	0	0	0	1	?
0	0	2	?	0	?	1	0	?	0	0	1	0	0	0	0
0	0	0	?	?	?	0	0	2	1	1	0	1	0	[12]	0
0	0	1	0	1	1	1	0	0	0	0	0	1	0		

Megalopsalis_nigricans

0	0	0	0	0	0	1	0	0	0	1	1	1	1	0	1
0	1	0	0	0	0	0	0	1	0	0	0	0	0	1	0
0	0	2	0	1	1	1	0	0	0	0	1	0	0	0	0
1	1	0	0	?	?	0	0	1	1	1	0	0	0	0	?
0	0	1	0	1	0	1	0	0	0	0	0	1	0		

Megalopsalis_porongorupensis

0 1 1 0 0 0 0 0 0 0 0 1 1 1 0 0
0 0 0 1 0 0 0 0 1 1 0 0 0 0 1 ?
0 0 2 ? 0 ? 1 0 ? 0 0 0 0 0 0 0
0 0 0 ? ? ? 0 0 2 1 1 0 1 0 2 0
0 0 1 0 1 0 0 ? 0 0 0 0 1 0

Megalopsalis_stewarti

0 1 1 0 0 0 1 0 0 0 0 1 1 1 0 0
0 1 0 0 0 0 0 0 1 1 1 0 0 0 1 1
0 0 2 1 1 1 1 0 0 0 0 0 0 0 0 0
0 0 1 1 ? ? 0 0 2 1 1 0 1 0 4 1
1 0 1 0 1 0 1 1 0 0 0 1 1 0

Megalopsalis_sublucens

0 1 1 0 0 0 0 0 0 0 0 1 1 1 0 ?
0 1 ? ? ? 0 0 0 1 1 1 0 0 0 1 ?
0 0 2 ? 2 1 0 1 1 0 0 0 0 0 0 0
0 0 0 ? ? ? 0 0 2 1 1 0 0 0 0 ?
0 0 1 0 1 1 0 ? 0 0 0 1 1 0

Megalopsalis_suffugiens

0 1 1 0 0 0 0 0 0 0 0 1 1 1 0 0
0 0 0 0 0 0 0 0 1 1 0 0 0 0 1 1
0 0 2 ? 0 ? 1 0 0 0 0 0 0 0 0 0
0 0 1 0 ? ? 0 0 2 1 1 0 0 0 1 [01]0
0 1 0 1 1 1 0 0 0 0 0 1 0

Megalopsalis_walpolensis

0 1 1 0 0 0 0 0 0 0 0 1 1 1 0 0
0 0 0 1 0 0 0 0 1 1 0 0 0 0 1 ?
0 0 2 ? 0 ? 1 0 ? 0 0 0 0 0 0 0
0 0 0 ? ? ? 0 0 1 1 1 0 1 0 1 1
0 0 1 0 1 0 0 ? 0 0 0 0 1 0

Megalopsalis_atrocidiana

0 1 1 0 0 0 1 0 0 0 0 1 1 1 0 ?
0 0 ? ? ? 1 0 0 1 1 1 1 0 0 1 0
0 0 2 1 1 0 1 0 1 0 0 0 0 0 0 1
0 0 0 1 ? ? 0 0 2 1 1 0 1 0 2 1
0 0 1 0 1 0 1 1 0 0 0 0 1 0

Megalopsalis_coronata

0 1 1 0 0 0 0 0 0 0 1 1 1 1 0 0
0 0 0 0 0 0 0 0 1 1 1 0 0 0 1 ?
0 0 2 1 1 0 1 0 0 0 0 1 0 0 0 1
0 0 0 ? ? ? 0 0 2 1 1 0 0 0 2 0
0 0 1 0 1 1 [01] 0 0 0 0 0 1 0

Megalopsalis_puerilis

0 1 1 0 0 0 0 0 0 0 1 1 1 1 0 0
0 0 0 1 0 0 0 0 1 1 1 1 0 0 1 ?
0 0 2 1 1 0 1 0 1 0 0 0 0 0 0 0
0 0 0 ? ? ? 0 0 1 1 1 0 0 0 1 1
0 0 1 0 1 1 [01]0 0 0 0 0 1 0

Megalopsalis_caeruleomontium

0 1 1 0 0 0 1 0 0 0 0 1 1 1 0 0
0 1 0 0 0 0 0 0 1 1 1 1 0 0 1 ?
0 0 2 1 1 0 1 0 0 0 1 1 1 1 0 0
0 0 0 0 ? ? 0 0 2 1 1 0 0 0 1 0
0 0 1 0 1 1 1 1 0 0 0 0 1 0